AMERICAN UNIVERSITY OF BEIRUT

INSIGHTS INTO THE DEREGULATIONS OF RBM20 IN
LAMIN A/C AND EMERIN RELATED CARDIOMYOPATHIES

by
DANA MHD HAZEM SEDKI

A thesis
submitted in partial fulfillment of the requirements
for the degree of Master of Science
to the Department of Biochemistry
of the Faculty of Medicine
at the American University of Beirut

Beirut, Lebanon
November 2015

AMERICAN UNIVERSITY OF BEIRUT

INSIGHTS INTO THE DEREGULATIONS OF RBM20 IN
LAMIN A/C AND EMERIN RELATED
CARDIOMYOPATHIES

By

DANA MHD HAZEM SEDKI

Approved by:

_____   Advisor
Marwan Refaat, Assistant Professor
Department of Biochemistry and Molecular Genetics

_____   Co-Advisor
Diana Jaalouk, Assistant Professor
Department of Biology

_____   Member of Committee
Georges Nemer, Professor
Department of Biochemistry and Molecular Genetics

_____   Member of Committee
Firas Kobaissy, Assistant Professor
Department of Biochemistry and Molecular Genetics

Date of thesis defense: November 12, 2015

AMERICAN UNIVERSITY OF BEIRUT

THESIS, DISSERTATION, PROJECT RELEASE FORM

Student Name: Sedki   Dana   MHD Hazem
     Last   First   Middle

◯ Master's Thesis ◯ Master's Project ◯ Doctoral Dissertation

☐ I authorize the American University of Beirut to: (a) reproduce hard or electronic copies of my thesis, dissertation, or project; (b) include such copies in the archives and digital repositories of the University; and (c) make freely available such copies to third parties for research or educational purposes.

☐ I authorize the American University of Beirut, **three years after the date of submitting my thesis, dissertation, or project,** to: (a) reproduce hard or electronic copies of it; (b) include such copies in the archives and digital repositories of the University; and (c) make freely available such copies to third parties for research or educational purposes.

_____

Signature   Date

ACKNOWLEDGEMENT

First of all, I would like to convey my warmest gratitude to my supervisor Dr. Marwan Refaat, who gave me the opportunity to conduct my study and my co-advisor Dr. Diana Jaalouk for their guidance, generous contribution of knowledge and experience, valuable comments and encouragement from the start until the end of my study. I could not have imagined having better advisors for my Master's study. Dr. Jaalouk welcomed me to her laboratory and guided me throughout my MSc thesis pursuit. She has been such a great inspiration and a role model to look up to. I'm deeply grateful for all the training, advice, enthusiasm, patience, and time she has invested in me. I owe a great deal of the progress I have achieved throughout my graduate study to her. Thank you for mentoring me and touching me on the personal level where you were always available for support and advice to help me realize the real essence of life.

Besides my advisors, I would like to thank the rest other members of my thesis committee: Prof. Georges Nemer and Dr. Firas Kobaissy for agreeing to serve on my thesis committee despite their busy schedules. I am sincerely grateful for their encouragement and insightful comments.

I am also very much grateful to the DJ lab members: Dima Diab El Harakeh, Hind Zahr, Ingrid Younes, and Sara Assi. I am fully indebted to Dima Diab el Harakeh for being a great friend and an amazing laboratory partner. I'm grateful to her not only for her help in acquisition of the confocal microscope images and with statistical analysis, but also for always being there to answer my questions and engage with me in critical analysis of my research work. Also, thanks to Hind and Ingrid for their friendship and contributing to my training when I first started laboratory work. I will never forget all the fun times and beautiful memories we shared during the past year. You have made the stressful and difficult times I've passed through much easier to tolerate.

Finally, my most profound gratitude goes to my family, my parents and elder brother, for their unflagging love and unconditional support throughout my life and my studies. This accomplishment would not have been possible without you. Thank you.

AN ABSTRACT OF THE THESIS OF

Dana Sedki   for   Master of Science
                              Major: Biochemistry

Title: Insights into the Deregulations of Rbm20 in Lamin A/C and Emerin Related Cardiomyopathies

Cardiomyopathies are among the leading causes of premature sudden death. Their etiology is genetically heterogeneous with more than 50 genes linked to them. The most substantial mutations involved in the cardiac phenotypes are those affecting the integrity and structure of the nuclear lamina; LMNA gene coding for Lamin A/C, and EMD gene coding for the inner nuclear membrane (INM) protein emerin. Additionally, recent studies identified mutations in the RBM20 gene coding for the intracellular RNA-binding protein as highly implicated in familial cardiomyopathies. We sought to get a better understanding of how Emery-Dreifuss Muscular Dystrophy (EDMD) and Dilated Cardiomyopathy (DCM) originate from deficiency and/or mutations in the LMNA and EMD genes. Accordingly, we aimed to investigate potential deregulations in Rbm20 transcript and protein expression in addition to intracellular localization in the context of Lmna and Emd deficiency. For the purpose of this pilot study, we used mouse embryo fibroblast (MEF) lines that were derived from mice lacking the expression of either Lamin A/C (Lmna-/-) or emerin (Emd-/Y) which have an EDMD phenotype, or mice expressing the Lmna N195K homozygote mutation (LmnaN195K/N195K) which have the DCM phenotype versus wild-type (WT) controls, under baseline conditions. We have also used Lmna null MEFs that were transduced by retroviral infection to re-express the Lmna WT or different mutant forms that result in EDMD (E358K, L530P). Real Time PCR quantification, Western Blot analysis, and immunofluorescence staining were performed on these cell lines to test for alterations in Rbm20 transcript or protein expression and intracellular localization. Rbm20 showed a significant reduction in the transcript levels in all the three mutant MEFs which was reversed upon re-expression of Lmna confirming the direct effect of lamina disruption on the expression of Rbm20. Likewise, the protein expression of Rbm20 was significantly reduced in the mutant cell lines compared to the wildtype, while there was no significant alteration in its intracellular localization. Taken together, our findings highlight the implication of Rbm20 in lamin A/C and emerin related cardiomyopathies. Ongoing work and future directions will focus on investigating the consequential aberrations in Rbm20 – mediated splicing of a number of targets that mediate key signaling pathways altered in these diseases.

CONTENTS

ILLUSTRATIONS

TABLES

ABBREVIATIONS

%	Percent
/	Per
°C	Degrees Celsius
μg	Micro gram
μl	Micro liter
AD-EDMD	Autosomal dominant Emery–Dreifuss muscular dystrophy
APS	Ammonium persulfate
AS	Alternative splicing
BAF	Barrier-of-autointegration factor
BRK	Baby rat kidney
BSA	Bovine serum albumin
CMT2	Charcot-Marie-tooth neuropathy type 2
Cnx	Connexins
Cys	Cysteine
DAPI	4',6-diamidino-2-phenylindole
DCM	Dilated cardiomyopathy
ddH$_2$O	Deionized distilled water
DNA	Deoxyribonucleic acid
ECM	Extracellular matrix
EDMD	Emery–Dreifuss muscular dystrophy
ER	Endoplasmic reticulum
ESCs	Embryonic stem cells
et al.	Et allii (and others)
FBS	Fetal bovine serum

FPLD	Familial partial lipodystrophy
g	Grams
GAPDH	Glyceraldehyde 3-phosphate dehydrogenase
HCM	Hypertrophic cardiomyopathy
HGPS	Hutchinson-gilford progeria syndrome
GWA	Genome-wide association
Ig-fold	Immunoglobulin-like fold
INM	Inner Nuclear Membrane
kDa	Kilo Dalton
LAP2	Lamina-associated protein 2
LBR	Lamin B receptor
LDB3	Lim domain binding 3
LEMD3/MAN1	Lem domain-containing protein 3
LGMD1B	Limb-girdle muscular dystrophy type 1B
LINC	Linker of nucleoskeleton and cytoskeleton complex
MAD	Mandibuloacral dysplasia
MAPK	Mitogen activated protein kinase
MEF	Mouse embryo fibroblast
Mef2a	Monocyte enhancer factor 2
Mg	Milligram
MKL1	Megakaryoblastic leukemia 1
ml	Milliliter
mm	Millimeters
mM	Millimolar
mRNA	Messenger RNA
MyoD	Muscle differentiation marker

NaOH	Sodium hydroxide
NE	Nuclear envelope
NF-κB	Nuclear factor kappa-light-chain-enhancer of activated B cells
NLS	Nuclear localization Signals
Nm	Nanometer
NPC	Nuclear pore complex
Nup	Nucleoporin
ONM	Outer nuclear membrane
PBS	Phosphate buffered Saline
PCNA	Proliferating cell nuclear antigen
PFA	Paraformaldehyde
PGM1	phosphoglucomutase 1
PKA	protein kinase A
PKC	protein kinase C
PLN	Phospholamban
PNS	Perinuclear space
pRb	Retinoblastoma protein
PTGR	Post transcriptional gene regulation
PVDF	Polyvinylidene fluoride
RBM20	RNA binding motif 20
RBP	RNA binding protein
RCM	restrictive Cardiomyopathy
RD	Restricted Dermopathy
RER	rough endoplasmic reticulum
RNA	Ribonucleic Acid

ROS	Reactive oxygen species
RRM	RNA recognition motif
RS	Arginine/serine
RYR2	Ryamodine receptor
SDS	Sodium dodecyl sulfate
SEM	Standard error of the mean
SFC	Splicing factor compartment
SiRNA	Small interfering RNA
snRNA	small nuclear RNAs
snRNPs	small nuclear ribonucleoproteins
SOD2	Superoxide dismutase 2
SREBP1	Sterol response element –binding protein 1
TEMED	Tetramethylethylenedi
TGF-β	Transforming growth factor beta 1 receptor
TMPO	Thymopoietin
Triton® X-100	t-Octylphenoxypolyethoxyethanol,
Tween20	Polyoxyethylene sorbitol ester
V	Volts
WRN	Classical Werner's syndrome
WS	Warner Syndrome
WT	Wild Type
X-EDMD	X-linked Emery-Dreifuss muscular dystrophy
ZMPSTE24	Zinc Metalloprotease related to Ste24

CHAPTER I

LITTERATURE REVIEW

A. Nucleus, Nuclear Structure and Organization

1. Overview

The nucleus, being the largest and most prominent organelle in eukaryotic cells, serves a conserved function of holding the cell's genetic information and controlling the major cellular processes such as growth and reproduction. Eukaryotic cells show a high level of complexity which explains the need for additional means for gene regulation manifested by the presence of a highly regulated double membrane called, the nuclear envelope (NE), nucleoma, or karyotheca. This nuclear envelope is a hallmark that distinguishes eukaryotic cells from those of prokaryotes. It serves to compartmentalize activities and separate the genetic material inside the nucleus from other cellular compartments (Gerace & Benson, 1984). Besides shielding the nuclear heterochromatin, the NE has an evolutionary role allowing for an additional level of gene expression regulation by effectively controlling the rate of mRNA transport in and out of the nucleus for translation in the cytoplasm. Moreover, it is mainly comprised of three morphologically distinct yet interconnected domains: the outer nuclear membrane (ONM), the inner nuclear membrane (INM), and nuclear pore complexes (NPCs) (Stewat & Burke, 2007; Zwerger et al., 2013) (Figure 1). The outermost membrane is a lipid continuation of the endoplasmic

1

reticulum (ER), which explains its enrichment of ER components and its similar protein composition. However, some integral proteins that are necessary for the nuclear positioning are characteristically expressed only on the NE. Both, the outer and the inner nuclear membranes are connected at the periphery of each NPC, and in between them lies a 40-50 nm perinuclear space (PNS) that is contiguous with the lumen of the ER (Burke & Stewart, 2013). The connection between the two membranes is through several points associated with NPCs where molecules are transported into and out of the nucleus. Despite being connected to the ONM, the INM comprises its own distinctive collection of cell type-specific integral membrane proteins. These proteins are responsible for anchoring the nuclear envelope to a protein meshwork known as the lamina.

The nuclear membranes forming the interface between the nucleus and the cytoplasm, along with the nuclear lamina that is tightly connected to the INM, all together work to establish the structure and support for the nucleus to perform its vital functions in DNA replication, ribosomal assembly, and RNA transcription. In the past two decades, the nuclear envelope and its constituents have gained a lot of interest due to the discoveries of several diseases associated with the disruption of its protein constituents.
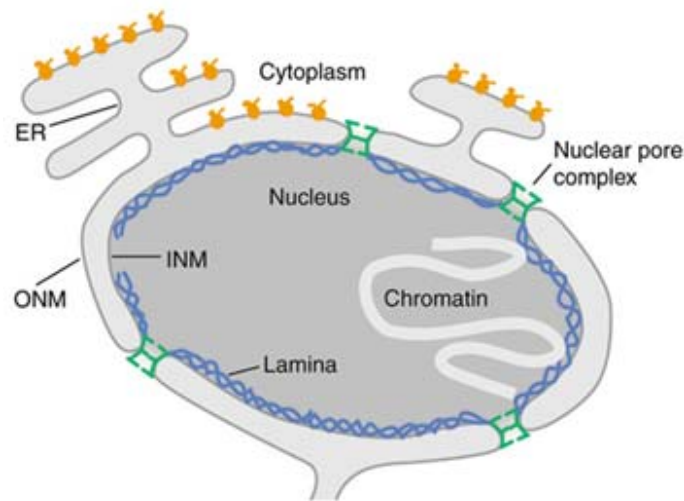
Figure 1 | A schematic of the nuclear envelope major components (Schirmer & Gerace, 2002).

2. *Lamins and the nuclear lamina*

a. <u>Lamin isoforms and expression pattern</u>

Nearly forty nine years ago, Fawcett and his colleagues first identified the nuclear lamina as a durable thin layer of intermediate filaments associated with the nuclear face of the INM of metazoan nuclear envelopes (Fisher & Blobel, 1986; Gerace & Benson, 1984). A decade later, the nuclear lamina was found to be associated with the NPCs and was categorized according to sequence homology, biochemical properties, and cell cycle specific cellular localization into three major components called lamin A, lamin B, and lamin C (Aaronson & Blobel, 1975; Dwyer & Blobel, 1976; Gerace & Blobel, 1978). A type lamins, are encoded by a single gene, *LMNA,* which is located on chromosome 1q21.2 and gives rise to four A-type lamins by alternative splicing: lamin A, lamin C, and the less frequently expressed isoforms, lamin AΔ10 and lamin C2. All four proteins are identical in

their amino acid composition except for their carboxy terminal tails (Burke & Stewart, 2013; Furukawa & Hotta, 1994; Holt & Morris, 2003). In contrast, B-type lamins are sub grouped into three types and are encoded by two distinct genes; *LMNB1* located on chromosome 5q23.3–q31.1 codes for lamin B1, and *LMNB2* located on chromosome 19p13.3 codes for lamin B2 and lamin B3. While A-type lamins are tightly associated with the surface of the chromosomes, B-type lamins remain bound to the INM vesicles during mitosis, thus anchoring the lamina to the nuclear membrane (Aebi & Gerace, 1986; Furukawa & Hotta, 1994).

The expression of A-type lamins is dependent on the state of differentiation of the cell. Generally, lamins A and C are ubiquitously expressed in most somatic cells, but seem to be expressed in diminished levels in undifferentiated cells, early embryos, hematopoietic cells, neuronal cells, and some types of cancers (Worman, 2012; Worman & Courvalin, 2005). On the other hand, B-type lamins are expressed in both embryonic and differentiated cells, except for lamin B3 strictly expressed in the male germ line (Burke & Stewart, 2013; Dittmer & Misteli, 2011). These differences in structure, localization, and expression among the different kinds of lamins are likely attributed to their variant functional roles.

b. <u>Structure and assembly of the nuclear lamins</u>

Similar to the cytoplasmic intermediate filaments, nuclear lamins are primarily comprised of a long central α-helical rod domain flanked by an N terminal head domain and a C terminal tail domain (Figure 2a). However, lamins differ in structure from their

cytoplasmic counterparts with their rod domains comprising additional 42 amino acids, and with their shorter head domains. Moreover, lamins constitute a nuclear localization signal (NLS) at their caboxy –terminus located in close proximity to an immunoglobulin like (Ig – fold) motif. The NLS is essential for the transport of lamins to the nucleus after their synthesis (Dechat et al., 2008; Fisher & Blobel, 1986; Worman, 2012). All lamins, except for lamin C comprise a -CAAX motif (where C is for Cys, an aliphatic residue and X is usually represented by a Met) at their carboxy terminal tail that is responsible for the initiation of post translational processing of lamins soon after their synthesis. A series of enzymatic reactions takes place starting with a farnesylation step, mediated by a farnesyl transferase, which enhances hydrophobic interactions to anchor lamins to the INM (Hutchison & Vaughan, 2001; Young & Michaelis, 2005).

Lamin A is initially synthesized as pre-lamin A. Once it is localized to the nuclear membrane, it undergoes multiple proteolytic cleavage reactions catalyzed by the enzyme ZMPSTE24, to remove the 18 amino acids of the c-terminus, and thus producing the maturelamin A. Conversely, the mature form of lamin B maintains its farnesyl moiety (Gerace & Benson, 1984, Weber & Traub, 1989) (Figure 2b). Lamins are subject to phosphorylation through the action of multiple specific kinases. The three main kinases working on lamins and altering their activities are, the mitotic kinase CDC2, protein kinase C (PKC), and protein kinase A (PKA). CDC2 phosphorylated residues lie within the head and coiled-coil domains of the lamina, explaining its role in their disassembly during mitosis (Peter & Nigg, 1990). PKA phosphorylates the nuclear lamina at sites hindering their ability to polymerize. Furthermore, PKC phosphorylation is important for the

regulation of lamin uptake into the nucleus (Collas & Courvalin, 1997; Molloy & Little, 1992).
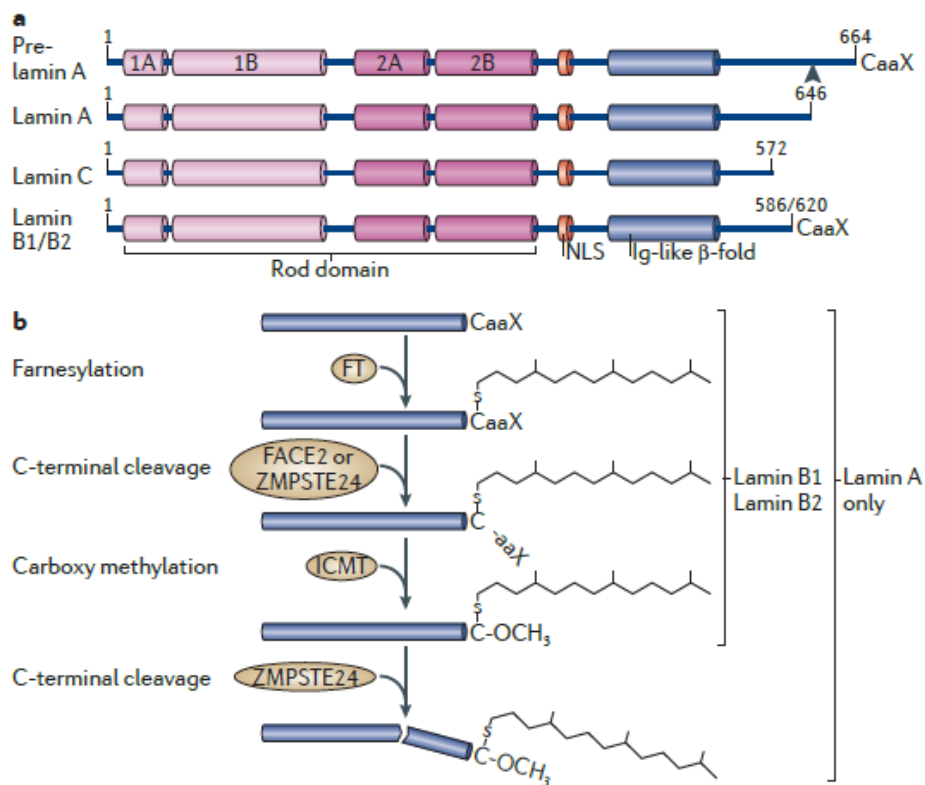
Figure 2 | A schematic representation of the structure and post translational modifications of A-type and B-type lamins (Burke & Stewart, 2013).

In order to establish nuclear envelope stability, lamins self-assemble to generate higher order structures with a coiled-coil dimer as the basic building block. They dimerize using the characteristic coiled-coil heptad repeated pattern in their α-helical rod domain.

The association of lamin filaments is hierarchical; beginning with parallel coiled-coil homodimers subjected to electrostatic interactions between the overlapping ends of their successive coiled-coil domains leading to their association to form the basic building block lamin dimer (McKeon & Caput, 1986) (Figure 3).Subsequently, a lamin polymer is developed through the lateral, antiparallel association of the previously formed head to tail assemblies. Further lateral interactions between two lamin polymers will produce proto-filaments which associate laterally to give rise to the intermediate filaments with an approximately 10nm diameter. Although lamin heteropolymers were able to form filaments *in vitro*, it is still not clear yet whether protein filaments *in vivo* may contain two types of filaments or whether lamins are separated into two distinct filaments (Kapinos et al., 2010; Worman & Courvalin, 2005).

In eukaryotic cells, the nuclear lamina structural integrity is under the cell cycle control. During the mitotic phase, after the chromosomal condensation in prophase, the nuclear envelope disintegrates and the nuclear lamins disassemble. As mentioned earlier, pre-lamin A undergoes proteolytic cleavage reactions to remove the farnesylation moiety, rendering it more soluble throughout the cytoplasm, whereas B-type lamins remain anchored to the INM through their retained farnesylation moiety. Phosphorylation of lamin proteins by PKC occurs before the disintegration of the nuclear envelope in prophase, expediting the disassembly of the lamina from the INM, whereas de-phosphorylation through the action of type 1 protein phosphatase reverses lamina back to the assembled state (McKeon & Caput, 1986; Thompson & Fields, 1997).
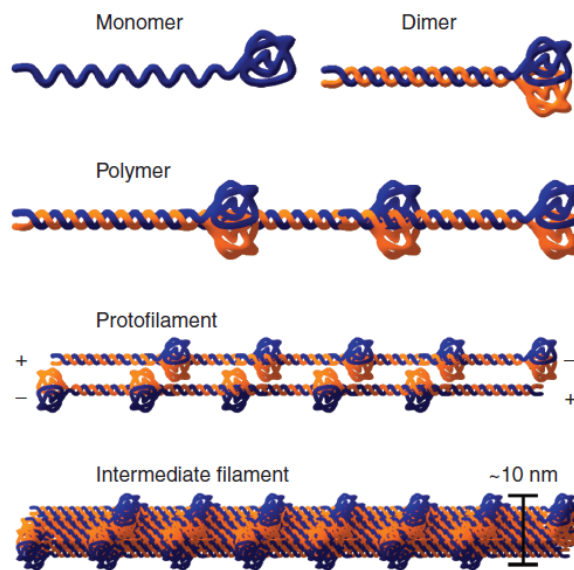
Figure 3 | An illustration of lamins polymerization and assembly. (Dittmer & Misteli, 2011).

c. Functions of lamins

Lamins were first recognized as merely structural proteins with the primary functions of delineating the nuclear morphology and providing mechanical support. This was concluded owing to their insolubility, filament forming properties, and lack of any apparent enzymatic activity (Aebi & Gerace, 1986; Dittmer & Misteli, 2011). However, subsequent studies unveiled the interactions of lamins with a large group of nuclear membrane integral proteins, chromatin, and DNA. Hence, it is now evident that the importance of lamins extends to carry a multitude of functions, ranging from structural support of the nucleus, to facilitating chromatin organization, gene regulation and DNA repair (Dechat & Goldman, 2010).

i. Regulation of nuclear shape and mechanical stability

The intermediate filaments, comprising the most prominent part of the nuclear lamina, are found to play a vital role specifying the nuclear morphology and size, and providing mechanical support to the nucleus. Mouse Embryo Fibroblasts (MEFs), depleted of lamins, assemble a deformed and fragile nuclei compared to those in control wild-type (WT) (Houben & Broers, 2007). This in turn, might explain the malleable and deformable properties of the embryonic stem cells lacking A-type lamins in their nuclear envelope (Pajerowski & Discher, 2007). Lamins mediate the linkage between the nucleus and the cytoskeleton by complexing with INM and ONM associated proteins and binding to cytoskeleton elements, further enhancing nuclear stability (Dittmer & Misteli, 2011) (Figure 4a). In addition, they play a vital role in the physical connection between the nucleus and the cytoskeleton, by virtue of their interactions with SUN proteins and nesprins, to form a protein complex symbolized as "the linker of nucleoskeleton and cytoskeleton complex" (LINC). LINC is required for cell migration, polymerization, and intracellular force transmission (Ho & Lammerding, 2012). Moreover, lamins play an evolutionary role in the assembly of the nucleus following mitosis; proven by the apparent inhibition of nuclear membrane assembly upon depleting lamin's expression in drosophila (Lenz-Bohme et al., 1997).

ii. Regulation of chromatin positioning and gene expression

Lamin A/C and binding partners are able to interact with chromatin, DNA, histones, and transcription factors. During differentiation, nuclear lamina regulates transcription by positioning chromatin to the nuclear envelope either through the direct interaction with chromatin, or indirectly by virtue of chromatin regulatory proteins (Figure 4b). This is supported by the findings that mutations in *LMNA* were shown to cause a disruption in differentiation, mainly in muscle and fat cells, highlighting the importance of an intact nuclear architecture for the differentiation process and regulation of gene expression (Puckelwartz & McNally, 2011). In addition, lamins, along with their associated proteins can sequester heterochromatin transcription factors, diminishing their availability in the nucleus for active transcription. Among these proteins involved in binding chromatin are the INM-localized lamin B receptor (LBR), barrier to autointegration factor (BAF), lamina-associated protein 2 (LAP2), LEM domain-containing protein 3 (LEMD3) also known as MAN1, and emerin (Burke & Stewart, 2013) (Figure 5c). Chromatin binding regions are found either in the lamina tail region or within the rod domain (Dittmer & Misteli, 2011). Interestingly, the nuclear lamina not only contains heterochromatin binding regions pertaining to transcriptional repression, but also other regions which do not associate with heterochromatin, and may even assist in genetic transcription (Peric-Hupkes et al., 2010). In addition, lamins regulate RNA polymerase-II-dependent gene expression. The inhibition of A-type lamins was found to disrupt the RNA polymerase-II transcription and affect the localization of the TATA-binding protein initiation factor (Dittmer & Misteli, 2011). Numerous examples of transcription factors were recognized as binding targets for

lamins or lamin-associated proteins. These include the retinoblastoma protein (pRb),

encoded by *RB*, and responsible for the regulation of S-phase entry and terminal

differentiation. Tethering of this transcriptional regulator to A-type lamins provides

stability, as pRb is subjected to rapid proteasomal degradation in *Lmna*-null mice cells

(Gruenbaum & Wilson, 2005).

iii. DNA replication and repair

Numerous studies support the pivotal role of lamins in regulating DNA replication

process. For instance, immuno depletion of major lamins prior to nuclear assembly in

Xenopus egg interphase extracts resulted in the inhibition of DNA replication. This

involvement of nuclear lamins in maintaining the elongation phase of replication is most

likely linked to its role in providing a support scaffold structure. Indeed, lamin A was found

grossly associated with different sites of early replication in primary fibroblasts, while

lamin B1 is co-localized with the replication factor proliferating cell nuclear antigen

(PCNA) during late S phase in the 3T3 cells (Dechat et al., 2008). Furthermore, recent

studies have shed the light on the importance of lamins in DNA repair. This role was

validated in samples derived from Hutchinson Gilford Progeria Syndrome (HGPS) patients,

who express an altered form of lamin A called, progerin. Whenever DNA damage takes

place, progerin hampers cells from actively recruiting the repair factor P53-binding protein

to the site of damage. Additionally, progerin alters the expression and localization of key

DNA damage regulators and break repair factors (Dittmer & Misteli, 2011). This confirms

11

the need for a normal lamin A function in DNA repair. However, the exact mechanism linking lamins to DNA repair needs to be further deciphered.

iv. Cellular signaling and transcriptional regulation

The nuclear lamina provides a platform for the assembly of protein complexes that are involved in signal transduction pathways (Figure 4d). The interplay between signal transduction pathways and lamins is essential for cellular homeostasis and differentiation. Lamins, by virtue of their interactions with other proteins, influence the availability of various proteins within signaling cascades. This is achieved by various mechanisms such as regulating post-translational modifications and degradation, seizing transcription factors in inactive complexes, and modulating transcriptional complexes. In fact, diseases caused by mutations in the *LMNA* gene are associated with deregulation in important signaling pathways including MAPK, TGF-β, Wnt-β -catenin, and notch pathways (Aebi & Gerace, 1986; Jaalouk & Lammerding, 2009).

A well-established example is the role of A-type lamins in the regulation of SMAD proteins, which mediate signaling cascades downstream of TGF-β. Lamin A inactivates SMADs by direct binding and sequestration to the nuclear envelope, and by interacting with their antagonists (MAN1 and PP2A) and positioning them in close proximity to SMADs. This positioning further dampens SMADs activity by dephosphorylation (Van Berlo et al., 2005). Another example is the AP1 (Jun/Fos) regulation via ERK/MAP kinase signaling. In this case, initial stimulation causes ERK1/2

12

phosphorylation and translocation into the nucleus. Phosphorylated ERK1/2 will then bind

lamin A, resulting in phosphorylation of the associated c-Fos. This releases c-Fos from the

nuclear envelope to dimerize with c-Jun, hence activating AP1 immediate-early genes

(Dittmer & Misteli, 2011).
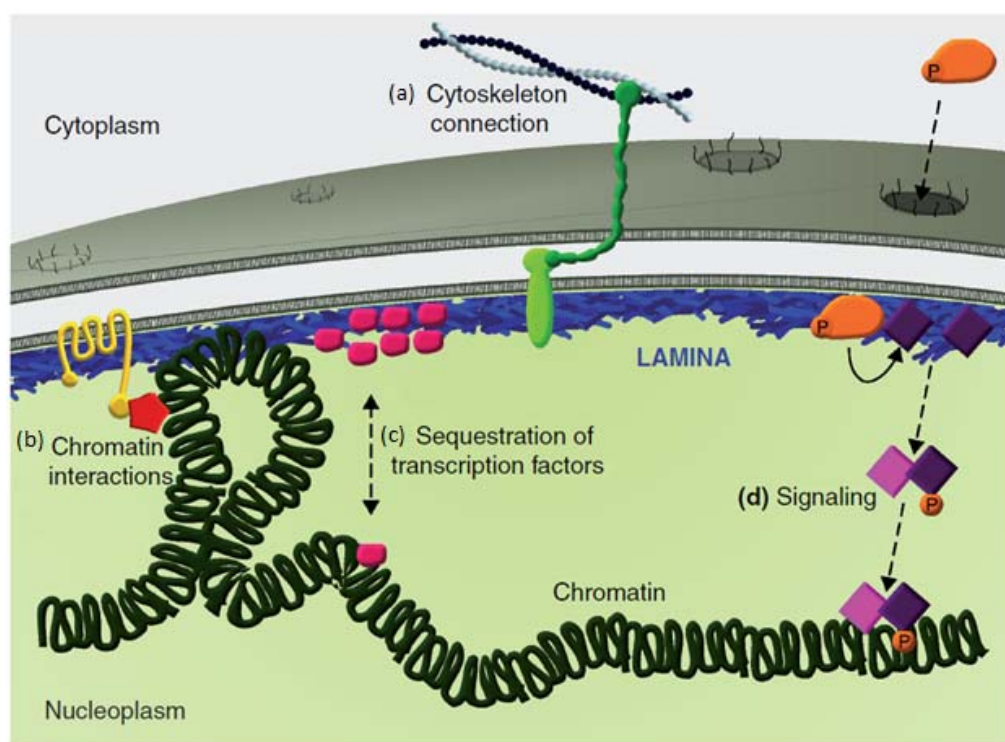
Figure 4 |An illustration of the primary functions of the nuclear lamina. (Edited from Dittmer & Misteli, 2011).

v. Cell cycle regulation**:**

At the onset of mitosis, the nuclear lamina phosphorylates and disassembles from the nuclear envelope to become completely soluble throughout the mitotic phase. As the nuclear lamina depolymerizes, B-type lamins remain attached to the nuclear envelope. In addition, some nucleoporins detach from the NPC in early mitosis to associate with kinetochores including Gle2, Nup107, and Nup358. NPC components which dissociate early in mitosis have an active role in mitotic progression given that the lack of Nup358 results in mitotic defects. This disassembly event is of utmost importance as its absence leads to cell cycle arrest. By the end of mitosis (anaphase, telophase), reassembly of the nuclear envelope and its associated structures takes place. These processes are highly regulated in a sequential manner starting with the cytoskeletal proteins tethering to the chromosomal surface, followed by the assembly of the NE, the formation of the NPCs to actively import the nuclear lamina, and finally the emergence of the nuclear lamina (Margalit & Foisner, 2005).

vi. <u>Apoptosis</u>

Apoptosis, also known as programmed cell death is an intrinsic property distinguishable for metazoan cells. It occurs normally during development or as a result of cellular stress signals (Lincz, 1998). The apoptotic process is defined by a series of morphological changes such as, nuclear membrane blebbing, chromatin condensation and detachment from the NE, DNA fragmentation, and the formation of apoptotic bodies. These changes eventually lead to the loss of both the structure and function of the nucleus. The

main players involved in the execution of apoptosis are cysteine proteases known as the caspase proteins. These are targeted by the nuclear lamina along with INM integral proteins and NPCs (Earnshaw, 1995). Indeed, lamins contain caspase recognition sequences, and their cleavage in vertebral cells is critical for the apoptotic process (Ruchaud et al., 2002). When this cleavage is inhibited in baby rat kidney (BRK) tissue culture cells, a significant delay in the onset of early apoptotic marks, but not the final stages of apoptosis, was observed (Gruenbaum & Wilson, 2005).

3. *Lamins and oxidative stress*

Reactive oxygen species (ROS) are natural by-products released by mitochondrial respiration and are normally eliminated by protective means such as the antioxidant defense mechanisms. A moderate increase in the levels of ROS acts to promote cellular proliferation and differentiation. However, under stress, the excess increase in these species damages DNA, proteins, and lipids. This causes defects in proliferation and longevity, eventually leading to cardiovascular and neurodegenerative disorders (Weinberg et al., 2010). Oxidative stress is the state where the production of ROS exceeds their removal. Interestingly, lamins have been shown to have an involvement in oxidative stress, proliferation, and longevity by modulating ROS. In fact, an interdependent relationship exists between lamins and oxidative stress. Oxidative stress alters the expression and the post translational modification of lamins, and conversely, mutations in the *LMNA* gene have been associated with affected oxidative stress responses (Shimi & Goldman, 2014).

Fibroblasts derived from patients harboring different *LMNA* mutations were shown to accumulate pre-lamin A associated with elevated oxidative stress, decreased expression of the mitochondrial respiratory chain proteins, and premature cellular senescence (Caron et al., 2007). These defects are mediated by altered levels of a wide range of antioxidant enzymes and transcription factors including Superoxide dismutase 2 (SOD2), pRb, and Sterol Regulatory Element Binding Protein (SREBP) (Mateos & Blanco, 2013). Further understanding of the mechanism by which lamins control ROS in normal and diseased conditions will offer new biochemical basis for therapeutic strategies.

B. Interactions of Lamins with Emerin and RNA Splicing Factor Compartments

1. *Overview*

The nuclear envelope is known to comprise an array of INM proteins that are in close association with the nuclear lamina. In fact, the nuclear lamins chiefly depend on these proteins for their attachment to the nuclear membrane and for the mediation of many of their functions including, gene regulation, chromatin organization, DNA transcription, RNA splicing, and DNA replication and repair (Osmanagic-Myers & Foisner, 2015; Worman & Courvalin, 2005). To date, eighty INM proteins have been identified. The structure and function of most of these proteins remain poorly characterized. It has been established that these proteins diffuse from their site of synthesis in the rough ER to the nuclear membrane, where they are retained by means of lamina and/or chromatin interactions. However, this diffusion is tightly regulated by nuclear pore complexes which

16

specify the proteins aimed to reach the INM (Worman & Courvalin, 2005). Scientists have

been able to identify and characterize in detail only around a dozen of INM proteins.

Among these are emerin, LBR, LAP1, LAP2, MAN1, and structural proteins; tubulin,

nesprin, actin, and myosin. Additionally, lamins interact with DNA replication centers in

replicating cells during the S phase, and RNA splicing factor speckles during interphase

(Dorner & Foisner, 2007; Melcon et al., 2006; Osmanagic-Myers & Foisner, 2015).

Interestingly, a very recent study was able to identify 130 nuclear proteins associating with

lamin A tail, most of which are novel lamin A interacting partners.These identified proteins

include components of the nucleolus and the nucleoplasm, nuclear speckles, Cajal Body,

nuclear bodies, paraspeckles, ribonucleoprotein and spliceosome complexes (figure 5).

Remarkably, a number of proteins involved in RNA processing and splicing were found to

be significantly enriched. Other lamin A binding candidates were associated with RNA

transport, processing, and translation (Depreux et al., 2015).

Several examples of how integral INM proteins help in establishing lamina

function have been reported. For instance, the interaction between lamins and the nuclear

envelope proteins (KASH and SUN) is essential for linking the cytoskeleton to the nucleus,

contributing in this manner to the maintenance of nuclear and chromatin arrangement

(Dechat & Goldman, 2010; Goldman & Shumaker, 2005). Another example is the

regulation of numerous signaling pathways represented by lamina interacting partners such

as the retinoblastoma protein (pRb), ERK1/2, cFOS, SREBP1 (Zwerger & Lammerding,

2011).
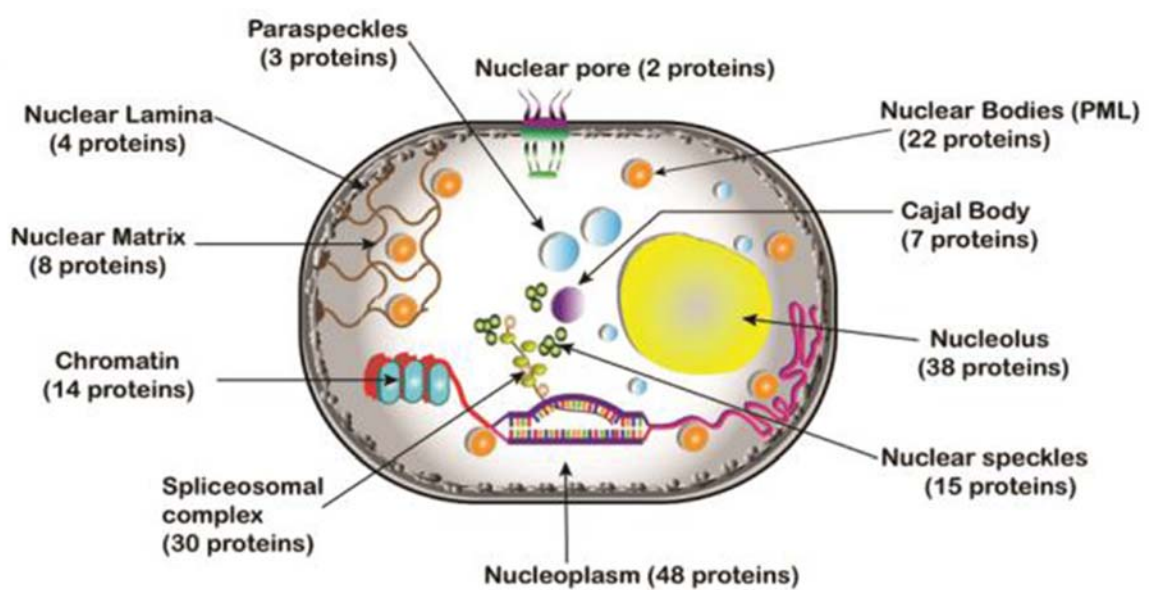
Figure 5 |A schematic representation for 130 proteins identified to bind the lamin A tail. (Depreux et al., 2015).

2. *Emerin*

a. Overview

Nearly two decades ago, Toniolo et al. identified *EMD* as the gene mutated in X-linked Emery-Dreifuss muscular dystrophy (X-EDMD). This gene was located in the X chromosome and codes for a 254 amino acid protein which they named emerin in honor of professor Emery (Bione et al., 1994). Soon after, emerin was identified as a nuclear

18

envelope protein, absent in the majority of subjects with X-linked EDMD. It constitutes a nucleoplasmic amino terminal domain, an individual transmembrane segment and a short luminal tail spanning the perinuclear space. Emerin is a member of the LEM domain family of nuclear proteins which constitutes a LEM binding domain located close to its amino terminus (Worman & Courvalin, 2005). Other members of this family include LAP2 and MAN1. LEM domains work to bind emerin to the BAF protein responsible for DNA bridging and anchoring of emerin to lamins A and C. Another functional domain is located in the central region and binds emerin to lamin A (Lee & Wilson, 2001). It is worth noting that lamin A/C is required for the proper localization of emerin. Indeed, *Lmna*^{-/-} and *Lmna*[N195K/N195K] MEFs yielded a more mobile and differentially localized emerin when compared to wild-type cells (Ho & Lammerding, 2012). Several lines of evidence confirm that the INM protein emerin interacts and associates with lamins at sites mapped to their tail domain that are specifically mutated in EDMD (Hutchison & Vaughan, 2001). Despite all the efforts made, many of emerin's protein-protein interactions and their significance in disease pathogenesis remain incompletely understood.

b. <u>Role of emerin and lamin A/C in skeletal muscle cells differentiation and disease</u>

Mutations in *LMNA* or *EMD* may lead to cardiac specific disorders, autosomal dominant EDMD (AD-EDMD) and X-linked EDMD (X_EDMD) respectively (Bione et al., 1994). The tissue specificity of diseases caused by mutations in the ubiquitously distributed *LMNA* and the X-linked *EMD* genes suggests their prospected role in tissue-specific gene expression, cellular signaling, and nuclear structure. A possible explanation

for the development of *LMNA* related dilated cardiomyopathies (DCM and EDMD) is the involvement of lamin A/C and emerin in the differentiation of muscle cells, resulting in a diminished expression of genes important for differentiation. This possibility emerged with the findings that the myoblasts treated with siRNA to reduce either lamin A/C or emerin expression also displayed a dramatically compromised differentiation potential when compared to the WT controls. The reduced levels of lamin A/C and emerin in myoblasts was associated with a reduction in four major differentiation proteins: desmin, myogenic regulatory factor MyoD, M-cadherin, and pRb (Favreau & Buendia, 2004; Frock & Kennedy, 2006; Melcon et al., 2006). These proteins are vital for the differentiation of myogenic precursor cells, termed satellite cell, to skeletal myocytes (Lammerding et al., 2004).

3. *Lamin A/C association with RNA splicing factor compartments*

Splicing factor compartments (SFCs) are dynamic nuclear compartments important for the storage and positioning of RNA splicing factors (Misteli & Spector, 1997). Transcription and pre-mRNA splicing are highly dependent on the SFC recruitment of splicing factors upon gene activation. Noteworthy is the close association of lamin A/C speckles with SFCs, co-localizing with 90% of RNA splicing factors. A study done by Kumaran and colleagues supports this statement with their findings that upon transcriptional inhibition, lamin A/C speckles along with RNA splicing factors rearrange and form large foci. This rearrangement was rapidly reversed by the removal of transcription inhibition, confirming the direct association between lamin A/C and the

organization of RNA splicing factors. Thus, there is a high necessity for proper nuclear architecture in pre-mRNA splicing and transcription organization (Kumaran & Parnaik, 2002).Additional examples for the redistribution of lamin speckles is noted during muscle differentiation. These direct association of lamins with DNA replication centers during S phase is an example of the cell cycle-dependent changes in the organization of nuclear lamina.

As mentioned earlier, in a recent study, 130 lamin A interacting partners have been identified. Of these, only 17 were previously recognized to interact with lamin A such as, BAF, emerin, LBR, Trim 28, and titin. Additionally, 30 proteins associated with RNA splicing in the spliceosomal complex were found to be significantly enriched. Matrin-3, a 125 KDa nucleoplasmic protein (847 aa), encoded by the *MATR3* gene, was further assessed and confirmed as a lamin A binding partner in C2C12 cells (Depreux et al., 2015). It is worth mentioning that mutations in the *MATR3* were found to be associated with inherited cardiovascular myopathy (Senderek et al., 2009), and that the splicing protein; RNA binding motif 20 (RBM20) is an important analog for this gene (http://www.genecards.org). RBM20 will be further discussed in more detail later in the text.

C. Laminopathies

1. Overview

The importance of the nuclear envelope and its associated proteins in both physiological and pathological states was emphasized by the discoveries of a group of

heritable disorders called "nuclear envelopathies". Although mutations in the genes encoding for the lamin associated proteins; emerin, MAN1, and LBR account for a number of these diseases, the majority result from mutation in the most mutated gene known to date; *LMNA*, with over than 400 discovered mutations linked to a variety of diseases termed "laminopathies". The first disease found to be caused by a mutation in the *LMNA* gene was the autosomal dominant Emery-Dreifuss muscular dystrophy. Since then, geneticists have discovered other *LMNA* mutations that are associated with a dozen of inherited sporadic diseases. Different missense mutations in the *LMNA* gene in different localizations are linked to distinct diseases (Worman, 2012) (Figure 6).This provides evidence that the "one gene-one disease" theory, previously assumed in early studies, is incorrect.

Laminopathies have variable clinical phenotypes and can broadly be categorized into 4 distinct groups with some overlap between them: (1) Skeletal muscle myopathies, (2) lipodystrophy syndromes, (3) peripheral neuropathy, and (4) accelerated aging disorders (Somech & Simon, 2005, Zaremba-Czogalla & Rzepecki, 2011).The fact that the *LMNA* geneis ubiquitously distributed in all cell types raises the enigma of how various mutations in one ubiquitously expressed gene lead to such a wide range of tissue-specific pathologies. Scientists proposed two mechanisms for these tissue-specific laminopathies "the structural hypothesis", and the "gene regulation hypothesis".

2. *Mechanistic insight into laminopathies*
a. <u>The structural hypothesis</u>

Many laminopathies are associated with nuclear structure anomalies such as nuclear blebbing and grossly misshapen nuclei, which may serve as diagnostic markers in these diseases. This suggests that some laminopathies may arise from the disruption and damage of the structurally compromised nucleus resulting from *LMNA* mutations. As it has been established, *LMNA* mutations lead to increased fragility and mechanical stability of the nucleus as evident in *Lmna*$^{-/-}$ mice showing these identical nuclear features. Moreover, loss of A-type lamins and mutations related to EDMD lead to disruption of the nuclear cytoskeleton coupling, causing nuclear movement and localizing impairment, and cytoskeletal organization disturbances (Ho & Lammerding, 2012).

Consequently, this hypothesis may provide a possible explanation for the skeletal and cardiac phenotypes, given the inherent continuous mechanical stress forced on these tissues. This is particularly the case observed in mechanically stressed cells such as striated muscle cells, eventually leading to the progression of various muscular dystrophies (Depreux et al, 2015; Jaalouk & Lammerding, 2009; Lammerding et al., 2004).

b. <u>The gene regulation hypothesis</u>

Different *LMNA* mutations my lead to lipodysrophic phenotypes not correlated to the integrity of the nuclear structure. These disorders may not be explained by the structural hypothesis, suggesting another part of the story. The "gene regulation hypothesis" proposes that other factors such as chromatin remodeling, impaired mechanosignaling, and altered interactions with tissue-specific transcription factors are major contributors to the disease

23

pathogenesis (Jaalouk & Lammerding, 2009; Lattanzi et al., 2011). For example, lamina's role in chromatin organization and subsequent transcriptional regulation explains the pathogenesis underlying HGPS where the detachment of heterochromatin and the miss-localization of nuclear pore complexes lead to impaired mRNA and protein trafficking (Dechat et al., 2008). Moreover, Lamins A/C bind transcription factors and RNA splicing factors, the alteration of which may lead to catastrophic physiological defects. For example, mutations in C terminal domain of *LMNA,* where BAF and SREBP1 bind, lead to the development of a lipodystrophic disease. BAF is important for cell division and ensures the proper localization and binding of emerin to lamin A, whereas SREBP1 is important for fatty acid synthesis and adipogenesis (Capell & Collins, 2006). This theory also explains how laminopathies often associate with a deregulation in important signaling pathways, particularly in the EDMD case associated with an upregulation in MAPK, ERK1/2 and JNK signaling (Muchir & Worman, 2007). In 2004, Lammerding et al, inspected *Lmna* deficient MEFs under stress and found that they have distorted nuclei, defective mechanotransduction, weakened strain-induced signaling, and decreased viability (Lammerding et al., 2004). Accordingly, the partitioning of the two hypotheses explaining the tissue specificity associated with laminopathies may be artificial.

3. ***Laminopathies affecting striated muscles***

a. <u>Emery-Dreifuss muscular dystrophy</u>

Emery-Dreifuss muscular dystrophy (EDMD) was first identified over 35 years ago. Years later, this disease was linked to the *EMD* gene on the X chromosome encoding for emerin, thereby captivating researchers attention who were later able to report around 70 different mutations in *EMD*, most of which result in an absolute deletion or delocalization of emerin in cardiac cells (Ellis, 2006). The manifestations of this disease originate particularly from the exerted effect on muscle cells at the subcellular level resulting ultimately in the loss of muscle cell integrity. Symptoms of EDMD include, early contractures of elbows, Achilles tendon, and slow progressive muscle wasting of the upper arms and the lower legs. The progression of this disease will ultimately lead to DCM with irregularities in the conduction system resulting in a high risk of cardiac arrest (Capell & Collins, 2006; Worman, 2012). Interestingly, EDMD is also caused by *LMNA* mutations. In fact, it was the first discovered human disease coinciding with mutations in the *LMNA* gene, which lead to the discovery that mutations in this gene may result in genetic disorders. This served as a platform for the finding of variant different inherited laminopathies (Bonne & Quijano, 2013; Worman & Wang, 2010). To date, around a hundred *LMNA* mutations have been reported in EDMD which accounts for almost 64% of *LMNA* mutations (Figure 6).In contrast to *EMD* mutations, those of the *LMNA* gene are normally autosomal dominant missense mutations with only few recessive reported cases. Furthermore, AD-EDMD patients present with more severe clinical disease phenotypes than X-EDMD patients, and the consequential cardiomyopathy arising from A-EDMD is of greater severity than X-EDMD patients.

b. <u>Dilated cardiomyopathy</u>

Dilated cardiomyopathy (DCM) is a heart disorder characterized by a dilation of the chambers of the heart with a thinning of the ventricular walls. One third of all DCM cases are of heritable origin, and mutations in the *LMNA* gene account for 6% of DCM cases. A study exclusive for familial DCM patients actually found 33% to have *LMNA* mutations (Arbustini et al., 2002). *LMNA* related cardiomyopathies are generally inherited in an autosomal dominant fashion. They usually present at early-mid adulthood, and are very aggressive, mostly resulting in premature death (Lu & Worman, 2011). By the age of 60, more than half of *LMNA* associated DCM patients die of cardiovascular arrest compared to 11% of DCM patients without *LMNA* mutations. Moreover, mutations in *LMNA* gene associated with DCM account for 18% of all *LMNA* mutations, and are found along the rod and tail domains of lamins A/C in all exons excluding exons 2 and 12, specifically in the protein coding region (Taylor et al., 2003) (Figure 6). One of these mutations, which alters highly conserved regions of *LMNA*, is the N195K missense mutation. Scientists have created a mouse model homozygous for *Lmna-N195K,* by homologous recombination in order to understand the mechanistic correlation between mutation in the nuclear lamin protein lamin A/C and the consequential cardiac phenotype. This mouse model displayed defects in the conduction system and developed DCM by 9 weeks of age. The conduction defects are believed to be outcomes for the disruption of gap junction proteins; connexins (Cnx) that are responsible for impulse conduction throughout the myocardium. Furthermore, The HF1b/Sp4 transcription factor is also deregulated in the hearts of these mice emphasizing the role of the nuclear lamina in regulating expression

patterns for genes that are important in tissue specific development (Mounkes & Stewart, 2005). The pathogenesis and the other genes involved in the development of DCM will be elaborated further later in the text.

c. Limb girdle muscular dystrophy

Limb girdle muscular dystrophy type 1B (LGMD1B) is dominantly inherited and chiefly characterized by progressive limb girdle weakness that usually affects the pelvic girdle before reaching to the humeral muscles. In the year 2000, LGMD1B was linked to mutations in A-type lamins with at least 6 mutations identified in patients suffering from this disease. Moreover, LGMD1B and EDMD-AD were discovered to be allelic, and it is now evident that both disorders may result from the same mutation (Rankin & Ellard, 2006). It is believed that mutations in the *LMNA* gene that cause LGMD1B impair lamin protein function leading to a fragile, easily damaged nucleus, and dysregulated gene expression affecting various cellular activities.

4. Laminopathies affecting the adipose tissue

a. Dunnigan-type familial partial lipodystrophy

Dunnigan-type familial partial lipodystrophy (FPLD) is a rare hereditary autosomal dominant disorder characterized by complete or partial loss of adipose tissue specifically from the trunk, limbs and buttocks and accumulation of fat in the face, neck, axillary and pelvic regions. It is often found to be associated with metabolic disturbances

including: diabetes mellitus, insulin resistance, liver steatosis and dyslipidemia (Jackson & Trembath, 1997; Shackleton et al., 2000). Like other laminopathies, FPLD is also caused by mutations in the *LMNA* gene. Generally, these mutations are amino acid substitution mutations that cluster only in exons 8 and 11 of *LMNA* gene and modify the surface charge, but not the overall structure of the Ig-like fold at tail domains of A-type lamins. Conversely, *LMNA* mutations at the same region which result in striated muscle disease yield a disruptive tertiary structure of this same fold (fig 6) (Cao & Hegele1, 2002; Lu & Worman, 2011; Vantyghem et al., 2004). The most frequent *LMNA* mutation linked to 85% of FPLD cases is a heterozygous R482Q substitution mutation. Interestingly, this mutation disturbs the interaction between the adipogenic transcription factor SREBP-1 and DNA suggesting the necessity of intact lamin A/C for lipid regulation. Lipodystrophy patients are subjects for developing insulin resistance, diabetes mellitus, hepatic steatosis and dyslipidemia. The mechanisms for the development of these metabolic complications are yet unclear and further studies must be performed (Garg, 2004; Wiltshire & Brownell, 2013).
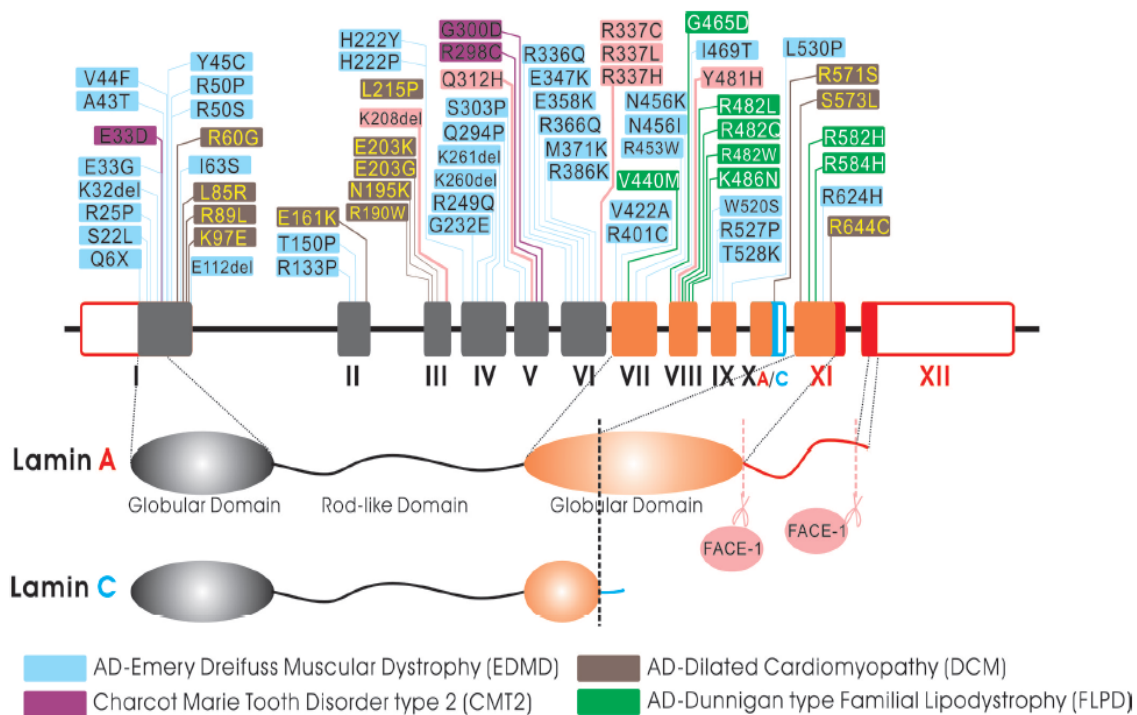
Figure 6 |Sequence localization of *LMNA* missense mutations causing different laminopathies. The resulting diseases are shown in the bottom by color code. (Liu & Zhou, 2008)

b. Mandibuloaclar dysplasia

Mandibuloacral dysplasia is rare autosomal recessive disorder that mainly arises by mutations in the *LMNA* gene. Characteristic signs and symptoms of this disease include bone abnormalities, growth retardation, patchy skin coloring, and loss of subcutaneous fatty tissue predominantly in the limbs owing to its fixation frequent association with partial lipodystrophy and insulin resistance (Al-Haggar et al., 2012). Indeed, at least four distinct *LMNA* mutations are causative for mandibuloacraldysplasia with type A lipodystrophy (MADA). The most common mutation substitutes the arginine with a histidine at 527 position; (527H). It is speculated that *LMNA* gene mutations alter the structure of lamin A and/or lamin C protein and affect their interaction with other inner nuclear membrane proteins, and thus disrupting the nuclear envelope stability. However, the exact mechanism for the development of the signs of symptoms of MADA are still not known (Al-Haggar et al., 2012; Novelli et al., 2002).

5. *Laminopathies affecting the peripheral nervous system*

a. <u>Charcot-Marie-Tooth neuropathy type 2</u>

Charcot-Marie-Tooth neuropathy (CMT) is recessively inherited disorder and represents one of the most common congenital disorders of the peripheral nervous system approximately affecting 1 in 2500 people (Krajewski et al., 2000). The neuropathy features of CMT2 include, damage of the peripheral nerves, atrophy of the muscles, loss of sensation, and foot deformities (hammer toe). At least one homozygous *LMNA* missense mutation, R298C, has been linked to Charcot-Marie-Tooth disease known as type 2B1 (CMT2). The *LMNA* gene mutation is thought to affect the function of the peripheral neurons leading eventually to their degeneration and communication damage (Azzedine & Chrast, 2012; De Sandre-Giovannoli et al., 2002).

6. *Laminopathies producing accelerated aging disorders*

a. <u>Hutchinson-Gilford Progeria Syndrome</u>

Hutchinson-Gilford Progeria syndrome (HGPS) exhibits the most dramatic phenotype among all diseases caused by *LMNA* mutations. It is a sporadic, heritable disorder, wherein features of premature aging manifest at early childhood. Its incident is very rare since carriers generally do not survive enough to reproduce. HGPS is a multi-system disorder affecting the overall growth, and the skin, fat, skeleton, and cardiovascular tissues. Children affected with this disease often display distinctive facial features of protruding ears, wrinkled skin, thin lips, protruding eyes, hair loss, inadequate joint

mobility, vertical midline groove in their chin and severe premature atherosclerosis. Inevitably, these patients die at an early age, often as a result of cardiac or cerebrovascular disease development (Liu et al., 2011; Sarkar & Shinton, 2001). It has been found that HGPS originates by mutations in lamin A. Sequencing of *LMNA* revealed that in 20 HGPS cases, 18 harbored an identical, *de novo*, single-base substitution mutation within exon 6 of GGC by GGT which results in the creation of a cryptic splice site within exon 1, producing an mRNA which encodes a truncated pre-lamin A lacking 50 amino acids of its carboxy terminus termed, progerin. This abnormal prelamin A retains its C-terminal domain in its farnesylated state, thus preventing the normal processing of lamin A. The incorporation of progerin into the nuclear lamina disrupts the structure of the nuclear envelope, and the accumulation of this protein will inevitably yield a dysfunctional nucleus that will eventually lead the cells to their fatal destiny (Mattout & Gruenbaum, 2006; Prokocimer & Gruenbaum, 2013).

b. Atypical Werner Syndrome

Werner syndrome (WS), also termed "adult progeria", is an autosomal recessive, rare disorder with an incidence rate of around 1 in 100,000 live births. Unlike HGPS patients, those of WS grow normally until puberty, but share similar characteristics of premature aging, growth retardation, alopecia, skin atrophy, atherosclerosis, and many anomalies. Moreover, they both have a high tendency for developing fatal cardiovascular diseases (Hasty & Vijg, 2003). Typically, WS arises from mutations in the *WRN* gene belonging to *RECQ* family of DNA helicases. Nonetheless, some cases were not associated

with and *WRN* mutations and were thus termed as atypical Werner's syndrome. These cases were attributed to *LMNA* missense mutations (Chen et al., 2003; Hisama & Oshima, 2012).

c. Restrictive dermopathy

Restrictive dermopathy (RD), also known as tight skin contracture syndrome, is an autosomal recessive, lethal disorder that possesses the distinctive characteristics of tight, translucent, erosive skin, sparse eyelashes, facial dimorphism, superficial vessels, and multiple joint ankyloses. Infants born with this disease often die within the first week after birth. Two mechanisms have been proposed for the origination of RD. First, a recessive mutation in the gene *ZMPSTE24* coding for the protein responsible for post translational cleaving of the farnesylated pre-lamin A (progerin) to yield the mature lamin. The second mechanism manifests in a direct mutation in the *LMNA* gene. Consequently, prelamin A accumulates in the nuclei instead of the mature lamin A isoform. RD shows similar pathophysiology to HGPS where the last lamin processing step is also hindered (Smigiel et al., 2010).

D. Dilated Cardiomyopathy

1. Overview

Despite all the medical advances, cardiomyopathies still rank as one of the leading causes of premature sudden death. They are the most prevalent form of genetic cardiac muscle diseases affecting approximately 0.5% of the general population with a linkage to over than 50 genes. Generally, they are divided into 5 different types with the dilated

cardiomyopathy (DCM) and hypertrophic cardiomyopathy (HCM) having the highest occurrence rate. Other cardiomyopathies include, the restrictive (RCM), arrhythmogenic right ventricular dysplasia, and non-compaction or hypertrabeculated cardiomyopathy (Arbustiniet al., 2014; report of the WHO/ISFC, 1980). All types share a characteristic pathology in the heart muscle rendering the heart incapable of adequately supplying the needs of the body, leading eventually to irregularities in heart rhythm (arrhythmias) and cardiac arrest. Idiopathic Dilatd Cardiomyopathy (DCM) is the most common form of cardiac muscle dysfunction. It is characterized by thinning of the walls of the heart chambers, dilation of the left ventricle, arrhythmias, and defective systolic function. In an attempt to compensate for myocytes loss and decreased heart conductive output, cardiomyocytes become hypertrophized. This in turn will increase the stress load on muscles cells, leading to their death and further increasing the conductive and contractile stress on the other remaining cells. Initially, patients may present as asymptomatic but develop orthopnea, exertional dyspnea, and left ventricle failure. Presenting features of this disease include arrhythmia, and mitral regurgitation, ultimately progressing to arrhythmic cardiac death (De Maria & Cappelli, 2015).

Numerous pathological mechanisms underlie DCM, including ischemia, autoimmune diseases, infections, toxins, drugs, and nutritional deficiency. Nevertheless, a heritable component is appreciated, given that one third of DCM cases are of familial origin. Genetic sequencing and screening have unraveled a big part of the genetic basis for hereditary cardiomyopathies. However, startling complexity has emerged, especially in DCM, conveying a large number of mutations linked to it. Moreover, cardiomyopathies are

beyond monogenic, meaning that multiple interactions rather than single gene mutations, contribute quantitatively to the phenotype (Cahill & Watkins, 2013). The exact molecular mechanisms underlying the disease are still in question, and many efforts and studies are pursued to screen for specific mutations related to this disease (Ku & Familial Cardiomyopathy Registry, 2013). Typically, inheritance pattern in DCM is autosomal dominant reported in 35% of heritable DCM cases, however, some cases of X-linked and autosomal –recessive transmission have been noted in many familial DCM patients.

2. *Genetics of dilated cardiomyopathy*

To date, genetic screening and genome-wide association studies (GWA) have led to the identification of a long list of around 42 involved genes (Figure 7). Most of these genes are related to the structure of the nuclear envelope (*LMNA* and *EMD* coding for lamin A/C and emerin respectively), the sarcomere (*TTN* coding for titin), and the cytoskeleton (*TNNT2,* and *MYH7* coding for cardiac troponin T, and β-myosin heavy chain respectively) (Arbustini et al., 2014; Parvari & Levitas, 2012). *TTN* gene, encoding for titin elastic muscle protein, is the most commonly mutated gene in DCM with a 25% occurrence rate among familial DCM cases and 18% in sporadic cases (De maria & Cappelli, 2015;Linke & Bucker, 2012). Relevant to our study, a novel mutation correlated with familial DCM was found to affect the function of the RNA binding motif protein 20 (RBM20). The major role of RBM20 is the alternative splicing of titin. This role provides a mechanistic explanation for the DCM phenotype observed with *RBM20* mutations (Linke & Bucker, 2012). Yet, the bio-functional relevance of RBM20 in cardiomyopathies is still

not fully understood, and further research is needed to gain a comprehensive and in depth understanding of its role in the disease initiation and progression. The large number of genes implicated in DCM denotes numerous cellular pathways. Hence, they can be broadly characterized in accordance to their pathophysiological effect and localization within the cell.

Sarcomere genes
MYH7, MYH3, MYL3, MYL2, TPM1, TNNT2, TNNI3, TNNC1, ACTC, PLN, MYBPC3

Z disk
TTN
LBD3
VCL
DES
CSRP3
TTID

Nuclear
TAZ
LMNA
EMD
EYA4
RBM20
SYNE1
TMPO

Mitochondrial
TTR, FRA
COX15, HFE

Cytoskeletal-Membrane Linkers
DMD, SGCG, SGCD, SGCB, SGCA, FKRP
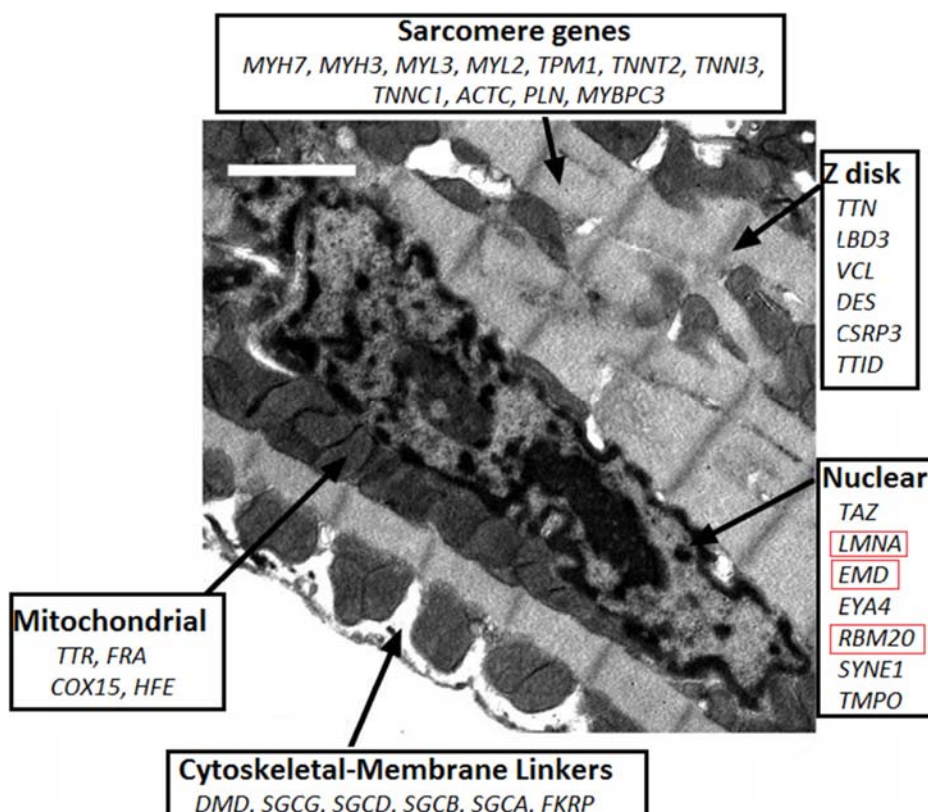
Figure 7 |Some of the genes linked to DCM. (Modified from Dellefave & McNally, 2010)

a. Contractile force generation and regulation

DCM may be caused by mutations in the sarcomere contractile proteins that are important for the generation and regulation of cardiac muscle contraction. The most commonly mutated sarcomeric gene is *MYH7,* coding for β-myosin heavy chain, and comprising 5-10% of familial DCM cases. Other mutations include those affecting the thin filament protein, cardiac actin (*ACTC1) (*Cahill et al., 2013)..

DCM mutations related to the sarcomere typically reduce the sensitivity of myofilaments to calcium ions as a common pathogenic mechanism for the disease (Dellefave & McNally, 2010). Indeed, aberrant intracellular Ca^{2+} homeostasis has been concurrent with DCM cases, and a link between alterations in the Ca^{2+} machinery and cardiomyopathy have been well established (Beraldi et al., 2014; Sheikh et al, 2012). Camk2d and serca2a proteins are important modulators of the Ca2+ machinery, and their elevation has been identified as a pathological feature in DCM cases (Beraldi et al., 2014).

One other major regulator of sarcomere contraction is the tropomyocin and troponin complex that is composed of three subunits; T, I, and C. Mutations in all three

subunits have been linked to DCM and are associated with reduced calcium sensitivity (Morimoto et al., 2002). In addition, mutations in phospholamban (*PLN*), a small phosphoprotein which modulates the calcium uptake by the sarcoplasmic reticulum, may cause autosomal dominant DCM (Cahill et al., 2013).

b. <u>Contractile force transduction and mechanosensing</u>

Force transduction along the sarcomere, cytoskeleton, and extracellular matrix (ECM) is vital for proper cardiac contraction. Several proteins involved in mechanosensing and force transduction were found to be linked to DCM. Examples of those are; titin, dystrophin, and desmin (Cahill et al., 2013).

Mutations in the *TTN* gene account for most of the heritable cases of DCM. In fact, *TTN* mutations were linked to a number of skeletal muscle titinopathies including, LGMD, hereditary myopathy, and tibial muscular dystrophy (Evila et al., 2014). The *TTN*-associated cardiomyopathy phenotype develops as a result of the expression of a truncated splice variant of *TTN*. RBM20 is the protein responsible for the proper splicing of *TTN*. Hence, mutations in *RBM20* have also been associated with the disease. A more in depth description for the alteration in *TTN* splicing and its contribution to the disease phenotypewill be provided later in the text.

Another gene related to cardiac force transduction is *DMD,* coding for dystrophin. Dystrophin is a big cytoskeletal protein that links the sarcolemma membrane proteins and the extracellular matrix, to stabilize the plasma membrane of the heart and skeletal muscles. Indeed, *DMD*, was the first reported DCM disease gene. Cardiac disorders caused by *DMD*

mutations are characterized by skeletal muscle weakness, and comprise the X-linked DCM and Duchenne and Becker muscular dystrophies (Guo & Fang, 2014).

Mutation in the desmin gene (*DES)* have been rarely reported in DCM. Desmin is an intermediate filament protein found in skeletal and cardiac muscles. It functions mainly to maintain the structure and function of myofibrils, and provide cytoskeletal support by linking Z bands and the plasma membrane. Other diseases associated with *DES* mutations include scapuloperoneal syndrome and myofibrillar myopathy (Cahill & Watkins, 2013).

Other proteins with the involvement of mechanosensing and sarcomeric function modulations have been linked to DCM. Lim domain binding 3 (LDB3) and α-actinin (*ACTC1*) are positioned at the lateral borders of the sarcomere and regulate mechanosensing and mechanotransduction. Irregularities in these proteins have been also suggested to cause DCM (Mohapatra et al., 2003).

c. Nuclear proteins

i. Lamin A/C

One of the most commonly implicated genes in familial DCM is the *LMNA* gene accounting for 5-8% of all DCM cases. As stated earlier, *LMNA* gene encodes for A-type lamin intermediate filament proteins which associate with the inner face of the nuclear lamina to provide structural support to the nucleus and a scaffold for various nuclear proteins. *LMNA* related DCM is clinically distinctive by its association with progressive

conduction disease. It is believed that the manifestations of cardiac disease related to *LMNA* originate principally from the effect on the subcellular level, leading eventually to the loss of muscle cell integrity. The striated muscle phenotype associated with mutations in the *LMNA* gene suggests that disruptions in A-type lamins enhance the cellular sensitivity to mechanical stress, thus leading to the degeneration of these cells due to impaired nuclear integrity and function (Frock & Kennedy, 2006; Worman & Courvalin, 2005). A second possibility is that A-type lamins regulate muscle differentiation by regulating genes that are important for differentiation and/or maintaining a stable differentiated state.

ii. Emerin

The *EMD* gene is located in the X chromosome, and encodes for the nuclear membrane protein, emerin. Mutations in this genes may cause X-linked Emery-Dreifuss muscular dystrophy (EDMD). Typically, patients with X-linked EDMD have skeletal involvement with progressive muscle weakness and contractures, ultimately leading to the development of DCM (Osmanagic-Myers & Foisner, 2015).

d. SR proteins – RBM20

The SR family comprises a number of structurally related proteins with the main function of pre-mRNA alternative splicing to generate proteomic diversity. Kong *et al* demonstrated the association of alternative splicing with cardiac disease. In their study,

they noted that human heart failure is associated with a notable reduction in the efficiency of mRNA splicing (Kong et al., 2010). In support of this, certain viral infections, resulting in the loss of function of splicing inhibition, were also found to cause the development of myocarditis and DCM (vercellotti, 2001). The SR protein family constitutes a numerous protein members, but of specific relevance to our study, is the RBM20 protein in which mutations were found to be associated with 3% of all genetic cases of DCM (Refaat et al., 2012).

E. RNA Binding Motif Protein 20 (RBM20)

1. *Overview*

RNA binding motif (RBM20) is a 134 kDa nuclear phosphoprotein, predominantly expressed in cardiac muscles and to a much lesser extent in the thymus and bone marrow (Guo et al., 2012). It is encoded by the *RBM20* gene located on the long arm of chromosome 10 at position 25.2, encoding a protein consisting of 1277 amino acids. *Rbm20* originating in murine species was found to have 4 different gene transcripts (splice variants), 3 of which encode proteins of 130, 87, and 56 kDa molecular mass (http://asia.ensembl.org). It belongs to the SR family of alternative splicing regulators, functioning to alternatively process specific sites in eukaryotic pre-mRNA segments by cleaving out introns and lysing exons, generating thereby proteomic diversity. It acts as a molecular switch orchestrating isoform transition of target cardiac genes. Typically, RBM20 binds a conserved RNA intronic sequence lying in close proximity to the differentially spliced exons and consequently repressing the splicing activity. Alteration in

40

splicing factors generally results in the production of abnormal gene products leading to the development of genetic diseases (Linke & Bucker, 2012). As such, mutations in *Rbm20* were the first cardiac splicing factors recognized to have an association with the pathogenesis of DCM, comprising 3% of individuals with the disease (Refaat et al., 2012). Specifically, the missense mutation in exon 9 of *RBM20* encoding for the RS region, at the chromosome 10q25, has been recognized as the same locus responsible for the emergence of DCM (Brauch et al., 2009). This mutation was later found to alter the normal splicing of *TTN* sarcomere gene, explaining in part the pathogenesis of *RBM20*-related DCM cases. Interestingly, a recent study on mice embryonic stem cells (mESCs) confirmed the early expression of *Rbm20* during cardiogenesis. As a crucial component of the RNA processing machinery, it is expected that Rbm20 regulates the expression of cardiac genes to ensure structural and morphological integrity of nascent cardiomyocytes. Moreover, the inhibition of *Rbm20* expression in mESCs portrayed an alteration in the expression of early stage cardiac genes, calcium overload, and atypical sarcomeric geometry. These findings establish that the disruption of Rbm20 is an early-onset mechanism of the cardiomyopathy phenotype (Beraldi et al., 2014).

RBM20 has been proposed to interact with a number of proteins previously identified to be associated with cardiomyopathies and heart failure including lamin A/C (http://string-db.org) (table 1). To date, a network of RBM20 interacting proteins has been proposed in that many of its members are responsible for the maintenance of sarcomere structure and function. Yet, none of these proposed partners have been validated to date. This, and the fact that our knowledge about the biological functions of RBM20 is only

limited to its ability to bind RNA, nucleotides, and zinc ions, emphasizes the urgent need to

broaden our scope of understanding of the relationship between RBM20 and DCM

progression.
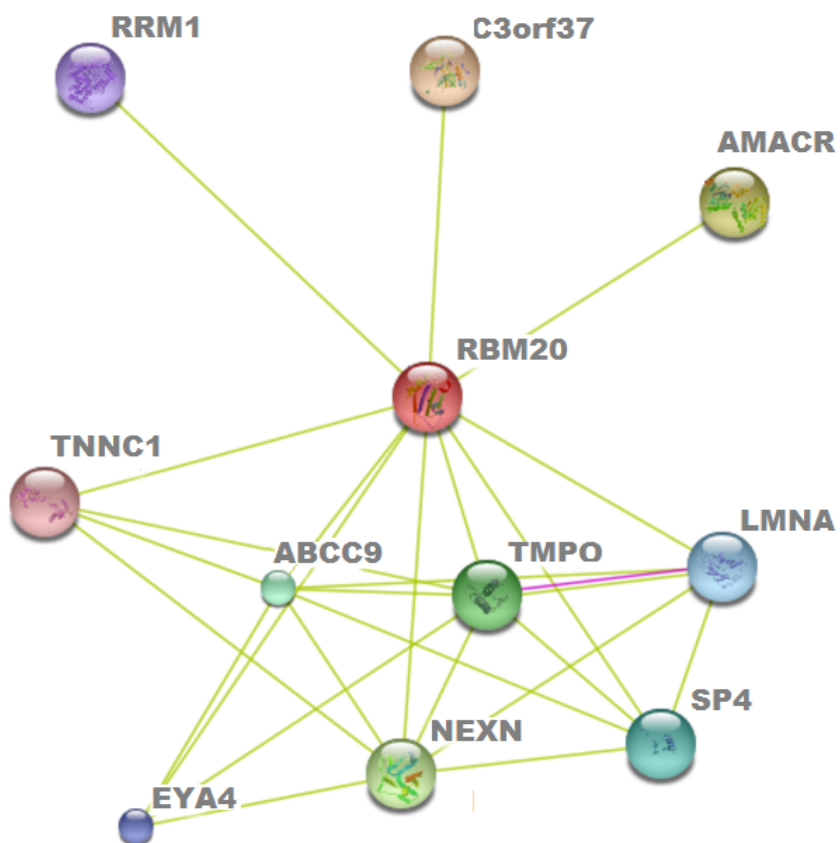
Predicted Functional Partners:

●	C3orf37	UPF0361 protein DC12
●	AMACR	alpha-methylacyl-CoA racemase
●	NEXN	nexilin (F actin binding protein)
●	TMPO	thymopoietin
●	ABCC9	ATP-binding cassette, sub-family C (CFTR/MRP), member 9
●	SP4	Sp4 transcription factor
●	LMNA	lamin A/C
●	EYA4	eyes absent homolog 4
●	RRM1	ribonucleotide reductase M1
●	TNNC1	troponin C type 1

Neighborhood
Gene Fusion
Cooccurrence
Coexpression
Experiments
Databases
Textmining
[Homology]

Table 1 |Predicted functional partners for RBM20 (Edited from http://string-db.org)

2. *Alternative splicing*

Post-transcriptional gene regulation (PTGR) refers to the processes that controls the expression at the RNA level, encompassing RNA maturation, transport, modification, and degradation. The main PTGR events include alternative splicing, mRNA translation, and RNA export. RNA-binding proteins (RBPs) are key players for alternative splicing through their binding with specific mRNA sequences (Gerstberger & Tuschl, 2014).

Alternative splicing (AS), also termed as differential splicing, is a process that complex eukaryotes highly depend on to increase the biodiversity of proteins encoded by one genome. It is a highly regulated phenomenon that takes place during gene expression allowing for a single gene to code for numerous proteins. This process allows for the 21,000 protein-coding genes in humans to be able to synthesize up to 100,000 various proteins (Weeland & Creemers, 2015). AS also allows for the generation of proteins with variant biological properties in terms of protein interactions, or catalytic ability (Kelemen et al., 2013). Interestingly, around 95% of the human genes undergo alternative splicing to generate numerous protein products with different cellular functions and conferring tissue-specific specialized properties (Martonfalvi et al., 2014). The most common method for alternative splicing is exon skipping, wherein specific exons may be introduced or excluded from the final mRNA product. Splicing activators and splicing repressors are the primary regulators for proper alternative splicing through binding on the transcripts cis-binding sites. Since alternative splicing regulates a large number of genes, it is not surprising that aberration in the splicing mechanism is frequently implicated in a number of human genetic diseases and many cancer types (Garcia-Blanco & Lasda, 2004; Tazi & Stamm, 2009).

3. *Alternative splicing mechanism and the SR protein family*

The exons to be retained from the pre-mRNA are primarily determined in the splicing process. The key player for the splicing event is the spliceosome which assembles by the activity of a large number of protein factors along with the U1, U2, U4, U5, and U6 small nuclear RNAs (snRNAs) that are complexed with proteins to small nuclear ribonucleoproteins (snRNPs). At first, the E complex intermediate is formed by means of

44

an ATP independent interaction of U1 and U2 auxiliary factor (U2AF) with the 5′ splice site and the polypirimidine tract respectively. Further ATP hydrolysis of this complex yields the formation of the A complex which provides functional commitment to the specific splice site. Finally, the incorporation and rearrangement of U4, U5, U6 produces B and C complexes responsible for the excision of introns and exons ligation, producing differential RNA products. It was found that RBM20 interacts with U1 and U2, but not U4, U5, and U6 snRNPs, suggesting its predominance in the A complex, but not in the catalytically active B complex of the spliceosome (Maatz et al., 2014). This concludes that the binding of mRNA to RBM20 actually prevents the activation of the spliceosome and represses splicing activity.

Further regulation of splicing events is reliant on intronic and exonic *cis*-acting sequences, flanking the spliced element, which can either endorse or inhibit splicing by inducing the recruitment of the spliceosome to a specific splice site depending on their location. Interestingly, RBPs binding these sequences are expressed in a tissue specific fashion, thus generating tissue specific mRNAs (Wang et al., 2008; Guo et al., 2012).

Genetic screening and fractionation experiments of RBPs led to the discovery of the SR proteinfamily. SR proteins are structurally related proteins, abundantly expressed, with some members manifesting among the most 2% translated genes. Unlike most of the ubiquitously expressed SR-related proteins, RBM20 is predominantly expressed in the striated muscles. Proteins of this family comprise an arginine/serine (RS) rich region, and at least one RNA recognition motif (RRM). The RRM is responsible for the recognition of

specific RNA segments and the RS domain is involved in the interactions of proteins with RNA or other proteins (Wang et al., 2014).Besides regulating alternative pre-mRNA splicing, members of the SR family of proteins are essential for RNA nuclear export, mRNA stability, and protein translation.

The expression of these SR proteins is tightly regulated to maintain proper transcriptome production and to ensure efficient splicing. Over a decade ago, two protein kinases families (SRPK and CLK) were found to phosphorylate the (RS) regions of SR proteins and alter their cellular distribution and activities (Colwill et al., 1996). The phosphorylation state of SR proteins triggers their relocation between the nucleus and the cytoplasm. Initially, proteins of the SR family are phosphorylated to enter the nuclease. In the nucleus, they mediate the spliceosome complex assembly and recruitment to the pre-mRNA by the interactions between the RRM and RS domains with the pre-mRNA and regulatory proteins respectively. Subsequently, de-phosphorylation catalyzes the splicing activity in the nucleus and nuclear export. Successive rephosphorylation is again required for the re-entry to the nucleus where the SR protein can start another cycle of splicing activity (Ghosh & Adams, 2011; Mueller & Hertel, 2011; Zhou & FU, 2013) (Figure 8). According to their orientation, SR proteins can exhibit either activating or inhibiting roles. Splicing repression may be due to the high affinity binding of SR proteins to introns.
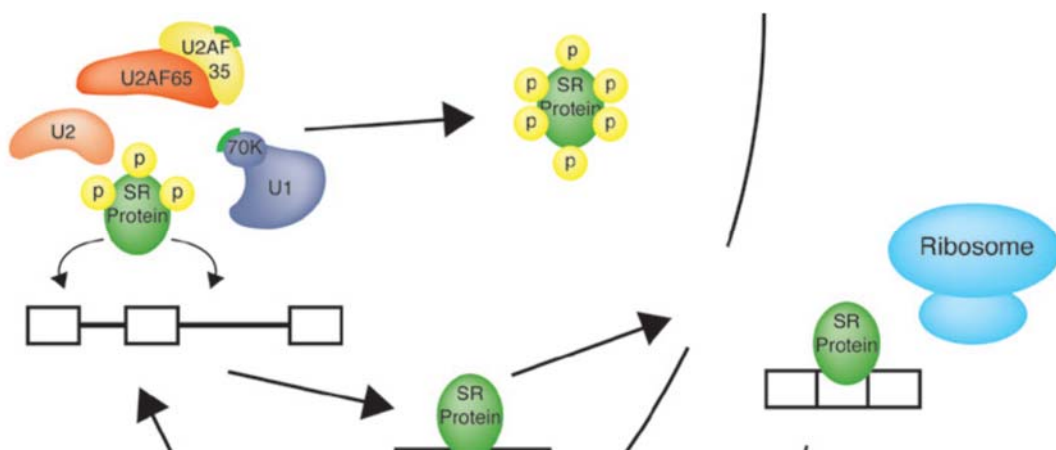
SR proteins:
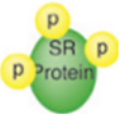
Phosphorylation State	Localization	Function
	Nuclear speckles	● Enter the nucleus to mediate spleceosomal assembly ● Splicing of mRNA
	Exported along with mRNA to cytoplasm	● Adaptor molecules for mRNA export

Figure 8 |A simplified model for the SR protein family phosphorylation and cellular localization. (Amended from Mueller & Hertel, 2011)

4. Alternative splicing in heart failure

During the last decade, much research has been conducted to broaden our understanding of the alternative splicing events and the specific role they play in heart development and disease. Key sarcomeric genes encoding for the basic contractile unit of muscle proteins such as; troponin T, filamin C, β-myosin heavy chain and titin were found to be substrates for alternative splicing. Moreover, during cardiac development, the process

of alternative splicing is intended to adapt to the changes in physiological conditions. For example, the increase in the passive stiffness that is required by the developing heart is achieved by regulating the expression of *TTN* splice variants. Upon stress, the heart reverts to the "fetal gene program" switching isoforms in the sarcomeric proteins, and failing hearts are often found to express differential splice variants (Kalsotra et al., 2008; Weeland & Creemers, 2015).

5. *RBM20 cardiac splicing targets related to DCM*

RBM20 affects multiple gene targets, many of which are involved in DCM pathogenesis. Next generation sequencing on human and rats presented 31 genes that are dependent on RBM20 for their alternative splicing. As expected, RBM20 regulates the alternative splicing of genes in bio-mechanics (*TTN,* and *TPM1)* andion homeostasis (*CAMK2D)* (Guo et al., 2012) (Figure 9). In another study, *Rbm20* knockdown in embryonic bodies (EBs) revealed 49 genes that were differentially spliced, and 21 genes with differential expression. 16 out of the 21 deregulated gene are linked to cardiac diseases including congenital heart diseases and cardiomyopathies (Beraldi et al., 2014).
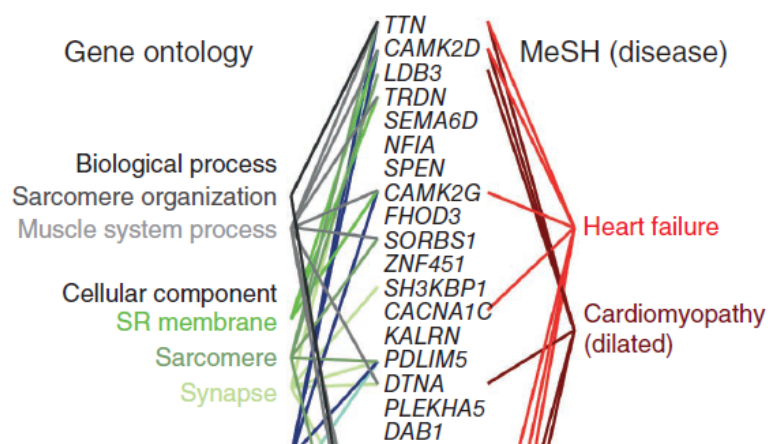
Figure 9 |A conserved set of RBM20 gene targets identified by next-generation sequencing of humans and rats. (Guo et al, 2012).

a. <u>Titin</u>

Titin, the largest protein in the human body, is a 3000 kDa sarcomere protein found in both cardiac and skeletal muscles. It spans half the length of the sarcomere with its amino terminus anchored to the Z disc and its carboxy terminus to the myosin thick filament. The main function of titin manifests in regulating tension, contraction, and sarcomere structural integrity through its action as an elastic molecular spring. It accounts for most of striated muscls passive tension by returning the sarcomere to its normal length after stretch, and repositioning thick and thin filaments (Osmanagic-Myers et al., 2015). Besides its mechanical function, during muscle development, titin works as a scaffold for the assembly of myofibrils and interacts with many structural proteins. Interestingly, the

49

huge 363 exons *TTN* gene is subjected to alternative splicing by RBM20 resulting in two diverse isoforms: the short and stiff, 2.97MDa, adult isoform (N2B), and the long compliant, 3.7MDa, neonatal isoform (N2BA). Stiffer titin isoforms increase their expression after birth to adapt to cardiac function and prevent overfilling of the ventricles during diastole due to the increase in the filling pressure (preload) (Makarenko et al., 2004). Accordingly, it is very important to maintain adequate isoform ratios as the titin-based passive tension regulates the stiffness of myocardial wall throughout ventricular filling.Recent studies confirmed that *TTN* splicing is aberrant in numerous cases of DCM. This stimulated further research into the RNA binding proteins that are associated with the expression of titin isoform. . Guo *et al.* identified a *titin* splice variant producing longer N2BA titin isoforms and developing DCM in rat strains with a deletion mutation of the gene encoding for Rbm20. The expression of this large isoform causes an increase in the titin-based elasticity, which further affects the diastolic function and ultimately leads to fibrosis due to a compensatory upregulation of collagen biosynthesis (Guo et al., 2012; Neagoe et al., 2002). Only recently, the molecular linkage between RBM and titin alternative splicing (AS) was delicately demonstrated. RBM20 specifically binds certain regions in the newly transcribed *TTN* pre-mRNA. This binding consequently blocks the removal of introns in these specific regions, whereas the rest of the *TTN* pre-mRNA resumes normal splicing. These partially spliced mRNA remain in the nucleus. Finally, splicing at the 5′ and 3′ splice sites of the exons flanking the region bound to RBM20 takes place, thereby skipping the introns and exons bound to RBM20 (Li et al., 2010).

b. Camk2d and ryanodine receptors

Further studies and genome-wide analysis revealed that RBM20 is a global regulator of cardiac alternative splicing. It is linked not only to the splicing of titin, but also a number of cardiac mRNAs like *CAMK2D, LDB3* and others. These genes serve important functions in regulating Ca^{2+} signaling, ion transport, and sarcomeric assembly (Guo et al., 2012).

Proper calcium transport is of ultimate importance for cardiac function, and is found to be altered in cardiomyopathy. *Camk2d,* another cardiac target for Rbm20 was found to be deregulated in *Rbm20* knock down mouse EBs (Beraldi et al, 2014). This deregulation manifested as the splicing out of exon 14 while including exons exons 15 and 16. This leads to the persistence of isoform A. noteworthy is that spliced exon 14 of *CAMK2D* comprises the nuclear localization signal, and that this isoform switch of *CAMK2D* has been associated with hypercontractility (Guo et al., 2012).

Targets downstream of CaMK2D include key proteins for the modulation of calcium ions handling include phospholamban (PLN) and ryanodine receptors (RyR2) (Mishra & Brown, 2011). *RYR2* is another target gene of RBM20 that is found primarily in heart muscles and plays a role in maintaining Ca^{2+} balance and excitation-contraction coupling. In both cardiomyopathy, and *Rbm20* deficiency cases, the N-terminus of *Ryr2* is mutated, leading to arrhythmias and cardiomyopathy (Maatz et al., 2014; Tang & Chen, 2012).

c. Lim domain binding 3

LDB3, coding for lim domain binding protein 3 (LDB3) was also found as a splicing target for RBM20. Mutations in *RBM20* were found to specifically affect the expression of exon 4. This altered LDB3 isoform expression diminishes phosphoglucomutase 1 (PGM1) binding sites. This leads to the disruption of the PGM1-recruitment to the Z disk (Maatz et al., 2014).

F. Gap in Knowledge, Study Rationale and Hypothesis

The increased health burden, and high incidence of mortality attributed to cardiomyopathies, calls for extensive research efforts and investigations to decipher the mechanisms giving rise to the disease phenotype. Genome-wide association studies identified mutations in *LMNA, EMD,* and *Rbm20* as causative factors for heritable EDMD and DCM cases. Mutations in the *LMNA* gene have been accredited to a number of tissue specific laminopathies. This tissue specificity, coinciding with the ubiquitously expressed *LMNA* gene, dazzled scientists for many years, and strived them to find the answers and cues for this phenomena. A simultaneous manifestation of two hypothesis, rendering tissue specificity, is highly plausible. The first, "structural hypothesis", suggests that the weakening of the lamina, leads to an injury to the structure and shape of the nucleus of cells subjected to high levels of stress as in cardiomyocytes. On the other hand, "the gene regulation hypothesis" claims that altered gene expression and signaling pathways take place whenever *LMNA* is mutated. A large subset of the molecular players that may be

52

implicated in the disruption of signaling pathways in muscular laminopathies have not been resolved to date. This prompted us to tackle specific postulated gene targets of which expression may be regulated by an intact nuclear lamina.

RBM20, being a nuclear matrix protein, responsible for splicing events important for cardiac function and differentiation has been recently identified as one of the leading causes for hereditary DCM. Mutations in this gene have been ascribed to altering splicing events of key genes responsible for the proper functioning and structure of the heart such as *TTN* sarcomere gene. A large network of RBM20 interacting proteins, including laminA/C have been acknowledged. Yet, none of these proposed interacting partners have been validated by means of biochemical analysis. These findings, in addition to the fact that A-type lamins have been found to co-localize with the RNA splicing compartments responsible for the recruitment and positioning of RNA splicing factors, directed us to investigate the behavior of RBM20 in the context of *LMNA* and *EMD* related cardiomyopathies.

The focus of this study is on investigating the putative role of RBM20 in *LMNA* and *EMD* related cardiomyopathies. Hence, we rationalized an alteration in RBM20 in terms of expression and/or localization in laminA/C and emerin related cardiomyopathies.

G. Objective of the Study and Specific Aims

Our ultimate objective is to gain a better insight into the complete repertoire of pathways perturbed in the hereditary form of *LMNA* and *EMD* related cardiomyopathies. Investigating the plausible interplay between three of the most prevalently mutated genes in

53

DCM and EDMD; *Rbm20, LMNA,* and *EMD* would provide new insight into the molecular pathways underlying the disease phenotype associated with these genes. The presence or lack thereof of Rbm20 expression and/or alteration in its localization associated with a deregulation in the postulated interacting partners; *LMNA* and *EMD,* provides a better understanding of the bio-functional interplay between these genes. Accordingly, for the purpose of this study, our specific aims are:

Specific Aim 1: To investigate the potential deregulation in *Rbm20* transcript expression under baseline conditions in MEF cell lines derived from *Lmna$^{-/-}$, Emd$^{-/y}$*, and *Lmna$^{N195K/N195K}$* mutant mice in comparison to wild-type controls, *Lmna$^{+/+}$*. This will be carried out through quantification of *Rbm20* expression by Real-Time PCR.

Specific Aim 2: To investigate the potential deregulation in Rbm20 protein expression under baseline conditions in the same MEF cell lines by quantification of the Rbm20 protein expression using immuno-blot analysis and immunofluorescence staining.

Specific Aim 3: To investigate the potential alterations in intracellular localization of Rbm20 protein under baseline conditions in the same MEF cell lines. This will be carried out by immunofluorescence staining and laser confocal microscopy imaging analysis.

H. Significance of the Study

Investigating the putative role of RBM20 in the context of lamin A/C deficiency (EDMD), emerin deficiency (EDMD), and the lamin A/C – N195K mutant form (DCM),

will provide new insights into the molecular and biochemical mechanisms and would unmask cellular pathways implicated in these diseases. Knowledge gained from this study would provide a better understanding of the development of cardiomyopathies emerging as a consequence of lamin A/C and emerin mutations. Extensive studies must be further performed to determine the initial points off divergence for these genetic diseases; in anticipation for the emergence of new therapies for cardiomyopathies, targeting the pathogenic consequences of lamin A/C and emerin mutations.

CHAPTER II

Materials and Methods

A. Cell Lines

Due to the technical hurdles and relatively high cost that are associated with the isolation, culturing, and maintenance of cardiac myocytes (neonatal or adult), all

experiments in this pilot study were performed using immortalized mouse embryo fibroblast (MEF) lines as surrogate models for preliminary testing of our hypotheses. These MEFs were derived from two EDMD mouse models being the Lamin A/C null ($Lmna^{-/-}$), and the emerin deficient ($Emd^{-/y}$). In addition, we tested our hypothesis in MEFs derived from the $Lmna^{N195K/N195K}$ mouse (DCM model). As for the control, the WT $Lmna^{+/+}$ MEFs were used. These cell lines were a kind gift from Dr. Jan Lammerding (Cornell, NY). It is worth mentioning that these cell lines are commonly used as a surrogate model in primary experiments to test hypotheses in pilot studies. Moreover, a number of researchers have used these cells lines previously to answer biochemical questions related to EDMD and DCM disease.

$Lmna^{-/-}$mouse model was generated by deleting the region from exon 8 to the center of exon 11 of $Lmna,$ removing 114 codons. The complete loss of lamin A/C expression was validated by Western Blot analysis on cellular extracts. Whereas $Lmna$ transcript expression loss was validated by Nothern Blot (Sullivan et al., 1999). At birth, mice from this model didn't show any characteristic features, but later during development, they were found to develop muscular dystrophy. Nuclei derived from $Lmna^{-/-}$MEFs were easily ruptured at low and had an increased fragility and deformability compared to nuclei isolated from WT MEFs controls (Lammerding et al., 2004; Sullivan et al., 1999).

$Lmna^{N195K/N195K}$ were generated by introducing a missense mutation replacing aspargine with lysine at amino acid 195 into the mice $Lmna$ gene through homologous recombination. Mice carrying this mutation were identified by PCR, and Northern Blot analysis confirmed that the introduction of the point mutation had no effect on the

expression levels or stability of the mutant gene. At the protein level, both lamin A and lamin C were downregulated in primary MEFs derived from the $Lmna^{N195K/N195K}$ mice. This mutation lead to the death of these mice due to the development of DCM. Nuclei in these cells are irregular in shape, and more elongated than nuclei derived from their WT controls (Lombardi & Lammerding, 2011; Mounkes et al., 2005; Zwerger et al., 2013).

The mouse model for the $Emd^{-/Y}$ was subjected to targeted deletion of the X-linked gene, *Emd*. These mice developed EDMD1 during their course of development. Nuclei of the MEFs derived from this mouse model looked generally normal with no distinct morphological changes, and no distribution abnormalities of other NE proteins were observed (Melcon et al., 2006).

1. *Cell culture*

MEF cell lines ($Lmna^{+/+}$, $Lmna^{-/-}$, $Lmna^{N195K/N195K}$, and $Emd^{-/y}$) were maintained in tissue culture using the DMEM-AQ media (Cat.# D0819, Sigma-Aldrich), supplemented with 1% penicillin/streptomycin (Cat.# DE17-602E,Lonza), 1% sodium pyruvate (Cat.# S8636, Sigma-Aldrich), and 10% Fetal bovine serum (FBS) (Cat.# F9665, Sigma-Aldrich), and incubated at 37°C and 5% CO2. When the confluency of the cells in 10 cc plates reached 80%, they were split. This was done first by washing once with 5ml of 1X Phosphate Buffered Saline (PBS) (Cat.# 17-517Q, Lonza) followed by detaching of the adherent cells by the addition of 1.5ml of 1X Trypsin (Lonza) and the incubation at 37°C and 5% CO2 for 2 minutes. Afterwards, 6.5 ml supplemented media was added to inactivate trypsin, and the cells were centrifuged at 600xg, 4°C, for 5 minutes. The pellet of

cells obtained from the centrifugation was resuspended in 1ml media and a relative ratio was pipetted into a new 10cc plate that is pre-labeled and prefilled with 10ml supplemented media.

2. Cell count

After the resuspension of the cell pellet with 1ml complete media, a sample was resuspended in media to obtain a dilution ratio of 1:10. Next, the diluted sample was diluted again in trypan blue (Cat# 0000414869) stain in a 1:2 ratio. The hemacytometer was used to accurately determine the number of viable cells, and to determine the volume needed for seeding, depending on the seeding density.

B. RNA Isolation

For all RNA extractions, (*Lmna*$^{+/+}$, *Lmna*$^{-/-}$, and *Emd*$^{-/y}$) MEFs were seeded in 6cm plates at $10*10^4$ cells per 1ml in specialized serum supplemented media. Whereas *Lmna*$^{N195K/N195K}$ MEFs were seeded at $13*10^4$ cells per 1ml media. After reaching 80% confluency, RNA samples were extracted from the MEF cell lines under baseline conditions using the TRI Reagent (TRIzol Reagent, T9424, Sigma Aldrich) based on the manufacturer's specifications and protocol. First, cells were washed once with PBS (1X), and then, 0.5 ml Trizol was added to each 6cm plate. After complete dissociation of the nucleoprotein complexes, 100µl chloroform was added. This was followed by a centrifugation at 12000 X g, 4°C, for 15 minutes, of which after, the aqueous phase was transferred to a new pre-labeled microcentrifuge tube. 250µl of isopropanol was added and

another centrifugation at 12000 X g, 4°C, for 10 minutes was carried. Next, the supernatant was removed and the RNA pellet was suspended with 500µl of 75% ethanol. A final centrifugation step was next done at 7500 X g, 4°C, for 5 minutes. The pellet obtained later, containing pure RNA, was left to completely dry out, and an appropriate amount of RNase/DNase free water (Lot# RNBC8413, SIGMA) was added and mixed. The quantity and purity of the extracted RNA samples were further assessed using the Nanodrop Spectrophotometer (Thermonanodrop 2000C). All RNA samples were stored at -80°C for later reverse transcription and Real-Time PCR analysis.

C. Reverse Transcription

After the assessment of the quality and purity of the RNA samples, 1µg of the extracted RNA was reverse transcribed into cDNA using the iScript cDNA Synthesis Kit (Cat3 1708890, Bio-Rad) based on the manufacturer's specifications and protocol. 1µg of each sample was mixed with 1µl of the iScript reverse transcriptase enzyme and 4µl of the 5X iScript Reaction Mix. The total volume was completed to 20µl using nuclease free sterile water (Lot# RNBC8413, SIGMA) in a labeled pre-cooled RNase free PCR tube and using barrier tips. Next, reverse transcription was carried on using the DNA engine machine (Peltier thermal cycler, Bio-Rad) following the protocol initiated with 25°C for 5 minutes to ensure proper annealing of the random primers. Subsequent the extension step of the cDNA strands was carried at 42°C for 30 mins, and the reverse transcription was completed with 5 min at 85°C. All cDNA samples were later stored at -20°C for later quantitative PCR analysis.

D. Quantitative Real-Time PCR

Real-Time PCR amplification was performed using the iQ SYBR Green Supermix (Cat.# S4438, Sigma-Aldrich). First, cDNA working stock of 1:20 was prepared by adding 5μl of the cDNA to 95μl of nuclease free sterile water. Specific forward and reverse primers for Rbm20 gene were also used. Primer pairs for the reference housekeeping gene *18s* were used as internal controls and for normalization. All primer pairs were diluted with nuclease free sterile water to the con oncentration of (1:10). Primer sequences were derived computationally from the MGH/Harvard Medical School Primer Bank Database (www.pga.mgh.harvard.edu/primerbank) (table 2). The validity of the primers were assessed by performing a dilution curve on known sample concentrations.

In each PCR tube, 4μl of the diluted cDNA (1:20) derived from each sample were added to 6.5μl of the nuclease free sterile water, 1μl of the forward primer and 1μl of the reverse primer for each gene, and finally 12.5μl of the Supermix completing the total volume to 25μl. Independent repeats were performed separately in duplicates, and samples were kept on ice throughout the experiment. In each repeat, 8 reactions were carried out relevant to the amplified gene. Subsequently, the reaction was executed using the Real-Time PCR machine (c-1000 Touch thermal cycler, Bio-Rad, CRSL facility, AUB). The protocol used consists of initial heating to 50°C for 2 minutes, followed by the DNA denaturing step at 95°Cfor 10 minutes, cooling at 60°C for 1 minute to insure proper annealing of primers to their complementary strands, and an extension at 72°C for 30 seconds were the Taq DNA polymerase extends the sequence-specific primer by

incorporating complementary nucleotides to the DNA template yielding a double-stranded DNA complex. This cycle was repeated 40 times, followed by final extension step was at 72°C for 10 minutes. For further analysis and recording of our obtained results, the Bio-Rad CFX Manager Software was used. Quantification of *Rbm20* transcript expression was further normalized to the expression of the*18s* reference gene in all independent experimental repeats.

Table 2 | List of the sequence for the forward and the reverse primers used to quantify the transcript expression of Rbm20. (www.pga.mgh.harvard.edu/primerbank).

E. Protein Extraction and Quantification from MEFs Cultured Under Baseline Conditions

Gene (species)	Primer	Sequence
18s (mouse)	Forward	5′ - GTAACCCTTGAACCCCATT - 3′
18s (mouse)	Reverse	5′ - CCATCCAATCGGTAGTAGCG - 3′
Rbm20 (mouse)	Forward	5′ - GGCCAAAACAAGCCCGATATT - 3′
Rbm20 (mouse)	Reverse	5′ – CCCTGTCTGAGGTAGGCTCT - 3′

1. Protein extraction with RIPA lysis buffer

For all protein extractions, *Lmna*$^{+/+}$, *Lmna*$^{-/-}$, and Emd$^{-/y}$ MEFs were seeded in 6cm plates at $10*10^4$ cells per 1ml in specialized serum supplemented media. Whereas

61

$Lmna^{N195K/N195K}$ MEFs were seeded at $13*10^4$ cells per 1ml media. After reaching 80%

confluency, cells were washed twice with 3 ml of pre-cooled PBS (1X). Subsequently,

150µl of the standard RIPA lysis buffer (Cat.# R-0278, Sigma Aldrich) was added after

fresh supplementation with a dilution of 1:1000 Protease Inhibitor Cocktail (P-8340, Sigma

Aldrich). Samples were then placed on ice and incubated on a nutator for 15 minutes. Next,

using the cell scraper, lysate cluster were lodged off the plates and transferred to pre-cooled

microfuge tubes and placed horizontally on ice on the nutator for another15 minutes.

Afterwards, lysates were centrifuged at 400xg at 4°C for 10 minutes. Thereafter, the

supernatant comprising the protein extracts from each sample was transferred to a pre-

labelled, pre-cooled sterile microfuge tube. Samples were then stored at -20°C. Protein

extracts from $Lmna^{+/+}$MEFs served as controls for comparison between the $Lmna^{-/-}$,

$Lmna^{N195K/N195K}$, and $Emd^{-/Y}$ panel of MEFs.

2. *Protein extraction with RIPA lysis buffer supplemented with phosphatase inhibitor*

The same procedure for protein extraction was implemented for one of the trials

with one slight variation in the lysis buffer used. RIPA lysis buffer was further

supplemented with 1:1000 phosphatase inhibitor cocktail (ab120386, abcam). This was

done in an attempt to obtain the 130kDa Rbm20 isoform which we were unable to detect in

Western Blot assays performed on proteins from MEFs extracted without the addition of

phosphatase inhibitor. Protein lysates were also stored at -20°C.

3. *Extraction of nuclear proteins*

Cells were rinsed once with 3ml of pre-cooled PBS (1X). Then, 2 ml of PBS (1X) supplemented with 20 μl of EDTA chelating agent were added to detach all the cells. The petri dishes were then placed on ice and incubated on a nutator for 15 minutes. Afterwards, cells were collected in Eppendorf tubes for centrifugation at 375xg for 90 seconds. Next, supernatant is was discarded, and the pellet was re-suspended with 800 μl of buffer A (10mM Tris pH 7.9, 0.1 mM EDTA, 0.1mM EGTA, 10mM KCl, 0.5mM DTT, 0.5mM PMSF, and 0.5 mM protease inhibitor cocktail (P-8340, Sigma Aldrich), along with 1 μl DTT (1M reducing agent), 2 μl protease inhibitor, and 1 μl PMSF (0.5 M). Contents were mixed, and the tubes were left standing in ice for 15 minutes. Next, 50 μl NP40 10% were added per tube, followed by vortexing and centrifugation at maximum speed for 90 seconds. The supernatant was again discarded, and the transparent pellet was suspended in 200 μl buffer C (20mM Tris pH 7.9, 1mM EDTA, 1mM EGTA, 400mM NaCl, 0.5 mM DTT, 0.5mM PMSF and 0.5 mM protease inhibitor cocktail. Tubes were then placed horizontally on the shaker in the cold room (T = 4°C) for 20 minutes. Afterwards, tubes were again centrifuged at maximum speed for 90 seconds. Pellets were then discarded, and the samples were stored at -20°C for later use.

4. *Protein extraction with high salt RIPA lysis buffer*

The same procedure was again repeated by using RIPA lysis buffer prepared with high salt concentration. The lysis buffer was prepared by adding 10mM Tris (Cat.# 161-0716, Bio-Rad) pH 7.5, 150mM sodium chloride,, 1% triton X-100 (Cat.# 2641C463,

Amresco), and 5mM EDTA pH 8 (Cat.# 3610C106, Amresco). The lysates were freshly

suspended with 1:1000 Protease Inhibitor Cocktail, and the same procedure as in the RIPA

lysis extraction was performed thereafter.

5. *Sample protein quantification*

Protein quantification was performed with the Optiblot Bradfors Reagent (Cat.#

ab119216, Abcam). Using a 96 well plate, the first two lanes were used for standardization

using specific dilutions of 1mg/ml of BSA (Bovine Serum Albumin, Cat.# 0332, Amresco)

in double distilled water (dd$_{H2O}$). The standards were done in duplicates with the following

protein content (μg): 0.0, 2.0, 4.0, 6.0, 8.0, and 10.0. In the subsequent rows, 5μl of each

sample were placed in duplicates. Later, 200μl of the Optiblot Bradford Reagent were next

added to each well for measurement of the protein content using the SpectraMax ascent

software (Multiskan EX, Thermo lab Systems).

F. SDS PAGE and Western Blot Analysis

1. *Casting and running the gels*

Cell lysates from MEF cell lines were extracted under baseline conditions. Next,

they were resolved using a 12% Tris-HCl buffer. The resolving and casting gels were

prepared manually using thick and thin plates with an integrated space of 1.5mm to allow

the loading of big volumes including high protein concentration. To prepare the 1.5mm

thick resolving gel, 3.2 ml Acrylamide/Bis (Cat.# 161-0158, Bio-Rad) was mixed with 2ml

1.5M Tris-HCl pH 8.8 (Cat.# 161-0798, Bio-Rad), and 2.8ml deionized distilled water.

Then, 140μl of APS (Ammonium Persulfate, Cat.# 161-0700, Bio-Rad) ,and 20μl of

TEMED (Tetramethylethylenediamine, Cat.# 0761, Ultra-pure grade, Amresco) was added

to the mixture. The mixture was then smoothly poured between the two plates. Immediately

after filling the space between the two plates up to the green line, the gels were topped with

isobutanol to insure obtaining a smooth horizontal line and prevent drying out of the gel.

Similarly, the stacking gel was prepared by mixing 750μl of 30% Acrylamide/Bis with

1250μl of 0.5M Tris-HCl pH 6.8(Cat.# 161-0799, Bio-Rad) and 3ml of deionized distilled

water. 140μl of APS and 20μl of TEMED were then mixed with the stacking gel solution

and poured between the glass plates until the top of the short plate was reached. The comb

was immediately placed in the stacking gel between the two plates, and the gels were left to

polymerize.

Meanwhile, the running buffer was prepared by dissolving 14.4g glycine (Cat.#

161-0724, Bio-Rad), 2.5g Tris-base (Cat.# 161-0719, Bio-Rad) and 1g SDS (Sodium

Dodecyl Sulfate, Cat.# 161-0302, Bio-Rad) in 1L deionized distilled water. Casted gels

were then placed in the running chamber filled with the prepared running buffer, and the

combs were carefully removed to obtain clean wells.

2. *Preparation of samples*

20μg of protein from each sample was prepared by resuspension with 5μl

Laemmli sample buffer composed of glycerol, SDS, 0.5M Tris-HCl pH 6.8 and traces of

bromophenol blue) freshly supplemented with 10% β-mercaptoethanol (BME) in a pre-cooled sterile microcentrifuge tube. The total volume was completed with double distilled water to obtain equal volumes for all lysates within each repeat. Denaturing of the protein samples was performed by boiling to 95°C for 5 minutes using the thermobloc. Samples were immediately placed on ice to prevent refolding. Samples were next loaded carefully into the wells. 5µl of the Precision Plus Protein standard (Cat.# 161-0373, Bio-Rad) was also loaded to be used as a molecular weight marker for the determination of the protein size. SDS-PAGE was then run at 200V for 45 minutes, while ice buckets surrounded the running chamber to prevent overheating.

3. Transfer of proteins from gel to membrane

Protein samples were transferred from gels to a polyvinylidene fluoride (PVDF) transfer membrane (Immuno-Blot ™ PVDF Membrane, Cat# 162-0177, Bio-Rad). First, membranes were activated by soaking in 100% methanol (Sigma-Aldrich) for 5 minutes. The transfer buffer was next prepared by diluting 14.4g glycine and 2.5g Tris-base in 800µl of double distilled water and 200µl of pure methanol. PVDF membranes, blotting papers, and sponges were all soaked in the transfer buffer before use. Next, gels were released from the plates and sandwiched along with the membranes between blotting papers and sponges in the cassette ensuring no bubbles were trapped between them. The sandwich was then placed in the transfer unit filled with the transfer buffer. The power supply was put on 100V for 90 minutes while the transfer unit was placed in ice to prevent overheating. Afterwards, the gels and the blotting papers were discarded in polyacrylamide waste

containers, and the membrane was soaked in 0.1% PBS-T (Phosphate Buffer Saline Tween20) washing buffer for few minutes prior to membrane blocking.

4. Blocking, washing and antibody incubation

Blocking of each membrane of the non-specific sites was done by soaking in 25ml of 5% non-fat dry milk (Regilait) diluted in the washing buffer at room temperature, on the ProBlot™ Rocker 25 at medium speed for 1 hour. The washing buffer (0.1% PBS-T) was prepared by diluting 100ml of 10X PBS without Ca and Mg, 900ml of deionized distilled water, and 1ml of primary antibody was incubated in Tween 20 (Polyoxyethylene sorbitol ester, Cat.# P1379, Sigma-Aldrich).

Incubation with the primary antibody was done after its dilution in 3.5ml of 5% non-fat dry milk prepared in 0.1% PBS-T on a ProBlot™ Rocker 25 at medium speed. Incubation with Rbm20 primary antibody was at 4°C, overnight, while GAPDH primary antibody incubation was done at room temperature, for 1 hour. The primary antibodies used for this study are Rbm20 rabbit polyclonal-IgG (P20140522331; rabbit polyclonal-IgG; 200µg/ml, Cloud-Clone Corp) used at 1:500, and Rbm20 goat polyclonal-IgG (D-20: Sc-243941, Santa Cruz Biotechnology, Inc.). As for the loading control, GAPDH rabbit polyclonal-IgG provided at 200µg/ml (FL-335-sc-25778, Santa Cruz Inc.) at 1:500 dilution was used. After incubation, three washes with 20ml of the 0.1% PBS-T washing buffer at room temperature on a ProBlot™ Rocker 25 at high speed was performed. Each wash for 10 minutes.

Incubation with the secondary antibody, corresponding to the primary antibody used, was performed at room temperature at the rocker at medium speed for 1 hour. The secondary antibody used for was the goat anti-rabbit-IgG, 0.8μg/μl, obtained from Jackson Immunoresearch. All secondary antibodies were used in 1:2500 dilution in 5ml 5% non-fat dry milk prepared in 0.1% PBS-T. Same washing steps which followed the primary antibody incubation were performed.

5. *X-ray film imaging*

Blots were developed with enhanced chemiluminescence; ECL reagents (ECL Western Blot Substrate, Abcam) composed of Reagent A (ab65628) and Reagent B (ab65629), and using X-ray film (AGFA), and XOMAT X-ray film processor (Optimax). Briefly, 1ml of each ECL reagent was added on the membrane and left for 1 minute for the complete reaction to take place in the dark. The membrane was then transferred to a cassette (Spectroline Monotec Cassette, Spectronics Corp). In the dark room, membrane was exposed to an X-ray film. For Rbm20 probed membranes, exposure time was 1-5 minutes. GAPDH probed membranes were exposed for 10-30 seconds.

6. *Membrane stripping and re-probing*

Stripping of probed membranes was performed by the addition of 15ml of 0.1M NaOH on the shaker at room temperature for 45 minutes. A 1 minute wash step with 10ml of 0.1% PBS-T wash preceded the blocking step. Blocking was performed for one hour, in the same manner mentioned earlier. This was followed by post primary antibody incubation

for the protein of interest. Washing, secondary antibody incubation, signal developing, and X-ray film imaging were repeated as previously mentioned in the text.

7. *Densitometry analysis*

Expression levels were quantified by densitometry using Image J 1.49 free Java image processing program software after normalization to the GAPDH loading controls. The software was downloaded from: http://imagej.nih.gov/ij/download.html. Developed X-ray films were scanned in tif format at 1200 dpi. Each lane was highlighted and enclosed with the rectangular selection tool in the Image J toolbar. This step was repeated for each band. Next, a profile plot was generated showing peaks that are correspondent to relative density of the band in the rectangle. To measure the area of each peak, the wand tool in the image J toolbar was used. Each measured peak was represented as a percentage of the total size of measured pics. Next, results were transferred to an excel sheet were the relative density of each peak was calculated relative to the standard by dividing the percent value of each lane by the percent value of the standard lane. Under baseline conditions, the density of each sample corresponding to $Lmna^{-/-}$, $Lmna^{N195K/N195K}$, and $Emd^{-/Y}$MEFs was measured relative to the protein expression levels in the $Lmna^{+/+}$ MEFs. Afterwards, the relative density of Rbm20 in each sample was normalized to the relative density of GAPDH loading control.

G. Immunofluorescence Staining

1. *Fixation of cells on coverslips*

MEF cell lines were first seeded in 6 well plates on a 22 x 22 mm wide and 0.17-

0.25mm thick square cover glass (Fisher Scientific) in specialized 4ml/well serum

supplemented media. WT-MEFs and the other three mutant cell lines were all seeded at a

similar density of $13*10^4$ cells per 1ml media. All cells were kept overnight in the incubator

(37°C and 5% CO2) to adhere and divide. After reaching 80% confluence, cells were

washed 2X with PBS for 5 minutes while gently stirring. Fixation of the cells was executed

with freshly prepared 4% Paraformaldehyde solution prepared from a 16% PFA solution

(Paraformaldehyde, Cat.# 15710, Electron Microscopy Sciences) at room temperature for

20 minutes. Next, cells were washed two times with 2 ml of 1X PBS, 5 minutes each time.

Cells were kept fixed at 4°C until the whole repeat set was ready to be permeabalized and

stained on the same day.

2. *Cellular permeablization and antibody incubation*

Fixed cells were treated with 0.2% Triton in PBS (t-

Octylphenoxypolyethoxyethanol, Cat.# T8787, Sigma-Aldrich) at room temperature for 10

minutes. This was done to permealize the cells and insure access of the antibody to bind to

its specific antigen. Subsequently, cells were washed three times with 2ml 1X PBS as

mentioned earlier, and blocked with freshly prepared 2% BSA in PBS (1µl/well), at room

temperature, for two hours. The blocking media was then removed, and the cells were

washed with 2 ml 1X PBS for 5 minutes. Each glass cover slip was later incubated with

300µl Rbm20 primary antibody (P20140522331; rabbit polyclonal-IgG; 200µg/ml, Cloud-

Clone Corp; and diluted in 1%BSA in PBS) used at 1:500 dilution, prepared in 1% BSA in

1X PBS at room temperature for 2 hours. This was followed by 3 washes with PBS on the ProBlot™ Rocker 25 at minimum speed at room temperature, for 5 minutes each. Next, the signal was developed by the specific secondary antibody Alexa Fluor® 488 conjugated goat anti-rabbit-IgG (H&L) provided at 1.5μg/μl (ImmunoResearch), used at 1:200 dilution in PBS only. Cells were again washed three times in 2ml 1X PBS, on the ProBlot™ Rocker 25 at minimum speed. Negative controls samples for each cell line were only stained with the secondary antibody and were used to demonstrate non-specific binding of the secondary antibody.

3. *Mounting of coverslips on microscopic slides*

Coverslips were mounted on microscope slides (Fisher Scientific) with a drop of the mounting medium (UltraCruz, Hard-set mounting medium, sc-359850, SantaCruz) containing 4',6-diamidino-2-phenylindole (DAPI) as a DNA counterstain. Cover slips were placed on top of the drop with the face holding the cells facing down. Excess mounting medium was removed, and the coverslips were sealed with transparent nail polish for storage in the dark overnight for the next day to obtain images. After imaging, slides were kept at 4°C for long-term storage.

4. *Microscopic imaging*

Image acquisition was performed within 24 hours of the staining with the use of the LSM710 Confocal Microscope (Carl Zeiss, DTS facility) at 63x / 1.40 oil DIC M27 objective magnification at optimum exposure times and excitation wavelengths. Eventually, the fluorescence intensity was analyzed by Image J 1.41 Ja. 7-9 frames were obtained for each sample slide of each independent repeat. As for the negative controls, 2 frames per slide were imaged. Nuclear to cytoplasmic scoring was done visually by plotting a (1) numeric for each cell viewed under the category that best describes the localization of the protein.

H. Statistical Analysis

In all the experiments performed, data were expressed as mean ± standard error of the mean (SEM) derived from 4 to 8 independent experiments per group. Real-Time PCR assays and IF staining were done in duplicates. Statistical analysis was carried out using Microsoft Excel Program and the IBM SPSS Statistics 20. Data were analyzed by using one-way ANOVA after which the 2-sided Dunnett post hoc test was performed for the comparisons of several groups with a control. Groups were considered significantly different at values of $P \leq 0.05$, with the symbols '*' *for $P \leq 0.05$*, '**' for $P \leq 0.01$ and '***' for $P \leq 0.001$.

CHAPTER III

RESULTS

A. Assess potential alterations in *Rbm20* transcript levels under baseline conditions in mouse embryo fibroblast (MEF) cell lines derived from mice either lacking A-type lamin or emerin expression (resulting in the EDMD phenotype), or homozygous for the *Lmna*-N195K mutant form (resulting in DCM phenotype), versus wild-type (WT) MEFs.

1. Rbm20 transcript expression is significantly down-regulated in Lmna$^{-/-}$ MEFs (Lamin A/C null), Lmna$^{N195K/N195K}$ MEFs and Emd$^{-/Y}$ MEFs (emerin null) under baseline conditions in comparison to Lmna$^{+/+}$ (wild-type) control MEFs.

To determine any alterations in the transcript expression levels of *Rbm20* in the panel of mutant MEFs (*Lmna$^{-/-}$, Lmna$^{N195K/N195K}$, and Emd$^{-/Y}$*) under baseline conditions, we performed quantitative Real-Time PCR (qRT-PCR) experiments on the aforementioned MEF cells after RNA extraction and cDNA synthesis, while ensuring consistent cell seeding density and confluence status amongst all cell lines and between independent repeats. Under baseline conditions, when normalized to the reference gene *18s* transcript levels, RT-PCR quantification data shows a reduction in the *Rbm20* expression levels in Lamin A/C null MEFs with a 0.19–fold (±0.06) of that of the WT control, suggesting an ~80% decrease in transcript expression. This reduction was statistically significant with a (*P-value<0.001*). In *Lmna$^{N195K/N195K}$* MEFs, the expression level of *Rbm20* transcript was also significantly down regulated, with a 0.51-fold (±0.06) of that of the control *Lmna$^{+/+}$* MEFs, reflecting an approximately ~50% reduction in total transcript expression, which also was determined to be statistically significant (*P-value<0.001*). A more prominent significant down-regulation in the *Rbm20* transcript expression was detected in the *Emd$^{-/Y}$* MEFs with a 0.04-fold (±0.01) of that of the control *Lmna$^{+/+}$* MEFs (*P-value<0.001*), hence

indicating an extreme decline in *Rbm20* expression level reaching ~95% in the emerin null background. Data is represented as mean fold difference ± SEM obtained from five independent experiments, each done in duplicates (Figure 10).
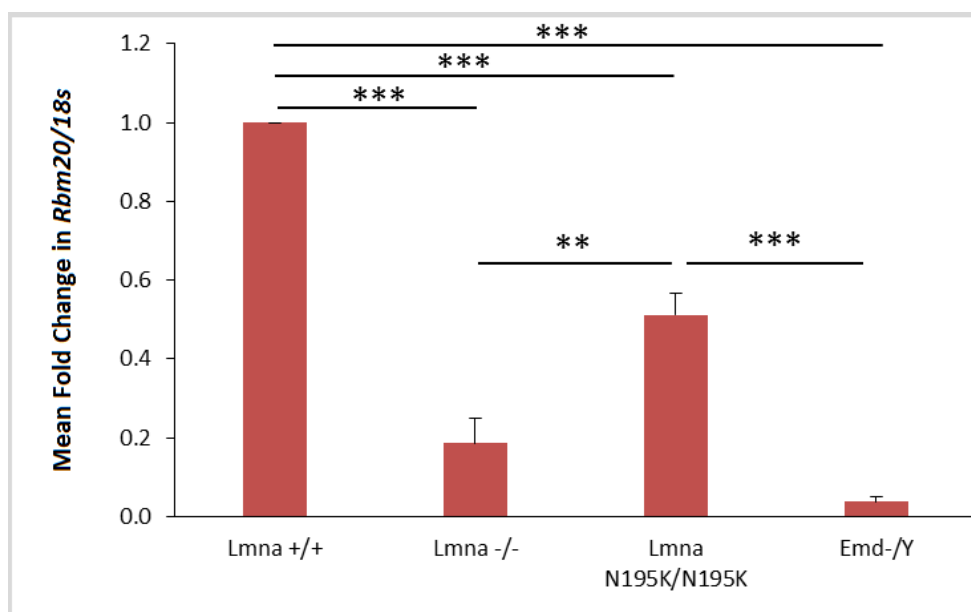
Figure 10 | Mean fold change in *Rbm20* transcript expression in *Lmna*^{-/-}, *Lmna*[N195K/N195K] and *Emd*[-/Y] MEF cells relative to the *Lmna*^{+/+} WT controls at baseline conditions. Real-Time PCR quantification data indicates a marked significant reduction in the *Rbm20* transcript expression levels in the mutant MEFs *Lmna*[N195K/N195K] (DCM model), *Lmna*^{-/-} and *Emd*[-/Y] MEF cells (EDMD model). *Rbm20* transcript expression levels were normalized to that of the *18s* reference gene. Data represents mean fold difference ± SEM relative to the WT controls derived from 5 independent experiments; each performed in duplicates. Two asterisks represent a statistical significance (*P-value <0.01*). Three asterisks represent a statistical significance (*P-value <0.001).*

2. ***Rbm20 transcript expression is significantly down-regulated in Lmna^{-/-} MEFs (Lamin A/C null), and Emd[-/Y] MEFs (emerin null) under baseline conditions in comparison to***

Lmna$^{N195K/N195K}$ mutant MEFs, but shows no significant difference in transcript expression between the Lmna$^{-/-}$ and the Emd$^{-/Y}$ (EDMD models).

Real-Time PCR quantification results, normalized to the transcript levels of *18s* reference gene, show a significant reduction in *Rbm20* transcript expression levels in the *Lmna$^{-/-}$* MEFs when compared to the *Lmna$^{N195K/N195K}$* mutant cells (*P-value <0.01*). Similarly, the *Rbm20* transcript expression levels in the *Emd$^{-/Y}$* MEFs also reflect a significant decline in comparison to the expression levels in *Lmna$^{N195K/N195K}$* (*P-value <0.001*). In contrast, no statistically significant difference in *Rbm20* transcript expression levels was found between the *Emd$^{-/Y}$* MEFs compared to the *Lmna$^{-/-}$* (*P-value>0.05*). The quantification data are represented as mean fold difference ± SEM generated from five independent experimental repeats, each done in duplicates (Figure 10).

B. Assess putative deregulation in the protein expression of Rbm20 under baseline conditions in mouse embryo fibroblast (MEF) cell lines derived from the EDMD mouse models with Lamin A\C and emerin deficiency, and the DCM mouse model homozygote for the *Lmna*-N195K mutant form, versus the wild-type (WT) control MEFs.

For the second aim of this study, our intention is to determine if there are any alterations in the Rbm20 protein expression under baseline conditions by employing Western Blot analysis, and using an Rbm20 specific antibody. The results were assessed with the relevant semi-quantitative densitometry analysis of the Western Blots and further supported by performing immunofluorescence staining of the same MEF cell line panel.

For the Western Blot analysis, protein lysates were obtained from MEFs in culture after reaching 80% confluence, under baseline conditions. This was done while ensuring

consistency in cell density and spreading among all tested samples, and between independent repeats. First, qualitative analysis was performed by observing and comparing the densitometry signals on autoradiography films between different samples. Subsequently, semi quantitative densitometry analysis was achieved using the image J software. In all films of all independent Western Blot repeats, no bands were visible for the full-length Rbm20 protein (expected at ~132-134 KDa); nonetheless we were able to detect the shorter isoforms of Rbm20 (expected at ~75-87kDa and 37-56kDa depending on protein modifications and/or cleavage state). All densitometry signals for Rbm20 were normalized to those of the GAPDH loading controls.

1. Total Rbm20 protein expression is significantly reduced in $Lmna^{-/-}$, $Lmna^{N195K/N195K}$, and $Emd^{-/Y}$ mutant MEFs in comparison to the control $Lmna^{+/+}$ MEFs by Western Blot analysis

The analysis of the densitometry signals pertaining to the expression of total Rbm20 protein (cumulative expression of both isoforms), normalized to GAPDH under baseline conditions in the MEF cell lines, reveals ~50% reduction of protein expression in all three $Lmna^{-/-}$, $Lmna^{N195K/N195K}$ and $Emd^{-/Y}$ mutant MEFs compared to the WT controls (Figure 11A). The semi-quantitative assessment of the densitometry signals on the autoradiography WB films further confirms these reductions in Rbm20 protein expression levels in all 3 mutant MEF cell lines (Figure 11B). $Lmna^{-/-}$ MEFs showed a 0.51-fold change (± 0.11) of protein expression when compared to the WT MEFs, reflecting a significant ~50% reduction in total Rbm20 protein expression (*P-value<0.001*). Similarly, the expression of both isoforms of Rbm20 was reduced to a 0.43-fold change (± 0.10) in the

$Lmna^{N195K/N195K}$ MEFs in comparison to the WT controls, which was also proven significant after statistical analysis (*P-value<0.001*). Likewise, the level of Rbm20 protein expression in the $Emd^{-/Y}$ was significantly reduced by nearly ~50%, with a 0.49-fold change ($\pm$ 0.08), when compared to the $Lmna^{+/+}$ control MEFs (*P-value<0.001*) (Figure 11B).

The expression levels of total Rbm20 protein were not significantly different between the $Lmna^{-/-}$ and $Lmna^{N195K/N195K}$ mutant cells under baseline conditions (*P-value>0.05*). Similarly, there was no significant difference in total Rbm20 expression between the $Lmna^{-/-}$ and the $Emd^{-/Y}$ MEFs (*P-value>0.05)*, or between the $Lmna^{N195K/N195K}$ and the $Emd^{-/Y}$ MEFs (*P-value>0.05)* (Figure 11B, see below). The quantification densitometry data of Rbm20 normalized to GAPDH loading control is represented as mean fold change $\pm$ SEM derived from eight independent experiments.
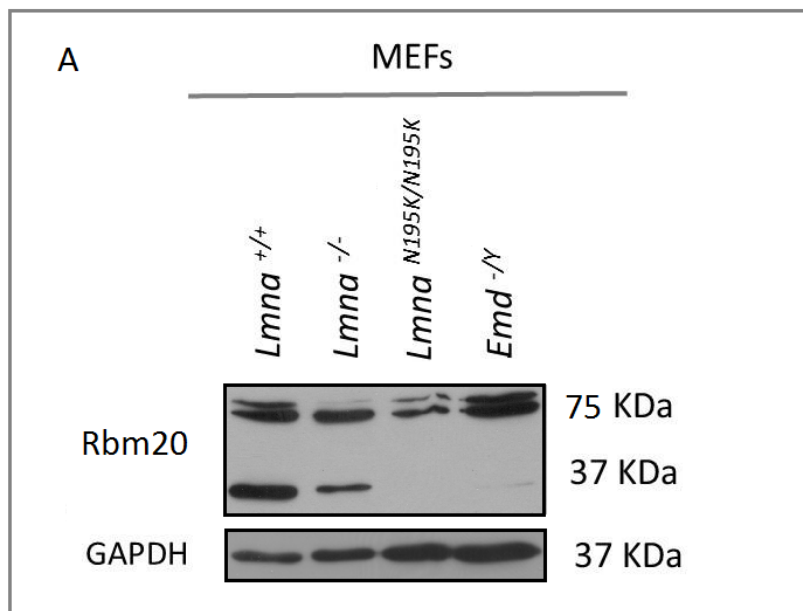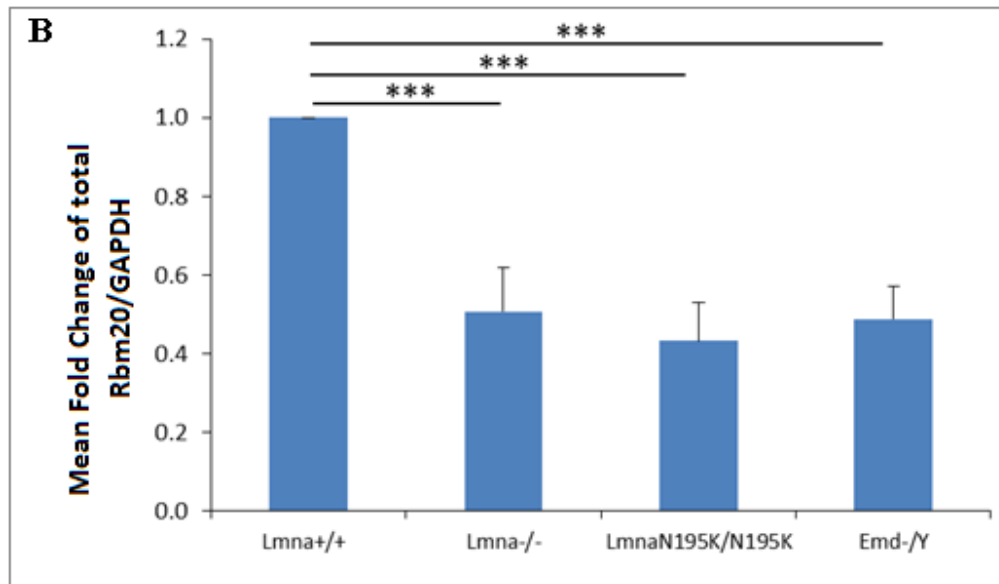
Figure 11| Western Blot analysis of total Rbm20 protein expression in *Lmna^{-/-}*, *Lmna^{N195K/N195K}* and *Emd^{-/Y}* mutant MEFs vs. WT control cells cultured at 80% confluence under baseline conditions. Panel (A); representative blot. Panel (B); Quantification and analysis of the Rbm20 densitometry signal, normalized to that of the GAPDH loading control, reveals a statistically significant decrease in the Rbm20 protein expression between the *Lmna^{-/-}*, *Lmna^{N195K/N195K}* and *Emd^{-/Y}* mutant MEFs compared to the *Lmna^{+/+}* WT control cells cultured under standard conditions. Data represent mean fold change ± SEM derived from 8 independent experiments. Three asterisks represent a statistical significance (*P-value <0.001*).

2. *The expression of the mid-size isoform of Rbm20 protein is reduced in the Lmna^{-/-}, Lmna^{N195K/N195K}, and Emd^{-/Y} mutant MEFs in comparison to the control Lmna^{+/+} MEFs by Western Blot analysis*

Qualitative Western Blot analysis and semi-quantitative densitometry signal

analysis of the mid-size Rbm20 isoform (75-87 KDa) normalized to GAPDH loading in the

panel of MEF cells propagated under standard cell culture conditions suggest a significant

reduction in this Rbm20 isoform in the N195K homozygote mutant MEFs (DCM model).

Lmna and *Emd* null MEFs (EDMD model) also showed reduced levels of this Rbm20

78

isoform expression compared to the WT control MEFs. However, this reduction was not statistically significant. A 0.59-fold (±0.15) was detected in the $Lmna^{N195K/N195K}$, reflecting a ~40% reduction in protein expression compared to the WT controls. The reduction was determined as statistically significant (*P-value<0.05*). On the other hand, the 0.63-fold (±0.11) noted in the $Lmna^{-/-}$ compared to the WT-MEF controls was not statistically significant (*P-value=0.06*). Likewise, this Rbm20 isoform in the $Emd^{-/Y}$ MEFs also revealed a differential expression from the WT control MEFs with a 0.64-fold (±0.13), but the reduction was not statistically significant (*P-value=0.07*) (Figure 12B). As was the case for the total Rbm20 protein expression pattern, the expression of the 75-87 KDa Rbm20 isoform showed no significant difference between the N195K homozygous mutant form (DCM model) and the lamin A/C or the emerin null MEFs (DCM model). Similarly, the statistical analysis confirmed no significant difference in expression between the lamin A/C null MEFs compared to the emerin-deficient MEFs (Figure 12B). The quantification densitometry data is represented as mean fold change ± SEM derived from eight independent experiments.
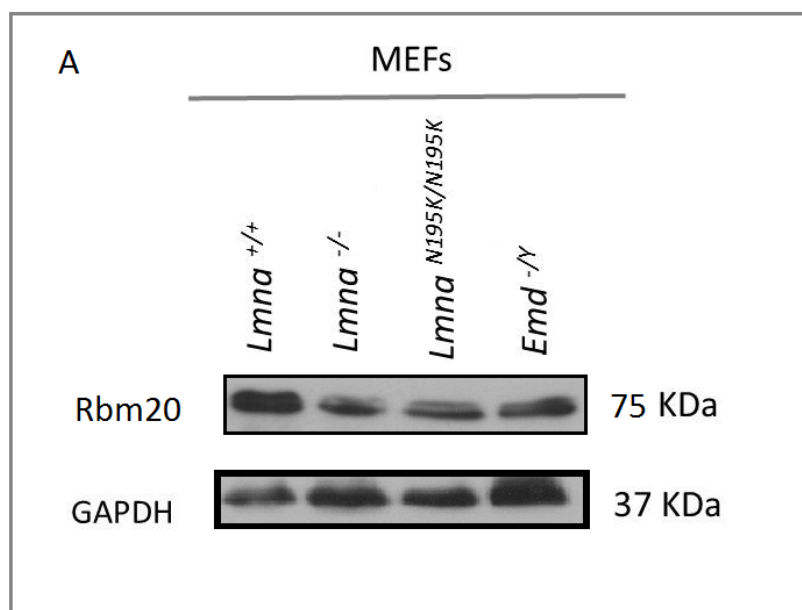
Figure 12| Western Blot analysis of the 75-87kDa Rbm20 protein isoform expression in $Lmna^{-/-}$, $Lmna^{N195K/N195K}$ and $Emd^{-/Y}$ mutant MEFs vs. control WT cells, cultured at 80% confluence. Panel (A); representative blot. Panel (B); semi-quantification and analysis of the Rbm20 densitometry signal, normalized to that of the GAPDH loading control, reveals a statistically significant decrease in the Rbm20 protein expression in the $Lmna^{N195K/N195K}$, and a reduction in the $Lmna^{-/-}$ and $Emd^{-/Y}$ mutant MEFs that was not statistically significant, when compared to the $Lmna^{+/+}$ WT control cells. Data represent mean fold change ±SEM derived from 8 independent experiments. One asterisk represents a statistical significance (*P-value <0.05*).

3. *The expression of the small size isoform of Rbm20 protein is significantly downregulated in $Lmna^{-/-}$, $Lmna^{N195K/N195K}$, and $Emd^{-/Y}$ mutant MEFs when compared to their control $Lmna^{+/+}$ MEFs by Western Blot analysis*

Qualitative assessment of autoradiography Western Blot films suggests an

extremely reduced expression of the smaller Rbm20 isoform (37-56kDa protein) in the

three mutant MEFs versus the WT control. The band was clearly detected in the $Lmna^{+/+}$

80

WT control lysates, but not consistently with the other three mutant MEF lysates. Image J densitometry quantification and analysis indicated an absence in the expression of this Rbm20 isoform in the $Lmna^{N195K/N195K}$ mutant cells (Figure 13B). On the contrary, $Lmna^{-/-}$ and $Emd^{-/Y}$mutant MEFs did show a slight expression of the smaller Rbm20 isoform. $Lmna^{-/-}$ showed a diminished expression in this Rbm20 isoform with a 0.09-fold (±0.05) change compared to the WT controls. Statistical analysis proved this change as significant (*P-value<0.001).*Likewise, the expression levels of this small Rbm20 isoform were markedly downregulated in the $Emd^{-/Y}$ mutant MEFs, with a 0.06-fold (±0.03) relative to the WT control. This reduction was also statistically significant (*P-value<0.001)* (Figure 13B, see below).

When comparing the expression levels of the 37-56kDa isoform of Rbm20 between the three mutant MEF cell lines, $Lmna^{-/-}$ and $Lmna^{N195K/N195K}$ showed no statistically significant difference (*P-value>0.05*). Similarly, there was no significant difference in this Rbm20 isoform expression between the $Lmna^{-/-}$ mutant MEFs compared to the $Emd^{-/Y}$, or between the $Lmna^{N195K/N195K}$and the $Emd^{-/Y}$counterparts (*P-value>0.05)* (Figure 13B). Densitometry data is represented as mean fold change ± SEM of six independent repeats.
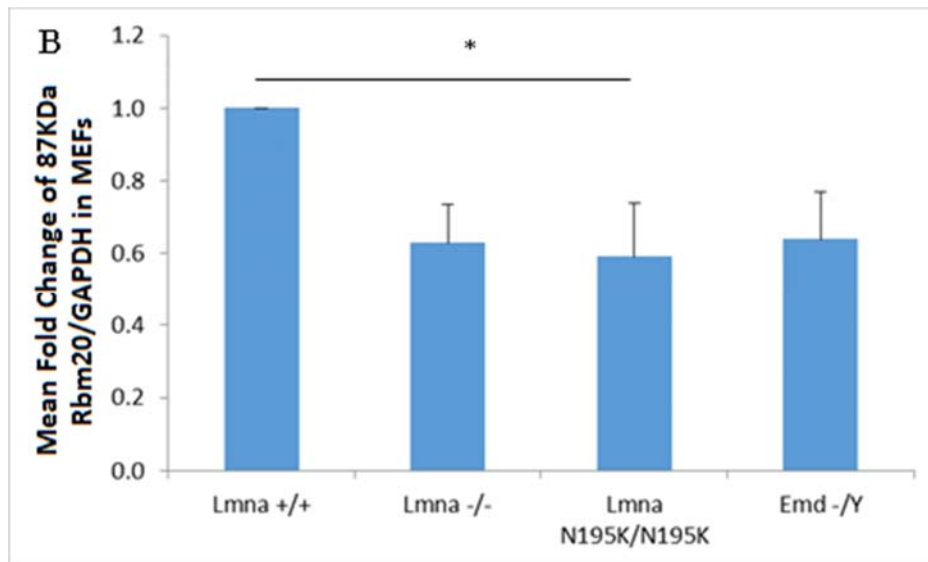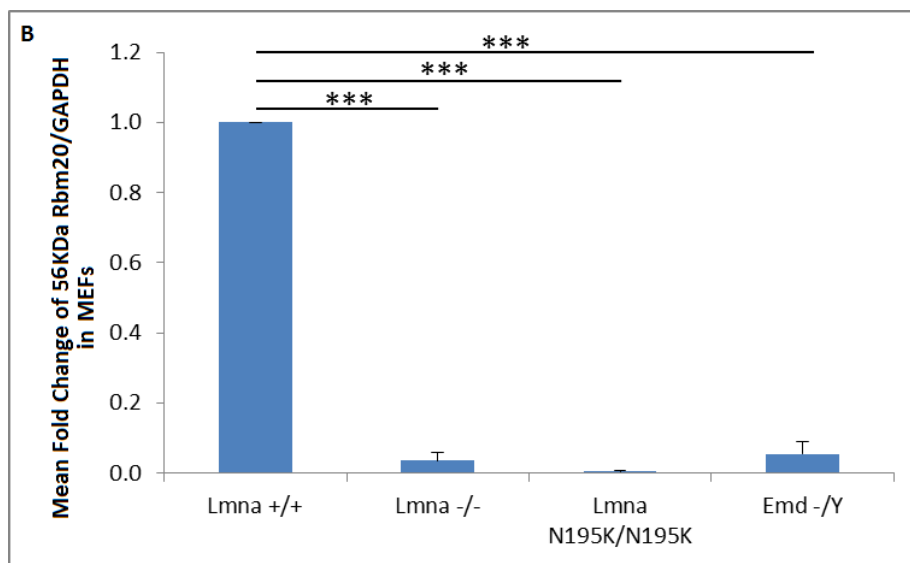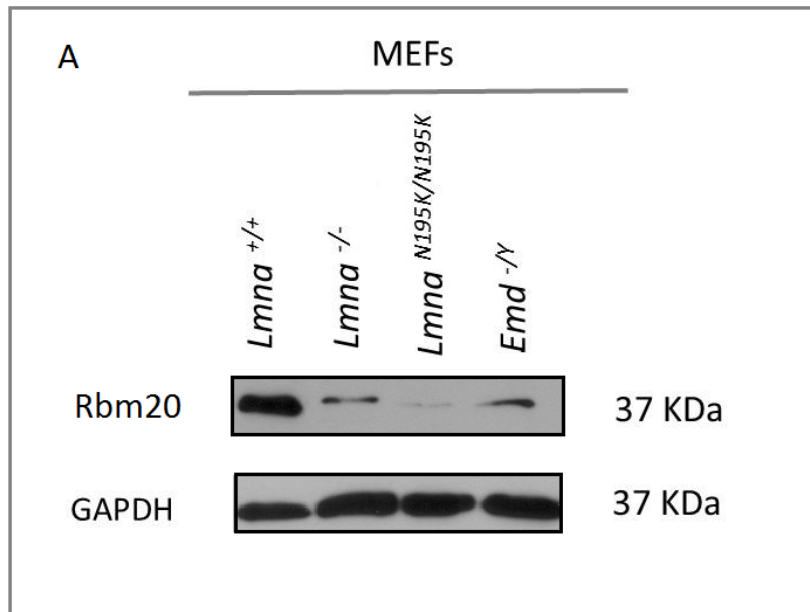
Figure 13| Western Blot analysis of the small Rbm20 isoform expression in *Lmna$^{-/-}$*, *Lmna$^{N195K/N195K}$* and *Emd$^{-/Y}$* mutant MEFs vs. control *Lmna$^{+/+}$* cells, cultured at 80% confluence. Panel (A); representative blot. Panel (B); Semi-quantification and analysis of the Rbm20 densitometry signal normalized to that of the GAPDH loading control reveals a statistically significant decrease in the 37-56kDa Rbm20 isoform expression between the *Lmna$^{-/-}$*, *Lmna$^{N195K/N195K}$* and *Emd$^{-/Y}$* mutant MEFs, when compared to the *Lmna$^{+/+}$* WT control cells cultured under baseline conditions. Data represent mean fold change ± SEM derived from 6 independent experiments. Three asterisks represents a statistical significance (*P-value <0.001*).

4. Total Rbm20 protein expression was reduced in the Lmna$^{N195K/N195K}$ and Emd$^{-/Y}$ mutant MEFs, but not significantly altered in Lmna$^{-/-}$ MEFs in comparison to the wild-type (WT) controls by immunofluorescence staining.

In order to further validate the reduction in the total Rbm20 protein observed by Western Blot analysis in the *Lmna$^{-/-}$, Lmna$^{N195K/N195K}$* and *Emd$^{-/Y}$* cells relative to the *Lmna$^{+/+}$* MEFs, we did immunofluorescence staining of PFA fixed cells with Rbm20 antibody. First, all cells were fixed with PFA after reaching 80% confluence. This was done while ensuring consistency in cell density and spreading among all tested samples and between independent repeats. Using the same exposure time and excitation wavelength, we obtained eight image frames for each cell line of the previously mentioned panel of MEFs. On average, 560 cells from each cell line were assessed. Semi-quantitative assessment of Rbm20 protein expression was performed using Image J software by measuring the relative fluorescence intensity of each cell normalized to the background for all tested samples. Fluorescent images were acquired in 2-D using laser confocal microscopy. The data indicates a significant down regulation in the protein expression of Rbm20 in *Lmna*-N195K MEFs with a 0.37-fold (± 0.09) reflecting a ~40% reduction in Rbm20 expression in comparison to the control WT MEFs (*P-value < 0.01*) (Figure 14B). Similarly, the immunofluorescence semi-quantification data also revealed a decline in the relative fluorescence intensity of Rbm20 in *Emd* - deficient MEFs. A 0.56-fold (±24) was quantified in these cells relevant to the WT controls. This reduction was not statistically significant (*P-value =0.06*) likely due to the high SEM. On the other hand, the reduction in the Rbm20 levels was less prominent in the *Lmna* null MEFs. The quantification of the

relative fluorescence intensity in the *Lmna*^{-/-} MEFs demonstrates a 0.83-fold (± 0.09) insignificant decrease relative to the WT controls (*P-value >0.05*) (Figure 14B).

When comparing the expression of Rbm20 between different mutant MEFs, a significant reduction was observed in the *Lmna*[N195K/N195K] cells compared to the *Lmna*[-/-,] (*P-value <0.05*). Conversely, there was no detected significant alteration in the expression levels of Rbm20 between the *Emd*-deficient MEFs and the *Lmna*-N195K homozygous mutants or the *Lmna*-deficient MEFs (*P-value >0.05*) (Figure 14B). Relative fluorescence intensity data is represented as mean fold change ± SEM of four independent repeats, with an average of 140 cells from each cell line, in each independent repeat (Figure 14B).
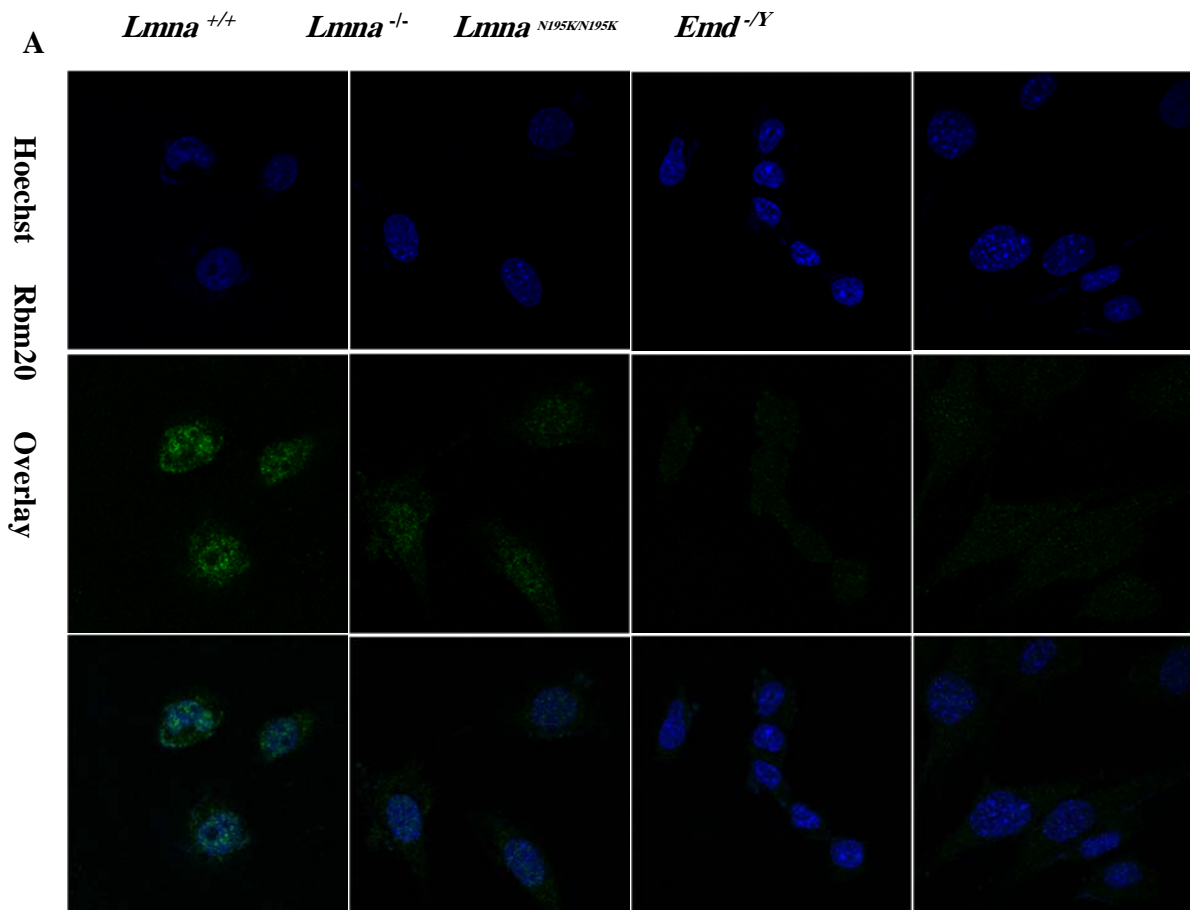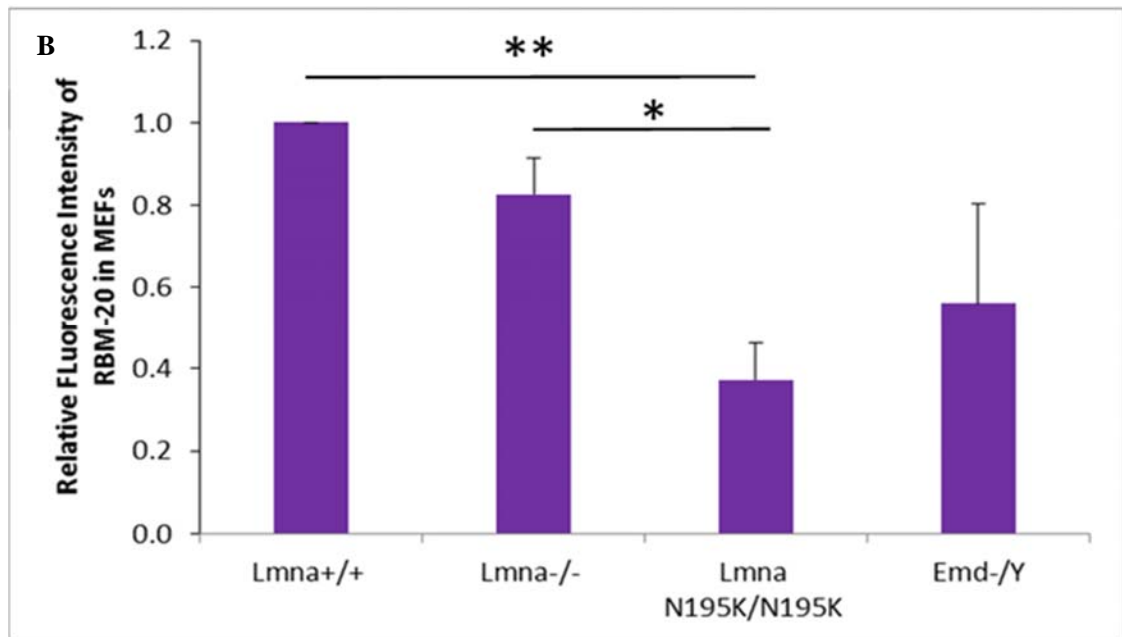
Figure 14| Immunofluorescence staining analysis of Rbm20 expression in *Lmna*^{-/-},
Lmna[N195K/N195K] and *Emd*[-/Y] mutant MEFs vs. control WT cells cultured at 80% confluence.
Images were acquired at 63x magnification. Panel (A); representative confocal microscope
images showing immunofluorescence staining of Rbm20 protein in MEF cells deficient in
A-type lamins and emerin, and in MEF cells expressing the N195K mutant form, in
comparison to the WT MEF cells. Hoechst stain was used to mark the nucleus (uppermost
panel). Semi-quantitative assessment of the relative fluorescence intensity of Rbm20
protein shows a reduction in the total Rbm20 expression in all mutant MEFs in comparison
to the WT cells. The reduction was shown to be statistically significant in MEFs derived
from mice homozygous for the N195K mutant form (DCM phenotype) (Panel B). Data
represent mean fold change ± SEM derived from 4 independent experiments, with an
average of 560 cells for each cell line. One asterisk represents a statistical significance
($P<0.05$). Two asterisk represents a statistical significance ($P<0.01$).

C. **Investigate putative alterations in the intracellular distribution of Rbm20 expression in mouse embryo fibroblast (MEF) cell lines derived from mice either lacking A-type lamin or emerin (EDMD phenotype), or homozygous for the *lmna-N195K* mutant form (DCM phenotype) versus wild-type (WT) controls by immunofluorescence staining**

1. *Cellular localization of Rbm20 protein is not significantly altered in Lmna$^{-/-}$, Lmna$^{N195K/N195K}$, and Emd$^{-/Y}$ mutant MEFs in comparison to the control Lmna$^{+/+}$ MEFs.*

   The same images used for the validation of the alteration in Rbm20 protein expression in the mutant MEFs were used here for the investigation of possible alteration in the intracellular localization of Rbm20 in the *Lmna$^{-/-}$, Lmna$^{N195K/N195K}$, and Emd$^{-/Y}$* MEFs compared to the WT controls. Qualitative analysis and nuclear to cytoplasmic scoring was performed visually, by observing and comparing the immunofluorescence stain for each individual cell. According to our observations, we subcategorized the pattern of Rbm20 expression into four categories: 1) Nuclear expression, 2) Nuclear > Cytoplasmic expression, 3) Nuclear = Cytoplasmic expression, and 4) Cytoplasmic expression (Figure 15 A, B, C, and D). Each cell was assigned to one of the four categories, and the total number of cells for each cell line, denoted to each category, was expressed as a percentage.

   Nuclear to cytoplasmic scoring and statistical analysis of the Rbm20 localization suggests that there exists no significant change in the localization of Rbm20 between *Lmna$^{-/-}$, Lmna$^{N195K/N195K}$* and *Emd$^{-/Y}$* mutant MEFs when compared to the WT cells, all cultured under baseline conditions (Figure 15E). Generally, we can state that the expression of

Rbm20 was preferentially restrained to the nucleus in all cell lines. The "Nuclear expression" category in the WT control MEFs was applicable to 41% of all cells, with somewhat comparable percentages of 44.4%, 45.7%, and 41.7% in the $Lmna^{-/-}$, $Lmna^{N195K/N195K}$ and $Emd^{-/Y}$ mutant MEFs respectively. There was no statistically significant difference in Rbm20 expression localization scores between the cell lines ($P\text{-}value>0.05$). Likewise, the "Nuclear > Cytoplasmic expression" category was also found to be insignificantly altered in all three mutant MEFs compared to the $Lmna^{+/+}$ control MEFs ($P\text{-}value>0.05$). 50.1% of all WT cells were assigned to this category, while 50.9% of $Lmna^{-/-}$, 50% of $Lmna^{N195K/N195K}$, and 55% of $Emd^{-/Y}$ mutant MEFs were fit under this group. The third category pertaining to Rbm20 protein expression localizing equally between the nucleus and the cytoplasm showed a slight insignificant reduction in the three mutants MEFs relative to the $Lmna^{+/+}$ WT controls ($P\text{-}value>0.05$). For this category, 4.4% of WT MEFs, 4.3% of the $Lmna^{-/-}$, 2.3% of the $Lmna^{N195K/N195K}$, and 3.3% of $Emd^{-/Y}$ mutant MEFs were scored. The fourth and final category representing the percentage of cells showing "Cytoplasmic expression" of Rbm20 included a minimal percentage of cells from all cell lines. Only 4.4% of all WT-MEFs, 0.4% of the $Lmna$-deficient MEFs, and 2% of the N195K homozygote MEFs were fit under this group. None of the Emd-deficient cells exhibited this localization. The difference in the percentages of cells from each cell line assigned to this category wasn't determined as statistically significant ($P\text{-}value>0.05$) (Figure 15E). Scoring analysis data is represented as mean percentages of four independent repeats. Each done in duplicates with an average of 140 cells per cell line in each repeat (Figure 14E).

87

A

Lmna^{+/+}   Lmna^{-/-} Lmna^{N195K/N195K}   Emd^{-/Y}

Hoechst   Rbm20   Overlay

B

Lmna^{+/+}   Lmna^{-/-}   Lmna^{N195K/N195K}   Emd^{-/Y}

Hoechst

Rbm20

Overlay

C

	Lmna $^{+/+}$	Lmna $^{-/-}$	Lmna $^{N195K/N195K}$	Emd $^{-/Y}$
Hoechst				
Rbm20				
Overlay				

D

	Lmna $^{+/+}$	Lmna $^{-/-}$	Lmna $^{N195K/N195K}$
Hoechst			
Rbm20			
Overlay			
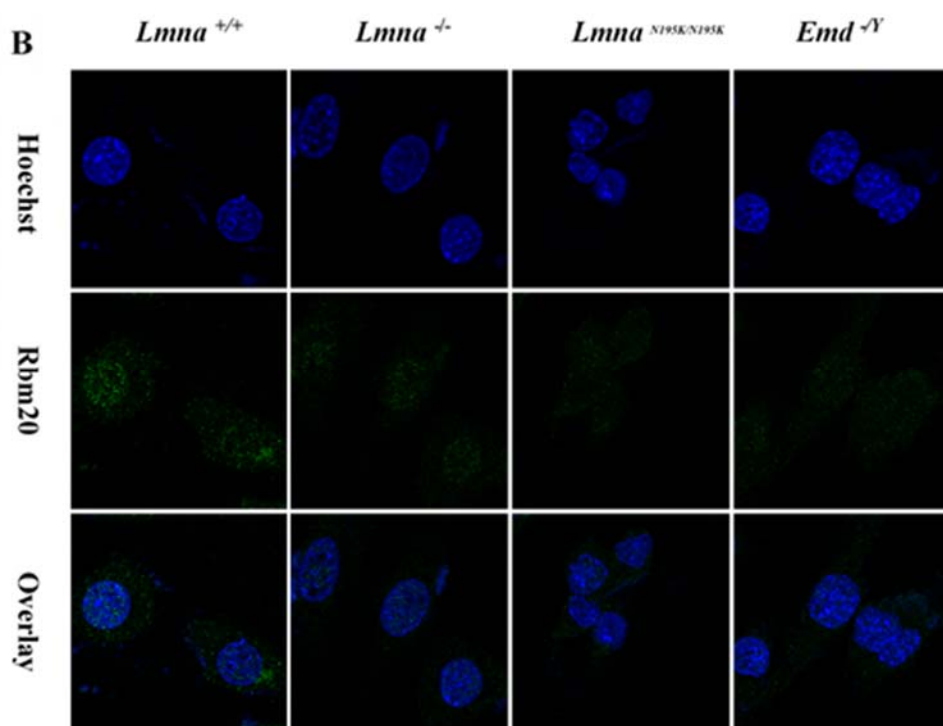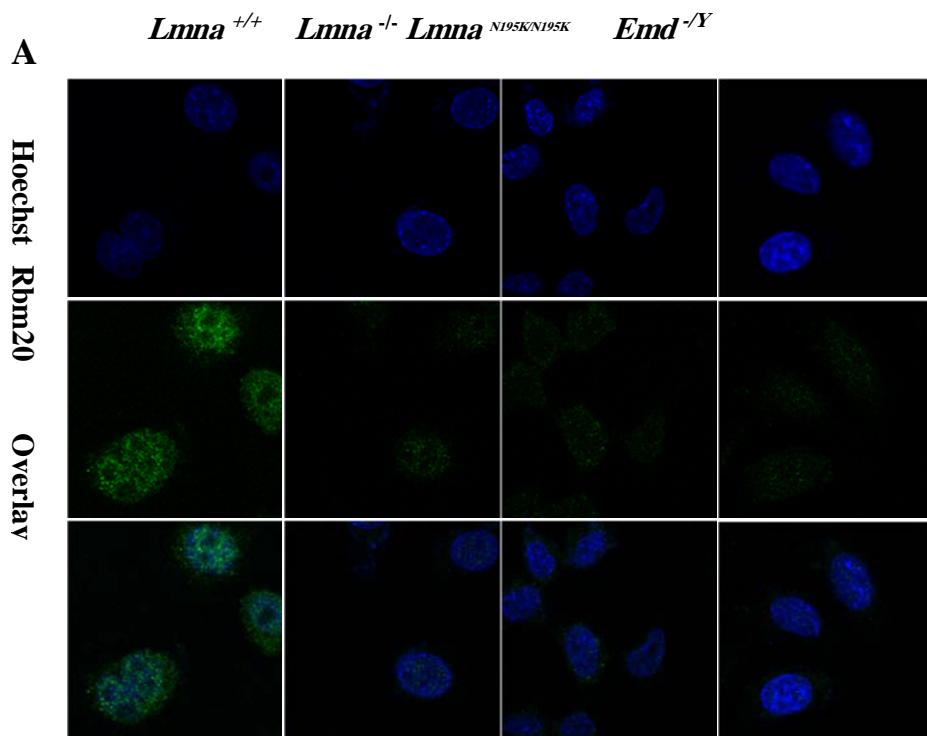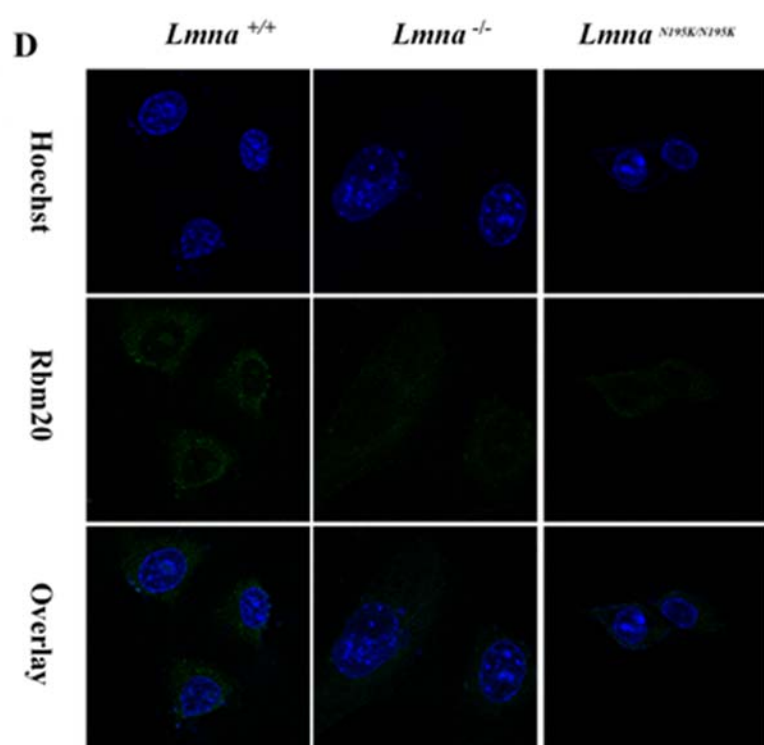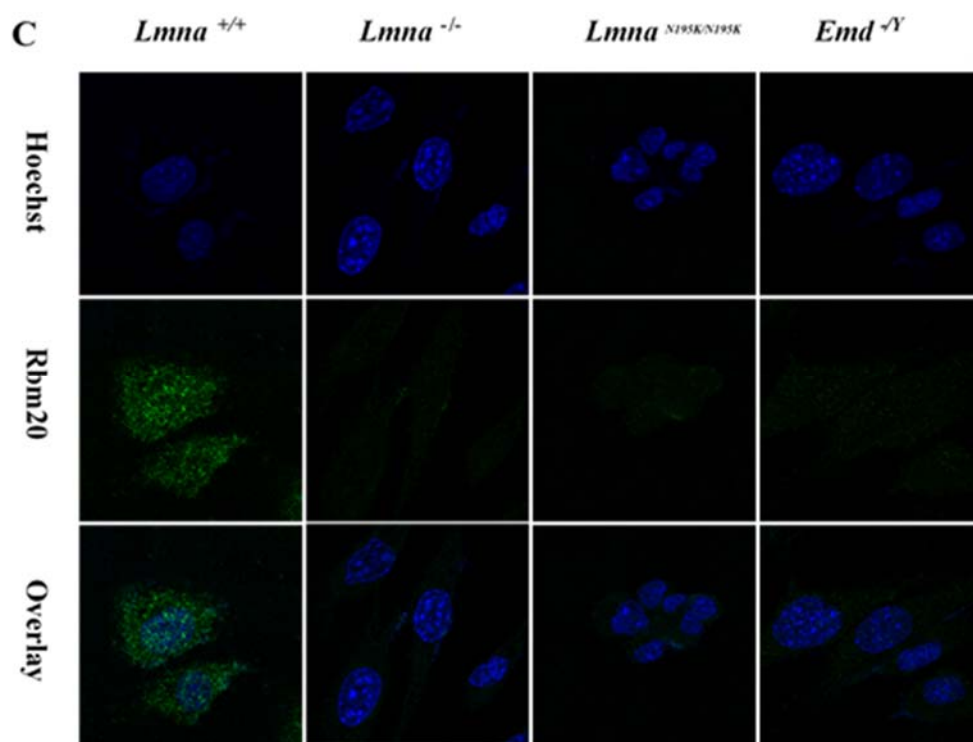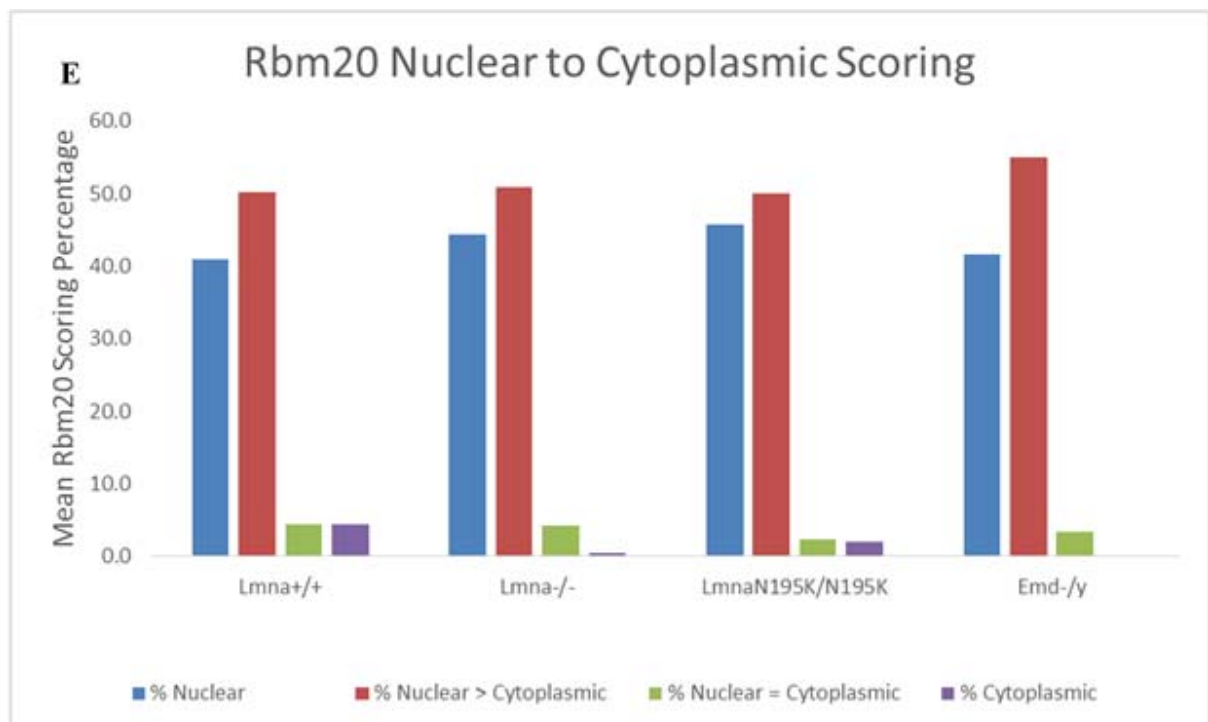
Figure 15| Nuclear to cytoplasmic scoring of Rbm20 protein expression in *Lmna*$^{-/-}$*, Lmna* $^{N195K/N195K}$, and *Emd*$^{-/Y}$ mutant MEFs vs. control *Lmna*$^{+/+}$ MEFs, cultured at 80% confluence. Images were acquired at 63x magnification. Nuclear to cytoplasmic scoring of Rbm20 protein expression localization as determined by immunofluorescence staining was assigned four categories. Panels A, B, C, and D are representative laser confocal microscope images showing respectively the "nuclear" pattern of Rbm20 protein expression, "nuclear >cytoplasmic" Rbm20 protein expression, "nuclear = cytoplasmic" protein expression and "cytoplasmic" expression of Rbm20 protein in lamin A/C- and emerin-deficient MEFs, and in MEF cells homozygous for the N195K mutation in *Lmna* relative to their WT control cells. Hoechst was used to stain the nuclei (uppermost panel). A strictly cytoplasmic expression of Rbm20 protein was not detected in the *Emd*$^{-/Y}$ MEFs. Visual scoring reveals no significant change in the intracellular localization of Rbm20

90

protein in the panel of mutant MEFs relative to the WT control cells (Panel E). Data represent mean percentages within each category derived from 4 independent repeats with an average of 560 cells scored for each cell line.

CHAPTER IV

DISCUSSION

Mutations in the *LMNA* gene lead to a diverse set of inherited tissue-specific pathologies including myopathies that affect both the heart and skeletal muscles. The question of how mutations in this single gene cause a broad spectrum of phenotypes have long been an area of interest, and scientists were able to propose and test several potential hypotheses. One of the leading cellular pathophysiological observations was the abnormal nuclear morphology associated with *LMNA* mutations. This led to the emergence of the "structural hypothesis", which postulates that *LMNA* mutations cause an increase in nuclear fragility and mechanical instability in cells undergoing mechanical stress, such as muscle cells. In addition, the altered desmin linkage of lamins to the cytoskeleton was found to associate with impaired contractility in dilated cardiomyopathy. These observations have led to the current model suggesting that the structural hypothesis probably explains the origin of the *LMNA*-related skeletal and cardiac muscle phenotypes. On the other hand, the

"gene regulation hypothesis" takes the functional roles of lamins into consideration. It states that mutations in *LMNA* lead to a disruption of gene regulation, and interaction with tissue-specific transcription factors. This takes place either directly, or through interacting inner nuclear membrane proteins. Consequently, vital regulatory cardiac genes are disrupted, contributing eventually to the observed phenotype. The cardiac muscle pathogenesis in emerin and lamin A/C related cardiomyopathies is likely multifold, as various nuclear functions are affected such as, gene expression, nuclear morphology and position, and many other cellular processes. In this study, we focused on RBM20, which was recently discovered to be defective in heritable cases of DCM. By virtue of its intracellular localization and functional role in cardiac muscles, we hypothesized that the disruption of lamin A/C and/or emerin may deregulate the expression and/or localization of RBM20, ultimately leading to the progression of the cardiac muscle phenotype in EDMD and DCM. In the context of the null or mutant *Lmna* and null *Emd* MEFs background, our data revealed a notable deregulation in Rbm20, in terms of transcript and protein expression, but not in its intracellular localization. This suggests the existence of a bio functional interplay between Rbm20, Lamin A/C and emerin.

When examining the transcriptional levels of *Rbm20*, our Real-Time PCR quantification data revealed a significant reduction in the *Rbm20* transcript levels in the *Lmna* and *Emd* null MEFs, as well as the *Lmna-N195K* mutant MEFs in comparison to the WT controls. It is worth noting that the specific primer pairs we used for quantification of Rbm20 transcript expression can recognize the mRNA sequences of 132 KDa full-length Rbm20 and the 75-87 KDa Rbm20 isoform. Moreover, the protein expression of Rbm20

was also downregulated in these cell lines when measured by Western Blot analysis and immunofluorescence staining. However, in these MEF cells and under the experimental parameters we used, we were unable to detect the full-length Rbm20 protein by Western Blot analysis. However, we were able to detect the smaller Rbm20 isoforms corresponding to the molecular weights of 75-87kDa and 37-56kDa, resulting from 2 different splice variants for *Rbm20* (that may also be subjected to further protein modifications and cleavage). In part, this could be due to inefficient extraction of the large molecular weight full-length form using standard RIPA lysis buffer to extract the proteins from total cell lysates. It is also worth noting that the full-length Rbm20 protein has been reported to primarily work on the splicing of genes that are related to cardiac muscle function, whereas our experiments were performed on mouse embryo fibroblast (MEF) cells. Thus, there could be tissue-specific expression of the Rbm20 splice variants vs. the full-length protein, hence favoring the expression of one isoform over the other according to the isoform-specific target genes in a given tissue or cell type. In the MEF cells, splice variants of Rbm20 may be favored over the full-length Rbm20. It is also plausible that the full-length Rbm20 protein gets expressed, but is then subjected to post-translational modifications and protein cleavage in MEF cells. Based on peptide similarity, it is estimated that Rbm20 has 4-to-8 peptide cleavage sites in its sequence. Nonetheless, both the full-length 132KDa protein and the 75-87kDa Rbm20 isoform have the same RNA recognition motif, suggesting that their splicing targets are probably the same. However, further investigation is needed to determine whether there are differences in Rbm20 isoform-specific splicing targets.

For the first aim of this study, the *Rbm20* transcript levels encoding for the 132kDa isoform were significantly reduced in the *Emd* null and *Lmna* null or mutant MEFs backgrounds. This reduction maybe linked to the role of the nuclear lamins in controlling gene expression through multiple mechanisms such as chromatin organization, epigenetic alteration, and regulation of transcription. Since the perturbation of the nuclear lamina leads to altered regulation of chromatin positioning and gene expression, it is likely that mutations in the *Lmna* and/or *Emd* change the configuration of chromatin, and hence the availability of *Rbm20*-specific transcription factors.

A recent study conducted by Beraldi and colleagues on embryonic bodies (EBs) with knock down of *Rbm20* expression, identified the *Mef2a* transcription factor as a direct splicing target of *Rbm20*. Three of the cardiac genes which are transcriptionally regulated by *Mef2a* were also differentially expressed in *Rbm20* deficient EBs including, *Act1,* the gene coding for actin *(*Beraldi et al., 2014). This correlates with the finding that actin dynamics are altered in *Lmna$^{-/-}$, Lmna$^{N195K/N195K}$*, and *Emd$^{-/y}$* mutant MEFs, and causes an impaired signaling of the megakaryoblastic leukemia 1(MKL1); a transcription factor that is essential for normal cardiac development and function (HO *et al*., 2013). Hence, our results, pertaining to the *Lmna*-dependent *Rbm20* expression might provide a plausible explanation for these changes in actin dynamics. Yet, further work needs to be done to complement these findings. First, it is necessary to confirm whether or not the reduction in *Rbm20* is a direct effect of the of *Lmna* and *Emd* disruption. For this, we could re-evaluate *Rbm20* transcript levels in the same MEFs panel after retroviral transfection, reintroducing *Lmna, Emd,* and different mutant forms of *Lmna*. Moreover, we could design primers that

94

are specific for the other two *Rbm20* splice variants, in order to determine possible alteration in the expression pattern, consistent with that found on the protein level. Our findings also need to be validated in lamin A/C and emerin null (or knock down) C2C12 myoblast cell line, and in H9C2 and HL-1 cardiomyocyte cell lines. Further assessment should be performed by qRT-PCR analysis on cardiac and skeletal tissue samples derived from *Lmna$^{-/-}$, Lmna$^{N195K/N195K}$*, and *Emd$^{-/y}$* mice in comparison to their WT and heterozygote littermates, age and gender matched.

As for the second aim of this study, WB densitometry analysis indicated an approximate 50% reduction in the total pool of detectable Rbm20 isoforms in the *Lmna$^{-/-}$, Lmna$^{N195K/N195K}$*, and *Emd$^{-/y}$* mutant MEFs compared to the *Lmna$^{+/+}$* MEFs. The reduction pattern of the 75-87kDa isoform was comparable to that of the overall protein, whereas the 37-56kDa isoform showed a minimal expression in all cell lines, and a more prominent decline in the expression levels in the mutant MEFs compared to the WT controls. The faint expression of the smallest isoform in all cell lines is likely due to the fact that this protein is a truncated protein, and transcription factors coding for it undergo nonsense - mediated decay. The different reduction levels obtained from each Rbm20 isoform in the cells either lacking lamin A/C, emerin, or expressing lamin-N195K mutant form indicates an alteration in the splicing of *Rbm20* itself. This is suggestive that the disruption in the nuclear lamina that results from lamin A/C or emerin deficiency not only impacts Rbm20 expression by reducing it, but it also affects the splicing of *Rbm20,* either by affecting the ability of Rbm20 to splice itself, or by affecting other splicing machinery responsible for the alternative splicing of *Rbm20.* From existing scientific literature, no studies have been done

95

to decipher the splicing mechanisms of Rbm20. Hence, further investigations should be done in that regard. The overall reduction in Rbm20 protein expression rules out the possibility that the reduced *Rbm20* transcript levels observed are due to increased translation of mRNA to protein. The reduction in *Rbm20* transcript levels noted in deficient or mutant lamin A/C or in emerin null background is concomitant with a reduction in the Rbm20 protein levels. It is plausible then that this reduction compromises the function of Rbm20 in the splicing of many cardiac target genes in the lamin A/C and emerin – associated cardiomyopathies. The *RBM20*-dependent post-transcriptional regulation and alternate splicing of the sarcomere structural *TTN* has been tested intensively. Interestingly, whole-exome sequencing (WES) of a family diagnosed with DCM revealed a doubly heterozygous mutation in both *LMNA* and *TTN* genes that is prevalent in those family members with the most severe cases (Roncarati et al., 2013). Moreover, lamin A was found to bind the C-terminus of nuclear titin, contributing to cardiac mechano-chemical transduction (Zastrow& Wilson, 2006). These findings, along with our results, suggest a role for RBM20 as a linker between mutations in A-type lamins and titin disruption that is leading to the cardiomyopathy phenotype. It would be interesting in future studies to test the possible direct or indirect interplay between lamin A/C, emerin, RBM20, and titin. Additionally, it is important to identify the specific cardiac targets for each Rbm20 isoform in order to attain a better assessment of the contribution of Rbm20 in lamin A/C and emerin related cardiomyopathies.

The findings from the analysis of immunofluorescence staining of Rbm20 expression in the tested MEF cell panel were generally consistent with the findings from

the Western Blot analysis in terms of reduced Rbm20 protein expression in the mutant MEFs vs. the WT controls. Nonetheless, for context-dependent validation of our findings, the expression of Rbm20 protein should be further assessed in C2C12 myoblast cells, and in cardiomyocyte cell lines with lamin A/C or emerin knockdown expression as well as in cardiac and skeletal muscle tissues derived from mice that are lacking *Lmna, Emd* or harboring variant *Lmna* mutations vs. their control littermates. Moreover, the relative expression of Rbm20 protein could be better quantified by performing cell-based or tissue-based ELISA assays in addition to Western Blot analysis, immunofluorescence and immunohistochemical staining.

On the other hand, the nuclear to cytoplasmic scoring of Rbm20 expression revealed no difference in the protein's localization, neither in the context of lamin A/C, nor with emerin disruption. It is worth noting that the acquired images were obtained in situ , and that the expression of Rbm20 was assessed in a planer, 2-D monolayer of cells. Hence, the results obtained here cannot be considered as conclusive by themselves. However, being somewhat consistent with the WB results, they provide support for the reduction of Rbm20 expression in the context of lamin A/C and emerin deficiency, and lamin-N195K mutation. This further confirms the necessity of an intact nuclear lamina for the proper functioning of Rbm20 in the splicing of its downstream cardiac-specific genes including, *Ttn* and *Mef2a* transcription factor.

As for the assessment of the localization of Rbm20 in the MEFs panel, our data suggests a very high nuclear retention of the Rbm20 expression compared to a very low occurrence of cytoplasmic expression in all four MEF cell lines. The fact that the

localization of Rbm20 depends on its phosphorylation state, and/or cell-cycle stage may explain the differential localization of Rbm20 in the same cell line, given that the fixed cells are not synchronized. When comparing the expression between different cell lines, no detectable difference was observed in the localization of Rbm20 in the mutant MEFs compared to the WT controls. This diminishes the prospects that A-type lamins and/or emerin may play a role in the delocalization of Rbm20 within the cell. Hence, suggesting that the lamin A/C and/or emerin related cardiomyopathy is associated with a reduction in the expression, but not with an altered localization of the Rbm20 protein. For future validation, immunofluorescence staining could be performed on C2C12 myoblasts and cardiomyocyte cell lines with lamin A/C or emerin knockdown as well as in cardiac and skeletal tissues derived from $Lmna^{-/-}$, $Lmna^{N195K/N195K}$, and $Emd^{-/y}$ mice compared to their WT and heterozygote littermate controls.

Our findings provide insight into the wide range of defects that result from mutations in the nuclear envelope proteins. In this study, we provide evidence that the proper expression (and hence function) of Rbm20 is reliant, at least in part, on an intact nuclear lamina. The validation of our findings in myocyte cells as well as in cardiac and skeletal muscle tissues would be essential to delineate the temporal sequential deregulations in Rbm20 expression and function that are implicated in lamin A/C and emerin related cardiomyopathies.

REFERENCES

Aaronson, R. P., & Blobel, G. (1975).Isolation of nuclear pore complexes in association with a lamina. *Proceedings of the National Academy of Sciences of the United States of America, 72*(3), 1007-1011.

Aebi, U., Cohn, J., Buhle, L., & Gerace, L. (1986). The nuclear lamina is a meshwork of intermediate-type filaments. *Nature, 323*(6088), 560-564.

Al-Haggar, M., Madej-Pilarczyk, A., Kozlowski, L., Bujnicki, J. M., Yahia, S., Abdel-Hadi, D., et al. (2012). A novel homozygous p.Arg527Leu LMNA mutation in two unrelated egyptian families causes overlapping mandibuloacral dysplasia and progeria syndrome. European Journal of Human Genetics : EJHG, 20(11), 1134-1140.

Arbustini, E., Narula, N., Tavazzi, L., Serio, A., Grasso, M., Favalli, V., et al. (2014).The MOGE(S) classification of cardiomyopathy for clinicians. *Journal of the American College of Cardiology, 64*(3), 304-318.

Arbustini, E., Pilotto, A., Repetto, A., Grasso, M., Negri, A., Diegoli, M., et al. (2002). Autosomal dominant dilated cardiomyopathy with atrioventricular block: A lamin A/C defect-related disease. *Journal of the American College of Cardiology, 39*(6), 981-990.

Azzedine, H., Senderek, J., Rivolta, C., & Chrast, R. (2012). Molecular genetics of charcot-marie-tooth disease: From genes to genomes. *Molecular Syndromology, 3*(5), 204-214.

Beraldi, R., Li, X., Martinez Fernandez, A., Reyes, S., Secreto, F., Terzic, A., et al. (2014). Rbm20-deficient cardiogenesis reveals early disruption of RNA processing and sarcomere remodeling establishing a developmental etiology for dilated cardiomyopathy. *Human Molecular Genetics, 23*(14), 3779-3791.

Bione, S., Maestrini, E., Rivella, S., Mancini, M., Regis, S., Romeo, G., et al. (1994). Identification of a novel X-linked gene responsible for emery-dreifuss muscular dystrophy. *Nature Genetics, 8*(4), 323-327.

Bonne, G., & Quijano-Roy, S. (2013). Emery-dreifuss muscular dystrophy, laminopathies, and other nuclear envelopathies. *Handbook of Clinical Neurology, 113*, 1367-1376.

Brauch, K. M., Karst, M. L., Herron, K. J., de Andrade, M., Pellikka, P. A., Rodeheffer, R. J., et al. (2009). Mutations in ribonucleic acid binding protein gene cause familial dilated cardiomyopathy. *Journal of the American College of Cardiology, 54*(10), 930-941.

Burke, B., & Stewart, C. L. (2013). The nuclear lamins: Flexibility in function. *Nature Reviews.Molecular Cell Biology, 14*(1), 13-24.

Cahill, T. J., Ashrafian, H., & Watkins, H. (2013).Genetic cardiomyopathies causing heart failure. *Circulation Research, 113*(6), 660-675.

Cao, H., & Hegele, R. A. (2000). Nuclear lamin A/C R482Q mutation in canadian kindreds with

Capell, B. C., & Collins, F. S. (2006). Human laminopathies: Nuclei gone genetically awry. *Nature Reviews.Genetics, 7*(12), 940-952.

Caron, M., Auclair, M., Donadille, B., Bereziat, V., Guerci, B., Laville, M., et al. (2007). Human lipodystrophies linked to mutations in A-type lamins and to HIV protease inhibitor therapy are both associated with prelamin A accumulation, oxidative stress and premature cellular senescence. *Cell Death and Differentiation, 14*(10), 1759-1767.

Chen, L., Lee, L., Kudlow, B. A., Dos Santos, H. G., Sletvold, O., Shafeghati, Y., et al. (2003). LMNA mutations in atypical werner's syndrome. *Lancet (London, England), 362*(9382), 440-445.

Collas, P., Thompson, L., Fields, A. P., Poccia, D. L., & Courvalin, J. C. (1997).Protein kinase C-mediated interphase lamin B phosphorylation and solubilization. *The Journal of Biological Chemistry, 272*(34), 21274-21280.

Colwill, K., Pawson, T., Andrews, B., Prasad, J., Manley, J. L., Bell, J. C., et al. (1996). The Clk/Sty protein kinase phosphorylates SR splicing factors and regulates their intranuclear distribution. *The EMBO Journal, 15*(2), 265-275.

De Maria, E., Patrizi, G., & Cappelli, S. (2015). Proarrhythmic effect of 'reverse mode switch' in a patient with dilated cardiomyopathy and drug-induced long QTc interval.Europace : European Pacing, Arrhythmias, and Cardiac Electrophysiology : Journal of the Working Groups on Cardiac Pacing, Arrhythmias, and Cardiac Cellular Electrophysiology of the European Society of Cardiology, 17(3), 423.

De Sandre-Giovannoli, A., Chaouch, M., Kozlov, S., Vallat, J. M., Tazir, M., Kassouri, N., et al. (2002). Homozygous defects in LMNA, encoding lamin A/C nuclear-envelope proteins, cause autosomal recessive axonal neuropathy in human (charcot-marie-tooth disorder type 2) and mouse. *American Journal of Human Genetics, 70*(3), 726-736.

Dechat, T., Adam, S. A., Taimen, P., Shimi, T., & Goldman, R. D. (2010). Nuclear lamins.*Cold Spring Harbor Perspectives in Biology, 2*(11), a000547.

Dechat, T., Pfleghaar, K., Sengupta, K., Shimi, T., Shumaker, D. K., Solimando, L., et al. (2008). Nuclear lamins: Major factors in the structural organization and function of the nucleus and chromatin. *Genes & Development, 22*(7), 832-853.

Dellefave, L., & McNally, E. M. (2010).The genetics of dilated cardiomyopathy. *Current Opinion in Cardiology, 25*(3), 198-204.

Depreux, F. F., Puckelwartz, M. J., Augustynowicz, A., Wolfgeher, D., Labno, C. M., Pierre-Louis, D., et al. (2015).Disruption of the lamin A and matrin-3 interaction by myopathic LMNA mutations. *Human Molecular Genetics, 24*(15), 4284-4295.

Dittmer, T. A., & Misteli, T. (2011).The lamin protein family.*Genome Biology, 12*(5), 222-2011-12-5-222. Epub 2011 May 31.

Dorner, D., Gotzmann, J., & Foisner, R. (2007). Nucleoplasmic lamins and their interaction partners, LAP2alpha, rb, and BAF, in transcriptional regulation. *The FEBS Journal, 274*(6), 1362-1373.

Dwyer, N., & Blobel, G. (1976).A modified procedure for the isolation of a pore complex-lamina fraction from rat liver nuclei. *The Journal of Cell Biology, 70*(3), 581-591.

Earnshaw, W. C. (1995). Nuclear changes in apoptosis. *Current Opinion in Cell Biology, 7*(3), 337-343.

Ellis, J. A. (2006). Emery-dreifuss muscular dystrophy at the nuclear envelope: 10 years on. *Cellular and Molecular Life Sciences : CMLS, 63*(23), 2702-2709.

Evila, A., Vihola, A., Sarparanta, J., Raheem, O., Palmio, J., Sandell, S., et al. (2014).Atypical phenotypes in titinopathies explained by second titin mutations. *Annals of Neurology, 75*(2), 230-240.

Favreau, C., Higuet, D., Courvalin, J. C., & Buendia, B. (2004). Expression of a mutant lamin A that causes emery-dreifuss muscular dystrophy inhibits in vitro differentiation of C2C12 myoblasts. *Molecular and Cellular Biology, 24*(4), 1481-1492.

Fisher, D. Z., Chaudhary, N., & Blobel, G. (1986). cDNA sequencing of nuclear lamins A and C reveals primary and secondary structural homology to intermediate filament proteins. *Proceedings of the National Academy of Sciences of the United States of America, 83*(17), 6450-6454.

Frock, R. L., Kudlow, B. A., Evans, A. M., Jameson, S. A., Hauschka, S. D., & Kennedy, B. K. (2006). Lamin A/C and emerin are critical for skeletal muscle satellite cell differentiation. *Genes & Development, 20*(4), 486-500.

Furukawa, K., Inagaki, H., & Hotta, Y. (1994).Identification and cloning of an mRNA coding for a germ cell-specific A-type lamin in mice. *Experimental Cell Research, 212*(2), 426-430.

Garcia-Blanco, M. A., Baraniak, A. P., & Lasda, E. L. (2004).Alternative splicing in disease and therapy. *Nature Biotechnology, 22*(5), 535-546.

Garg, A. (2004). Acquired and inherited lipodystrophies. *The New England Journal of Medicine, 350*(12), 1220-1234.

Gerace, L., Blum, A., & Blobel, G. (1978).Immunocytochemical localization of the major polypeptides of the nuclear pore complex-lamina fraction.interphase and mitotic distribution. *The Journal of Cell Biology, 79*(2 Pt 1), 546-566.

Gerace, L., Comeau, C., & Benson, M. (1984).Organization and modulation of nuclear lamina structure. *Journal of Cell Science.Supplement, 1*, 137-160.

Gerstberger, S., Hafner, M., Ascano, M., & Tuschl, T. (2014).Evolutionary conservation and expression of human RNA-binding proteins and their role in human genetic disease. *Advances in Experimental Medicine and Biology, 825*, 1-55.

102

Ghosh, G., & Adams, J. A. (2011).Phosphorylation mechanism and structure of serine-arginine protein kinases. *The FEBS Journal, 278*(4), 587-597.

Goldman, R. D., Goldman, A. E., & Shumaker, D. K. (2005). Nuclear lamins: Building blocks of nuclear structure and function.*Novartis Foundation Symposium, 264*, 3-16; discussion 16-21, 227-30.

Gruenbaum, Y., Margalit, A., Goldman, R. D., Shumaker, D. K., & Wilson, K. L. (2005). The nuclear lamina comes of age. *Nature Reviews.Molecular Cell Biology, 6*(1), 21-31.

Guo, W., Schafer, S., Greaser, M. L., Radke, M. H., Liss, M., Govindarajan, T., et al. (2012). RBM20, a gene for hereditary cardiomyopathy, regulates titin splicing. *Nature Medicine, 18*(5), 766-773.

Hasty, P., Campisi, J., Hoeijmakers, J., van Steeg, H., & Vijg, J. (2003). Aging and genome maintenance: Lessons from the mouse? *Science (New York, N.Y.), 299*(5611), 1355-1359.

Hisama, F. M., Kubisch, C., Martin, G. M., & Oshima, J. (2012). Clinical utility gene card for: Werner syndrome. *European Journal of Human Genetics : EJHG, 20*(5), 10.1038/ejhg.2011.265. Epub 2012 Jan 18.

Ho, C. Y., Jaalouk, D. E., Vartiainen, M. K., & Lammerding, J. (2013). Lamin A/C and emerin regulate MKL1-SRF activity by modulating actin dynamics. *Nature, 497*(7450), 507-511.

Ho, C. Y., & Lammerding, J. (2012). Lamins at a glance. *Journal of Cell Science, 125*(Pt 9), 2087-2093.

Holt, I., Ostlund, C., Stewart, C. L., Man, N., Worman, H. J., & Morris, G. E. (2003). Effect of pathogenic mis-sense mutations in lamin A on its interaction with emerin in vivo. *Journal of Cell Science, 116*(Pt 14), 3027-3035.

Houben, F., Ramaekers, F. C., Snoeckx, L. H., & Broers, J. L. (2007).Role of nuclear lamina-cytoskeleton interactions in the maintenance of cellular strength. *Biochimica Et Biophysica Acta, 1773*(5), 675-686.

Hutchison, C. J., Alvarez-Reyes, M., & Vaughan, O. A. (2001). Lamins in disease: Why do ubiquitously expressed nuclear envelope proteins give rise to tissue-specific disease phenotypes? *Journal of Cell Science, 114*(Pt 1), 9-19.

Jaalouk, D. E., & Lammerding, J. (2009). Mechanotransduction gone awry. *Nature Reviews.Molecular Cell Biology, 10*(1), 63-73.

Jackson, S. N., Howlett, T. A., McNally, P. G., O'Rahilly, S., & Trembath, R. C. (1997). Dunnigan-kobberling syndrome: An autosomal dominant form of partial lipodystrophy.*QJM : Monthly Journal of the Association of Physicians, 90*(1), 27-36.

Kalsotra, A., Xiao, X., Ward, A. J., Castle, J. C., Johnson, J. M., Burge, C. B., et al. (2008). A postnatal switch of CELF and MBNL proteins reprograms alternative splicing in the developing heart. *Proceedings of the National Academy of Sciences of the United States of America, 105*(51), 20333-20338.

Kapinos, L. E., Schumacher, J., Mucke, N., Machaidze, G., Burkhard, P., Aebi, U., et al. (2010). Characterization of the head-to-tail overlap complexes formed by human lamin A, B1 and B2 "half-minilamin" dimers. *Journal of Molecular Biology, 396*(3), 719-731.

Kelemen, O., Convertini, P., Zhang, Z., Wen, Y., Shen, M., Falaleeva, M., et al. (2013). Function of alternative splicing. *Gene, 514*(1), 1-30.

Kong, S. W., Hu, Y. W., Ho, J. W., Ikeda, S., Polster, S., John, R., et al. (2010). Heart failure-associated changes in RNA splicing of sarcomere genes. *Circulation.Cardiovascular Genetics, 3*(2), 138-146.

Krajewski, K. M., Lewis, R. A., Fuerst, D. R., Turansky, C., Hinderer, S. R., Garbern, J., et al. (2000). Neurological dysfunction and axonal degeneration in charcot-marie-tooth disease type 1A.*Brain : A Journal of Neurology, 123 (Pt 7)*(Pt 7), 1516-1527.

Ku, L., Feiger, J., Taylor, M., Mestroni, L., & Familial Cardiomyopathy Registry.(2003). Cardiology patient page.familial dilated cardiomyopathy.*Circulation, 108*(17), e118-21.

Kumaran, R. I., Muralikrishna, B., & Parnaik, V. K. (2002). Lamin A/C speckles mediate spatial organization of splicing factor compartments and RNA polymerase II transcription. The Journal of Cell Biology, 159(5), 783-793.

Lammerding, J., Schulze, P. C., Takahashi, T., Kozlov, S., Sullivan, T., Kamm, R. D., et al. (2004). Lamin A/C deficiency causes defective nuclear mechanics and mechanotransduction. *The Journal of Clinical Investigation, 113*(3), 370-378.

Lattanzi, G., Benedetti, S., Bertini, E., Boriani, G., Mazzanti, L., Novelli, G., et al. (2011). Laminopathies: Many diseases, one gene. report of the first italian meeting course on laminopathies. *Acta Myologica : Myopathies and Cardiomyopathies : Official Journal of the Mediterranean Society of Myology / Edited by the Gaetano Conte Academy for the Study of Striated Muscle Diseases, 30*(2), 138-143.

Lee, K. K., Haraguchi, T., Lee, R. S., Koujin, T., Hiraoka, Y., & Wilson, K. L. (2001). Distinct functional domains in emerin bind lamin A and DNA-bridging protein BAF. *Journal of Cell Science, 114*(Pt 24), 4567-4573.

Lenz-Bohme, B., Wismar, J., Fuchs, S., Reifegerste, R., Buchner, E., Betz, H., et al. (1997). Insertional mutation of the drosophila nuclear lamin Dm0 gene results in defective nuclear envelopes, clustering of nuclear pore complexes, and accumulation of annulate lamellae. *The Journal of Cell Biology, 137*(5), 1001-1016.

Li, D., Morales, A., Gonzalez-Quintana, J., Norton, N., Siegfried, J. D., Hofmeyer, M., et al. (2010).Identification of novel mutations in RBM20 in patients with dilated cardiomyopathy. *Clinical and Translational Science, 3*(3), 90-97.

Lincz, L. F. (1998). Deciphering the apoptotic pathway: All roads lead to death. *Immunology and Cell Biology, 76*(1), 1-19.

Linke, W. A., & Bucker, S. (2012). King of hearts: A splicing factor rules cardiac proteins. *Nature Medicine, 18*(5), 660-661.

Liu, B., & Zhou, Z. (2008).Lamin A/C, laminopathies and premature ageing. Histology and Histopathology, 23(6), 747-763.

Liu, G. H., Barkho, B. Z., Ruiz, S., Diep, D., Qu, J., Yang, S. L., et al. (2011). Recapitulation of premature ageing with iPSCs from hutchinson-gilford progeria syndrome. Nature, 472(7342), 221-225.

Lombardi, M. L., & Lammerding, J. (2011).Keeping the LINC: The importance of nucleocytoskeletal coupling in intracellular force transmission and cellular function. Biochemical Society Transactions, 39(6), 1729-1734.

Lu, J. T., Muchir, A., Nagy, P. L., & Worman, H. J. (2011). LMNA cardiomyopathy: Cell biology and genetics meet clinical medicine. *Disease Models & Mechanisms, 4*(5), 562-568.

Maatz, H., Jens, M., Liss, M., Schafer, S., Heinig, M., Kirchner, M., et al. (2014). RNA-binding protein RBM20 represses splicing to orchestrate cardiac pre-mRNA processing.*The Journal of Clinical Investigation, 124*(8), 3419-3430.

Makarenko, I., Opitz, C. A., Leake, M. C., Neagoe, C., Kulke, M., Gwathmey, J. K., et al. (2004). Passive stiffness changes caused by upregulation of compliant titin isoforms in human dilated cardiomyopathy hearts. *Circulation Research, 95(7),* 708-716.

Margalit, A., Vlcek, S., Gruenbaum, Y., & Foisner, R. (2005). Breaking and making of the nuclear envelope. *Journal of Cellular Biochemistry, 95*(3), 454-465.

Markiewicz, E., Ledran, M., & Hutchison, C. J. (2005). Remodelling of the nuclear lamina and nucleoskeleton is required for skeletal muscle differentiation in vitro. *Journal of Cell Science, 118*(Pt 2), 409-420.

Martonfalvi, Z., Bianco, P., Linari, M., Caremani, M., Nagy, A., Lombardi, V., et al. (2014). Low-force transitions in single titin molecules reflect a memory of contractile history. *Journal of Cell Science, 127*(Pt 4), 858-870.

Mateos, J., De la Fuente, A., Lesende-Rodriguez, I., Fernandez-Pernas, P., Arufe, M. C., & Blanco, F. J. (2013). Lamin A deregulation in human mesenchymal stem cells promotes an impairment in their chondrogenic potential and imbalance in their response to oxidative stress. Stem Cell Research, 11(3), 1137-1148.

Mattout, A., Dechat, T., Adam, S. A., Goldman, R. D., & Gruenbaum, Y. (2006). Nuclear lamins, diseases and aging. *Current Opinion in Cell Biology, 18*(3), 335-341.

McKeon, F. D., Kirschner, M. W., & Caput, D. (1986).Homologies in both primary and secondary structure between nuclear envelope and intermediate filament proteins. *Nature, 319*(6053), 463-468.

Melcon, G., Kozlov, S., Cutler, D. A., Sullivan, T., Hernandez, L., Zhao, P., et al. (2006). Loss of emerin at the nuclear envelope disrupts the Rb1/E2F and MyoD pathways during muscle regeneration. *Human Molecular Genetics, 15*(4), 637-651.

Mishra, S., Gray, C. B., Miyamoto, S., Bers, D. M., & Brown, J. H. (2011). Location matters: Clarifying the concept of nuclear and cytosolic CaMKII subtypes. *Circulation Research, 109*(12), 1354-1362.

Misteli, T., Caceres, J. F., & Spector, D. L. (1997).The dynamics of a pre-mRNA splicing factor in living cells. Nature, 387(6632), 523-527.

Molloy, S., & Little, M. (1992).p34cdc2 kinase-mediated release of lamins from nuclear ghosts is inhibited by cAMP-dependent protein kinase. *Experimental Cell Research, 201*(2), 494-499.

Morimoto, S., Lu, Q. W., Harada, K., Takahashi-Yanaga, F., Minakami, R., Ohta, M., et al. (2002).Ca(2+)-desensitizing effect of a deletion mutation delta K210 in cardiac troponin T that causes familial dilated cardiomyopathy. *Proceedings of the National Academy of Sciences of the United States of America, 99*(2), 913-918.

Mounkes, L. C., Kozlov, S. V., Rottman, J. N., & Stewart, C. L. (2005). Expression of an LMNA-N195K variant of A-type lamins results in cardiac conduction defects and death in mice. *Human Molecular Genetics, 14*(15), 2167-2180.

Muchir, A., Pavlidis, P., Bonne, G., Hayashi, Y. K., & Worman, H. J. (2007). Activation of MAPK in hearts of EMD null mice: Similarities between mouse models of X-linked and autosomal dominant emery dreifuss muscular dystrophy. *Human Molecular Genetics, 16*(15), 1884-1895.

Mueller and Hertel 2011, http://jeeves.mmg.uci.edu/hertel/pdfs/MuellerHertel11.pdf

Neagoe, C., Kulke, M., del Monte, F., Gwathmey, J. K., de Tombe, P. P., Hajjar, R. J., et al. (2002). Titin isoform switch in ischemic human heart disease. *Circulation, 106*(11), 1333-1341.

Novelli, G., Muchir, A., Sangiuolo, F., Helbling-Leclerc, A., D'Apice, M. R., Massart, C., et al. (2002). Mandibuloacral dysplasia is caused by a mutation in LMNA-encoding lamin A/C. *American Journal of Human Genetics, 71*(2), 426-431.

Osmanagic-Myers, S., Dechat, T., & Foisner, R. (2015). Lamins at the crossroads of mechanosignaling. *Genes & Development, 29*(3), 225-237.

Pajerowski, J. D., Dahl, K. N., Zhong, F. L., Sammak, P. J., & Discher, D. E. (2007). Physical plasticity of the nucleus in stem cell differentiation. *Proceedings of the National Academy of Sciences of the United States of America, 104*(40), 15619-15624.

Parvari, R., & Levitas, A. (2012). The mutations associated with dilated cardiomyopathy.*Biochemistry Research International, 2012*, 639250.

Peric-Hupkes, D., Meuleman, W., Pagie, L., Bruggeman, S. W., Solovei, I., Brugman, W., et al. (2010). Molecular maps of the reorganization of genome-nuclear lamina interactions during differentiation. *Molecular Cell, 38*(4), 603-613.

Peter, M., Nakagawa, J., Doree, M., Labbe, J. C., & Nigg, E. A. (1990).In vitro disassembly of the nuclear lamina and M phase-specific phosphorylation of lamins by cdc2 kinase. *Cell, 61*(4), 591-602.

Prokocimer, M., Barkan, R., & Gruenbaum, Y. (2013).Hutchinson-gilford progeria syndrome through the lens of transcription.*Aging Cell, 12*(4), 533-543.

Puckelwartz, M. J., Depreux, F. F., & McNally, E. M. (2011).Gene expression, chromosome position and lamin A/C mutations. *Nucleus (Austin, Tex.), 2*(3), 162-167.

Rankin, J., & Ellard, S. (2006). The laminopathies: A clinical review. *Clinical Genetics, 70*(4), 261-274.

Refaat, M. M., Lubitz, S. A., Makino, S., Islam, Z., Frangiskakis, J. M., Mehdi, H., et al. (2012). Genetic variation in the alternative splicing regulator RBM20 is associated

with dilated cardiomyopathy. *Heart Rhythm : The Official Journal of the Heart Rhythm Society, 9*(3), 390-396.

Report of the WHO/ISFC task force on the definition and classification of cardiomyopathies.(1980). *British Heart Journal, 44*(6), 672-673.

Roncarati, R., Viviani Anselmi, C., Krawitz, P., Lattanzi, G., von Kodolitsch, Y., Perrot, A., et al. (2013). Doubly heterozygous LMNA and TTN mutations revealed by exome sequencing in a severe form of dilated cardiomyopathy. *European Journal of Human Genetics : EJHG, 21*(10), 1105-1111.

Ruchaud, S., Korfali, N., Villa, P., Kottke, T. J., Dingwall, C., Kaufmann, S. H., et al. (2002). Caspase-6 gene disruption reveals a requirement for lamin A cleavage in apoptotic chromatin condensation. *The EMBO Journal, 21*(8), 1967-1977.

Sarkar, P. K., & Shinton, R. A. (2001).Hutchinson-guilford progeria syndrome. *Postgraduate Medical Journal, 77*(907), 312-317.

Schirmer, E. C., & Gerace, L. (2002). Organellar proteomics: The prizes and pitfalls of opening the nuclear envelope.*Genome Biology, 3*(4), REVIEWS1008.

Senderek, J., Garvey, S. M., Krieger, M., Guergueltcheva, V., Urtizberea, A., Roos, A., et al. (2009). Autosomal-dominant distal myopathy associated with a recurrent missense mutation in the gene encoding the nuclear matrix protein, matrin 3. *American Journal of Human Genetics, 84*(4), 511-518.

Shackleton, S., Lloyd, D. J., Jackson, S. N., Evans, R., Niermeijer, M. F., Singh, B. M., et al. (2000). LMNA, encoding lamin A/C, is mutated in partial lipodystrophy. *Nature Genetics, 24*(2), 153-156.

Shimi, T., & Goldman, R. D. (2014).Nuclear lamins and oxidative stress in cell proliferation and longevity. *Advances in Experimental Medicine and Biology, 773*, 415-430.

Smigiel, R., Jakubiak, A., Esteves-Vieira, V., Szela, K., Halon, A., Jurek, T., et al. (2010). Novel frameshifting mutations of the ZMPSTE24 gene in two siblings affected with restrictive dermopathy and review of the mutations described in the literature. *American Journal of Medical Genetics.Part A, 152A*(2), 447-452.

Somech, R., Shaklai, S., Amariglio, N., Rechavi, G., & Simon, A. J. (2005).Nuclear envelopathies--raising the nuclear veil.*Pediatric Research, 57*(5 Pt 2), 8R-15R.

Stewart, C. L., Roux, K. J., & Burke, B. (2007). Blurring the boundary: The nuclear envelope extends its reach. *Science (New York, N.Y.), 318*(5855), 1408-1412.

Sullivan, T., Escalante-Alcalde, D., Bhatt, H., Anver, M., Bhat, N., Nagashima, K., et al. (1999). Loss of A-type lamin expression compromises nuclear envelope integrity leading to muscular dystrophy. The Journal of Cell Biology, 147(5), 913-920.

Tang, Y., Tian, X., Wang, R., Fill, M., & Chen, S. R. (2012). Abnormal termination of Ca2+ release is a common defect of RyR2 mutations associated with cardiomyopathies. *Circulation Research, 110*(7), 968-977.

Taylor, M. R., Fain, P. R., Sinagra, G., Robinson, M. L., Robertson, A. D., Carniel, E., et al. (2003).Natural history of dilated cardiomyopathy due to lamin A/C gene mutations. *Journal of the American College of Cardiology, 41*(5), 771-780.

Tazi, J., Bakkour, N., & Stamm, S. (2009). Alternative splicing and disease. *Biochimica Et Biophysica Acta, 1792*(1), 14-26.

Thompson, L. J., Bollen, M., & Fields, A. P. (1997).Identification of protein phosphatase 1 as a mitotic lamin phosphatase. *The Journal of Biological Chemistry, 272*(47), 29693-29697.

Van Berlo, J. H., Voncken, J. W., Kubben, N., Broers, J. L., Duisters, R., van Leeuwen, R. E., et al. (2005). A-type lamins are essential for TGF-beta1 induced PP2A to dephosphorylate transcription factors. *Human Molecular Genetics, 14*(19), 2839-2849.

Vantyghem, M. C., Pigny, P., Maurage, C. A., Rouaix-Emery, N., Stojkovic, T., Cuisset, J. M., et al. (2004). Patients with familial partial lipodystrophy of the dunnigan type due to a LMNA R482W mutation show muscular and cardiac abnormalities. *The Journal of Clinical Endocrinology and Metabolism, 89*(11), 5337-5346.

Vercellotti, G. M. (2001). Overview of infections and cardiovascular diseases.The Journal of Allergy and Clinical Immunology, 108(4 Suppl), S117-20.

Wang, E. T., Sandberg, R., Luo, S., Khrebtukova, I., Zhang, L., Mayr, C., et al. (2008).Alternative isoform regulation in human tissue transcriptomes. *Nature, 456*(7221), 470-476.

Wang, M., Zhang, P., Shu, Y., Yuan, F., Zhang, Y., Zhou, Y., et al. (2014). Alternative splicing at GYNNGY 5' splice sites: More noise, less regulation. *Nucleic Acids Research, 42*(22), 13969-13980.

Weber, K., Plessmann, U., & Traub, P. (1989). Maturation of nuclear lamin A involves a specific carboxy-terminal trimming, which removes the polyisoprenylation site from the precursor; implications for the structure of the nuclear lamina. *FEBS Letters, 257*(2), 411-414.

Weeland, C. J., van den Hoogenhof, M. M., Beqqali, A., & Creemers, E. E. (2015). Insights into alternative splicing of sarcomeric genes in the heart. *Journal of Molecular and Cellular Cardiology, 81*, 107-113.

Weinberg, F., Hamanaka, R., Wheaton, W. W., Weinberg, S., Joseph, J., Lopez, M., et al. (2010). Mitochondrial metabolism and ROS generation are essential for kras-mediated tumorigenicity. *Proceedings of the National Academy of Sciences of the United States of America, 107*(19), 8788-8793.

Wiltshire, K. M., Hegele, R. A., Innes, A. M., & Brownell, A. K. (2013).Homozygous lamin A/C familial lipodystrophy R482Q mutation in autosomal recessive emery dreifuss muscular dystrophy. Neuromuscular Disorders : NMD, 23(3), 265-268.

Worman, H. J. (2012). Nuclear lamins and laminopathies. *The Journal of Pathology, 226*(2), 316-325.

Worman, H. J., & Courvalin, J. C. (2005).Nuclear envelope, nuclear lamina, and inherited disease. *International Review of Cytology, 246*, 231-279.

Worman, H. J., Ostlund, C., & Wang, Y. (2010).Diseases of the nuclear envelope. *Cold Spring Harbor Perspectives in Biology, 2*(2), a000760.

Young, S. G., Fong, L. G., & Michaelis, S. (2005). Prelamin A, Zmpste24, misshapen cell nuclei, and progeria--new evidence suggesting that protein farnesylation could be important for disease pathogenesis. *Journal of Lipid Research, 46*(12), 2531-2558.

Zaremba-Czogalla, M., Dubinska-Magiera, M., & Rzepecki, R. (2011). Laminopathies: The molecular background of the disease and the prospects for its treatment. *Cellular & Molecular Biology Letters, 16*(1), 114-148.

Zastrow, M. S., Flaherty, D. B., Benian, G. M., & Wilson, K. L. (2006). Nuclear titin interacts with A- and B-type lamins in vitro and in vivo. *Journal of Cell Science, 119*(Pt 2), 239-249.

Zhou, Z., & Fu, X. D. (2013).Regulation of splicing by SR proteins and SR protein-specific kinases. *Chromosoma, 122*(3), 191-207.

Zwerger, M., Ho, C. Y., & Lammerding, J. (2011).Nuclear mechanics in disease. *Annual Review of Biomedical Engineering, 13*, 397-428.

Zwerger, M., Jaalouk, D. E., Lombardi, M. L., Isermann, P., Mauermann, M., Dialynas, G., et al. (2013). Myopathic lamin mutations impair nuclear stability in cells and tissue and disrupt nucleo-cytoskeletal coupling. *Human Molecular Genetics, 22*(12), 2335-2349.